

**Red Dog Mine  
Closure and Reclamation Plan**

---

**SD C5: Stability Analysis for Future Raises to Closure,  
Tailings Main Dam  
(URS, 2007)**

**REPORT  
STABILITY ANALYSIS FOR  
FUTURE RAISES TO CLOSURE  
TAILINGS MAIN DAM  
RED DOG MINE, ALASKA**

For

**TECK COMINCO ALASKA, INC.  
URS JOB NO. 33757098  
April 13, 2007**

April 13, 2007

Mr. Gary Coulter  
Teck Cominco Alaska, Inc.  
3105 Lakeshore Drive, Blvd. A, Suite 101  
Anchorage, Alaska 99517

**Stability Analysis Report  
Red Dog Tailings Main Dam  
Future Raises to Closure  
Red Dog Mine, Alaska  
PO # 1257477, Contract # RD-02-06  
URS Job No. 33757098**

Dear Mr. Coulter:

URS Corporation is pleased to submit one copy of our report to Teck Cominco Alaska, Inc. (TCAK) on the stability analysis of the Red Dog Tailings Main Dam future raises to closure. The analysis was completed under TCAK Purchase Order No. 1257477 of Contract No. RD-02-06 dated July 25, 2004, and Change Order Nos. 002, 003, 004 and 005.

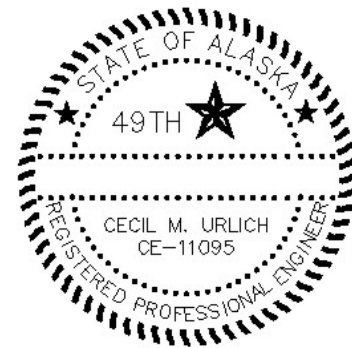
This stability analysis was completed of the tailings main dam to the planned closure height and three assumed interim raise stages. A permanent water cover was assumed over the tailings at closure. The report was prepared in association with URS geotechnical investigation, dam history and seepage analysis reports that have been completed, and a conceptual design report that is in progress.

We thank you for the opportunity to provide engineering support for the tailings main dam future raises to closure. Please call if you have any questions or need additional information.

Sincerely,  
URS Corporation

Suren Balendra  
Staff Geotechnical Engineer

Sri Rajah, Ph.D., P.E.  
Senior Geotechnical Engineer



Cecil M. Urlich, P.E.  
Vice President and Project Manager

Cc: Mr. George Thornton, TCAK, Red Dog Mine (1)  
Mr. Daryl Hockley, SRK, Vancouver (1),

# TABLE OF CONTENTS

	Page
<b>EXECUTIVE SUMMARY .....</b>	<b>V</b>
<b>1.0 INTRODUCTION.....</b>	<b>1</b>
<b>2.0 PURPOSE AND SCOPE .....</b>	<b>1</b>
<b>3.0 HISTORIC REVIEW AND FUTURE PLANS .....</b>	<b>2</b>
3.1 FUTURE RAISES TO CLOSURE .....	3
3.1.1 Embankment Raises to Closure .....	3
3.1.2 Stability of Embankment .....	3
3.1.3 Closure Cover Options .....	3
3.2 HISTORIC STABILITY ANALYSIS .....	4
3.3 TAILINGS MANAGEMENT FOR CLOSURE .....	4
<b>4.0 FACTORS INFLUENCING STABILITY.....</b>	<b>5</b>
4.1 DAM GEOMETRY .....	5
4.2 GOUGE ZONES .....	6
4.2.1 Stability Analyses for Stages I to VI .....	6
4.2.2 Stability Analyses for Stages VII-A and B .....	7
4.2.3 Re-evaluation of Gouge Presence and Strength.....	7
4.2.4 Stability Analyses for Future Raises to Closure .....	7
4.3 SHEAR STRENGTH OF DAM AND FOUNDATION MATERIALS .....	8
4.3.1 Stability Analysis for Stages I-VI.....	8
4.3.2 Stability Analysis for Stages VII-A and B.....	8
4.3.3 Reevaluation of Gouge Strength.....	8
4.3.4 Stability Analysis for Stages for Future Raises to Closure .....	9
4.4 SEISMIC LOADING .....	9
4.4.1 Seismic Design of Tailings Main Dam.....	10
4.4.2 Seismic Criteria used for Stages I to VI .....	11
4.4.3 Seismic Criteria used for Stages VII-A and B .....	12
4.5 PHREATIC SURFACES .....	12
4.5.1 Historical Records .....	13
4.5.2 Phreatic Surface at Closure.....	13
4.6 CONSTRUCTION IMPACT .....	13
4.7 LONG-TERM STABILITY .....	14
<b>5.0 ANALYSIS APPROACH.....</b>	<b>14</b>
5.1 SEISMIC HAZARD ANALYSIS .....	14
5.2 STABILITY ANALYSIS.....	15
5.3 DEFORMATION ANALYSIS .....	16
<b>6.0 SEISMIC HAZARD ANALYSIS .....</b>	<b>17</b>
6.1 REGIONAL TECTONIC SETTING .....	18
6.2 REGIONAL SEISMICITY .....	18
6.3 SIGNIFICANT SEISMIC SOURCES .....	18
6.4 SITE GEOTECHNICAL CONDITIONS .....	18
6.5 PROBABILISTIC SEISMIC HAZARD ANALYSIS .....	19
6.5.1 Probabilistic Hazard Model .....	19
6.5.2 Seismic Source Models.....	19
6.5.3 Attenuation Equations .....	22
6.6 COMPUTATIONS OF MEAN GROUND MOTION .....	25
6.7 RESULTS.....	25
6.8 COMPARISON WITH USGS VALUES.....	26

<b>7.0</b>	<b>STABILITY ANALYSIS</b> .....	<b>27</b>
7.1	SEISMIC CRITERIA.....	27
7.2	LIQUEFACTION POTENTIAL OF TAILINGS.....	28
7.2.1	Selection of Earthquake Magnitude.....	28
7.2.2	Liquefaction Evaluation.....	29
7.3	DESIGN PHREATIC SURFACE FOR CLOSURE .....	29
7.3.1	Upstream Phreatic Surface .....	29
7.3.2	Downstream Phreatic Surface.....	30
7.4	PORE PRESSURE COEFFICIENT.....	34
7.5	STABILITY ANALYSES.....	35
7.6	SENSITIVITY ANALYSES.....	38
7.6.1	Pore Pressure Coefficient .....	38
7.6.2	Shear Strength of Gouge Material .....	38
7.6.3	Sensitivity to No Liner in Dam.....	39
<b>8.0</b>	<b>DEFORMATION ANALYSIS</b> .....	<b>40</b>
8.1	SIMPLIFIED DEFORMATION ANALYSIS .....	40
8.1.1	Determination of Yield Acceleration, $k_y$ .....	41
8.1.2	Determination of Earthquake Induced Acceleration, $k_{max}$ .....	42
8.1.3	Estimation of Permanent Displacement.....	43
8.2	DEFORMATION ANALYSIS RESULTS .....	43
8.2.1	Makdisi and Seed (1978).....	43
8.2.2	Franklin and Chang (1977).....	44
8.2.3	Bray and Rathje (1998).....	44
8.2.4	Martin and Qiu (1994).....	44
<b>9.0</b>	<b>CONCLUSIONS AND RECOMMENDATIONS</b> .....	<b>45</b>
9.1	CONCLUSIONS .....	45
9.2	RECOMMENDATIONS .....	46
<b>10.0</b>	<b>REFERENCES</b> .....	<b>46</b>

## TABLES

Table 3-1	Summary of Upstream and Downstream Slopes of the Dam
Table 4-1	Material Unit Weight and Strength Parameters
Table 4-2	Summary of Seismic Criteria for Stages I to VII-B
Table 6-1	Seismicity-based Recurrence Equations in PSHA
Table 6-2	Annual Recurrence of Characteristic Earthquakes
Table 6-3	Attenuation Equations for PSHA
Table 6-4	Five Percent Damped Uniform Probability Spectral Accelerations in g for Bedrock
Table 6-5	Five Percent Damped Response Spectral Accelerations in g for Site Class C
Table 6-6	Comparison of Bedrock PGA (g) Results from This Study and USGS
Table 7-1	Seismic Hazard for Tailings Main Dam
Table 7-2	Representative Underdrain Piezometer and Pumpback Rate Records
Table 7-3	Design Downstream Piezometric Heads
Table 7-4	Material Parameters for Stability Analyses
Table 7-5	Summary of Stability Analysis Results

Table 7-6	Factor of Safety Values for Different Values of $R_u$
Table 7-7	Factor of Safety Values with Gouge Friction Angle of 19 degrees
Table 7-8	Summary of Stability Sensitivity Analysis Results for Seismic Loading Condition
Table 8-1	Summary of Deformation Analysis Results

## FIGURES

Figure 4-1	Site Plan and Location of Soil Profiles (Conceptual Design)
Figure 4-2	Downstream Slope Options for Conceptual Closure Design
Figure 4-3	Material Types and Parameters for Stability Analyses
Figure 4-4	Soil and Rock Profile (Cross Section H-H')
Figure 4-5	Maximum Recorded Water Levels of Underdrain Piezometers and Design Phreatic Surface
Figure 4-6	Permafrost and Phreatic Profile along Dam Longitudinal Axis
Figure 4-7	Historical Permafrost Degradation along Stage VI Axis of the Dam
Figure 6-1	Alaska Seismicity showing Magnitude of Earthquakes Recorded Since 1899
Figure 6-2	Alaska Seismicity Recorded Since 1899 Color Coded by Focal Depth
Figure 6-3	Alaska Seismicity, $M \geq 6$ .
Figure 6-4	Seismic Source Zones
Figure 6-5	Recurrence Equation based on the historical seismicity for the Brooks Range
Figure 6-6	Site-Specific Bedrock Response Spectra
Figure 6-7	Site-Specific Response Spectra for Site Class C
Figure 7-1	Seismic Hazard Map for OBE
Figure 7-2	Seismic Hazard Map for MDE
Figure 7-3	Probabilistic Seismic Hazard Deaggregation for OBE
Figure 7-4	Probabilistic Seismic Hazard Deaggregation for MDE
Figure 7-5	Historical Temperature Profile at Thermistor TDAM-T1
Figure 7-6	Historical Temperature Profile at Thermistor TDAM-T15
Figure 7-7	Historical Effectiveness of Tailings Beach on Seepage
Figure 7-8	Critical Block Failure Surface - 2.75H: 1V with Berm for Long Term Condition under MDE Loading
Figure 7-9	Critical Block Failure Surface - 2.75H: 1V without Berm for Long Term Condition under MDE Loading
Figure 7-10	Critical Circular Failure Surface - 2.75H: 1V with Berm for Long Term Condition under MDE Loading
Figure 7-11	Critical Circular Failure Surface - 2.75H: 1V without Berm for Long Term Condition under MDE Loading
Figure 7-12	Critical Block Failure Surface - 3H: 1V Slope for Stage VIII under MDE Loading
Figure 7-13	Critical Block Failure Surface with $R_u = 0.1$ -- Static End-of-Construction Case 2.75H: 1V Slope

Figure 7-14 Critical Block Failure Surface with  $R_u = 0.2$  – Static End-of-Construction Case 2.75H: 1V Slope

Figure 7-15 Downstream Phreatic Surface for Closure 900 feet Beach, No Liner

Figure 7-16 Critical Block Failure Surface with  $R_u = 0$  – Static Long Term Design Condition Case, 900 beach, No Liner; 3H: 1V Slope

## Executive Summary

This report describes stability analyses that were completed by URS Corporation for Teck Cominco Alaska Inc. (TCAK) for the tailings main dam future raises to closure at Red Dog Mine. The conceptual design of the dam at closure assumes three raises (Stages VIII, IX and X) of heights 10, 10 and 6 feet, and crest elevations at 970, 980 and 986 feet, respectively.

This final crest level at El. 986 may change slightly as the closure plan is being developed for the tailings impoundment, and possibly as tailings production, water discharge and storage area projections are updated. However, slight changes in the crest level will not significantly impact the stability analyses described in this report.

The primary purpose of the stability analyses was to support the closure plan that is currently being developed for the mine and specifically for the tailings impoundment, and to enable the conceptual designs of Stages VIII, IX and X to be prepared to the Stage X crest elevation of 986 feet (El. 986) at closure. This report describes the following:

- Seismic review and site specific probabilistic seismic hazard analysis (PSHA)
- Revised seismic criteria based on the PSHA results and updated seismic information
- Stability and deformation analyses and the results of these analyses.

URS developed the following seismic design criteria and conclusions:

- Red Dog Mine is located in a region that has low seismicity and no known active faults.
- Two design-level earthquakes for dam designs in Alaska are defined by ADNR (2005) as:
  - Operating Basis Earthquake (OBE): 10% probability of exceedance in 50 years (return period of 475 years)
  - Maximum Design Earthquake (MDE): 2 % probability of exceedance in 50 years (return period of 2,475 years).
- The following seismic hazard was interpolated at the mine site from a 2005 USGS seismic hazard map for Alaska, which was developed by means of a PSHA at nodal points of a grid:
  - OBE - PGA is 0.10 g for bedrock and 0.11 g for Site Class C
  - MDE - PGA is 0.23 g for bedrock and 0.25 g for Site Class C
- A site specific seismic hazard analysis was performed based on a site specific PSHA for the mine site , and the following seismic hazard was obtained:
  - OBE - PGA is 0.077 g for bedrock and 0.084 g for Site Class C
  - MDE - PGA is 0.18 g for bedrock and 0.20 g for Site Class C
- Seismic criteria for the dam future raises to closure were established to be as follows:
  - OBE - conceptual design PGA is 0.11 g
  - MDE - conceptual design PGA is 0.25 g
- Seismic coefficients for pseudo-static stability analyses of the dam were selected to be:
  - OBE - seismic coefficient is 0.055
  - MDE - seismic coefficient is 0.125
- For the seismic criteria established for closure, the predominant moment magnitude of earthquake for both OBE and MDE events is 5.23.

- The liquefaction potential of the tailings is low for ground shaking induced by the OBE and MDE events.
- The shear strength of the gouge zones under the dam is the critical parameter for designing stable dam slopes. From the geotechnical data, it is estimated that the gouge zones have a shear strength corresponding to an internal friction angle of 22 degrees and zero cohesion.

The stability and deformation analysis results and conclusions using a gouge material internal friction of 22 degrees and zero cohesion are as follows:

Design Condition	Loading Conditions	Minimum Required FS	Computed FS (for gouge friction angle 22 deg. & cohesion 0)						
			2.75H:1V				3H:1V		
			Stage VIII	Stage IX	Closure		Stage VIII	Stage IX	Closure
				with berm	without berm				
End-of-Construction Ru =0.1	Static, Block	1.3	1.46	1.44	1.45	1.35	1.54	1.50	1.53
	Static, Circular	1.3	1.73	1.68	1.65	1.45	1.88	1.70	1.58
Long Term Condition	Static, Block	1.5	1.61	1.58	1.59	1.52	1.70	1.65	1.67
	Static, Circular	1.5	1.81	1.77	1.74	1.59	1.96	1.82	1.71
	Seismic (OBE) Block	1.2	1.23	1.23	1.23	1.18*	1.27	1.27	1.29
	Seismic (OBE) Circular	1.2	1.47	1.46	1.39	1.26	1.55	1.42	1.38
	Seismic (MDE) Block	1.0	0.98*	0.98*	1.00	0.96*	1.01	1.02	1.06
	Seismic (MDE) Circular	1.0	1.22	1.18	1.14	1.04	1.23	1.15	1.14

\* Does not meet minimum FS criteria

- With an internal friction angle of 22 degrees and zero cohesion for the gouge material, the steepest stable downstream slope of the Stage X dam and interim Stage VII and IX raises is 3.0H: 1V. The final dam would be stable during the MDE.
- For the extreme “no liner” case of a failed geomembrane, the dam will be stable with a factor of safety (FS) of 1.36, which is less than the required minimum FS of 1.5. The FS could be increased by further widening the beach to lower the phreatic surface in the dam.
- The deformation analyses show that a maximum permanent horizontal crest displacement of the dam during the maximum anticipated earthquake at the site will be up to 21 inches, which is not a dam safety concern because of the adequate freeboard that will be in place.
- Using the simplified approach of deformation analysis, it is estimated that the maximum shear strain in the dam during the maximum anticipated earthquake at the site would be about 0.19%.

The dam stability was found to be sensitive to the shear strength of the gouge material. For example:

- With an internal friction angle of 19 degrees and zero cohesion for the gouge material, the downstream slope of 3.0H: 1V will be stable for static and OBE seismic conditions, but will not be stable under MDE seismic loading and will likely deform under this loading.

On the basis of the stability analysis, URS developed the following recommendations:

- A downstream slope of 3.0H:1V is recommended for the tailings main dam future raises to closure, and would provide a stable embankment with required long-term factors of safety
- During construction of the future raises, the pore pressure coefficient in the foundation materials should be maintained less than 0.2.

## 1.0 INTRODUCTION

The tailings main dam at Red Dog Mine is a 182-foot high rockfill embankment that was raised in stages to the current Stage VII-B configuration. The mine operator, Teck Cominco Alaska, Inc. (TCAK), and SRK Consulting (Canada) Inc., are developing a mine closure plan that is based on operations to about year 2030. This will require raising the dam by 26 feet from the current crest elevation of 960 feet (El 960) to a final crest at El 986.

In order to provide technical input to the closure plan for the tailings facility part of the mine, TCAK retained URS Corporation to complete a conceptual design of the tailings main dam at closure. This conceptual design assumes that the dam will be raised in three stages (VIII, IX and X) of heights 10, 10 and 6 feet, to crests at El 970, 980 and 986 feet, respectively. The final dam will be 208 feet high.

In order to develop the conceptual design, URS completed a geotechnical investigation for the Stage VII-B and closure configurations, a historical review of the dam, a seepage analysis of the dam from Stage VII-B through the future raises to closure, and a stability analysis of the dam for the raises to closure (URS 2006, 2007a, 2007b and 2007c).

This URS report presents the results of the stability analysis for the conceptual design at closure and for the Stage VII-B dam raise that is now under its third and final season of construction. The stability analysis was completed under TCAK Purchase Order No. 1257477 of Contract No. RD-02-06, dated July 25, 2004, and Change Orders Nos. 002, 003, 004 and 005.

The stability analysis work also fulfils a State of Alaska Department of Natural Resources (ADNR) request for “a *detailed engineering evaluation of the expected performance of the next raise and in subsequent raises up to the final configuration of the system*” in a letter to TCAK (2005b) titled “Multiple Accounts Analysis for Red Dog Tailings Disposal”, dated June 2, 2005.

## 2.0 PURPOSE AND SCOPE

The primary purpose of the URS stability analysis of the tailings main dam at Red Dog Mine was to support the closure plan for the tailings impoundment as follows:

- Evaluate the stability of tailings main dam for future raises to closure with a range of downstream slopes
- Determine the inclination of the steepest stable downstream slope for the raise and closure configurations
- Estimate the crest deformation during the maximum seismic event that could reasonably be anticipated at the site

In order to achieve this purpose, the scope of this stability analysis for the tailings main dam included the following tasks:

- Review the design, construction, operation and instrumentation records of the dam
- Review the historic dam inspection, instrumentation, and thermal analysis reports
- Compile the impoundment water level, pumpback rate, and dam phreatic surface data
- Consolidate the geotechnical data from the past and current geotechnical investigations

- Analyze the extent and strength of gouge zones in the bedrock within the dam foundation
- Perform a site specific probabilistic seismic hazard analysis (PSHA) for the mine site
- Update the seismic design criteria based on current seismic hazard maps for the region
- Determine the site specific PSHA for the tailings main dam
- Evaluate the liquefaction potential of the tailings using the updated seismic design criteria
- Perform stability analyses of the dam using a two-dimensional model for four conditions:
  - Static stability for “end-of-construction”
  - Static stability for “long-term” design conditions
  - Seismic stability for “Operational Basis Earthquake (OBE)” design conditions
  - Seismic stability for “Maximum Design Earthquake (MDE)” design conditions
- Evaluate the stability of the dam under interim raise construction stages
- Complete a deformation analysis of the dam under the maximum earthquake that could be reasonably expected at the site.

The stability analysis findings, conclusions and recommendations are described in this report which is organized as follows:

- Section 1.0 provides the introduction to the report
- Section 2.0 outlines the purpose and scope of the stability analysis
- Section 3.0 describes the dam’s stability history and future raises to closure
- Section 4.0 describes the factors that influence the stability of the dam
- Section 5.0 describes the stability and deformation analysis approaches
- Section 6.0 describes the site specific seismic hazard analysis and results
- Section 7.0 describes the stability analysis and results
- Section 8.0 describes the deformation analysis and results
- Section 9.0 presents conclusions and recommendations
- Section 10.0 is a list of references used in completing the analysis

### **3.0 HISTORIC REVIEW AND FUTURE PLANS**

Descriptions of the tailings dam site, design and construction history, construction material types, primary seepage control system, secondary seepage control system, and dam instrumentation history were provided in the Stage VII-A construction report (URS 2004a), Stage VII-B drawings (URS 2005b), geotechnical report (URS 2006) and dam history report (URS 2007a)

Concurrent with the stability analysis, URS completed seepage analyses and conceptual designs of the tailings main dam to closure that are described in separate reports (URS 2007b and 2007c, respectively). The planned future raises to closure, the historic stability analysis, and the planned seepage controls for closure are presented in this section.

### 3.1 FUTURE RAISES TO CLOSURE

#### 3.1.1 Embankment Raises to Closure

The conceptual design of the tailings main dam future raises to closure (URS 2007c) consists of raising the dam by a total of 26 feet from the current Stage VII-B crest at El. 960 to the closure crest at El. 986, by completing the following construction activities:

- Widen the embankment downstream to provide a footprint for the raises
- Raise the embankment to a final crest elevation of El 986
- Extend the wing wall out from the east abutment to a final crest at El 986
- Construct an open channel spillway along the hillside around the west abutment.

For purposes of the conceptual design, it is assumed that the 26 feet of future raises from the current Stage VII-B crest at El. 960 to the closure crest at El. 986 will be built in three stages as follows:

- Stage VIII Ten feet high from crest El. 960 to 970
- Stage IX Ten feet high from crest El. 970 to 980
- Stage X Six feet high from crest El. 980 to 986.

The planned maximum tailings and water levels at closure would be El 975 and El 985.6, respectively, based on the water cover closure option (SRK 2005, SRK 2006, URS 2007b). For the seepage analysis, a surface pond water level at El 980.2 was used. This includes a permanent water cover of 2.0 feet and autumn and spring inflow of 3.2 feet on top of the maximum tailings of El. 975, as described in the conceptual design report (URS 2007c).

#### 3.1.2 Stability of Embankment

URS identified seven major factors that affect the stability of the tailings main dam embankment:

- Dam geometry
- Gouge zones
- Shear strengths
- Seismic loading
- Phreatic surface
- Construction impact
- Long-term stability

These factors are described in Section 4.0. URS performed the stability analysis for the future raises to closure by considering all of these factors to achieve a safe and optimum design of the dam.

#### 3.1.3 Closure Cover Options

Several closure options were evaluated for closure and reclamation of the tailings main dam, and the following four options were selected for detailed consideration (SRK, 2006):

- **Contaminated water cover:** Contaminated inflows would be stored in the tailings impoundment for annual treatment and discharge

- **Clean pond water cover:** Contaminated inflows would be diverted to an alternate storage location and clean water inflows will be stored in the tailings impoundment.
- **Dry soil cover:** A soil/rock layer would cover the tailings and the water level would be below the base of the cover. Contaminated inflows would be diverted elsewhere.
- **Wet soil cover:** A soil/rock layer would cover the tailings and the water level will be maintained within the cover.

For the seepage analysis model presented in seepage report (URS, 2007b), a contaminated water cover, which represents conditions similar to the clean pond water cover and wet soil cover options, was considered. A sensitivity analysis of a potential dry cover option was also completed.

### 3.2 HISTORIC STABILITY ANALYSIS

Stability analyses of the tailings main dam were completed during the design of Stages I to VI (Dames & Moore, 1986), modifications such as the pipe bench (Dames & Moore, 1999) and dust control structures (URS, 2001) and the Stages VII-A and B raises (URS, 2002a and 2002b). Upstream and downstream slope configurations of the dam for various stages were selected by considering the long-term static and seismic stability and the short-term end-of-construction stability (URS 2004a, 2005b).

The upstream and downstream slopes of the Stage I starter dam were 3H: 1V and 2H: 1V respectively. The upstream slopes for the subsequent Stage II to VII-B raises has been 2.5H: 1V. The downstream slopes had two different inclinations: 4H: 1V for the Stage II to VI raises; and 3H: 1V for the upper part of the Stage VII-A and B raises above a hinge point on the slope. The upstream and downstream slopes and the hinge point elevations for Stages I to VII-B are summarized in Table 3-1 below.

**Table 3-1: Summary of Upstream and Downstream Slopes of the Dam**

Dam Stage	Upstream Slope	Downstream Slope		
		Above Hinge (H:V)	Hinge El (feet)	Below Hinge (H:V)
Starter Dam (Stage I)	3.0H:1V	2.0H:1V	No Hinge	2.0H:1V
Stage II	2.5H:1V	3.0H:1V	877.5	4.0H:1V
Stage III	2.5H:1V	3.0H:1V	887.5	4.0H:1V
Stage IV	2.5H:1V	3.0H:1V	895.0	4.0H:1V
Stage V	2.5H:1V	3.0H:1V	902.5	4.0H:1V
Stage VI	2.5H:1V	3.0H:1V	907.5	4.0H:1V
Stage VII-A	2.5H:1V	3.0H:1V	880.0	4.0H:1V
Stage VII-B	2.5H:1V	3.0H:1V	852.5	4.0H:1V

### 3.3 TAILINGS MANAGEMENT FOR CLOSURE

Recognizing the benefits of a wider tailings beach to reduce the seepage rate and lower the phreatic surface in the tailings main dam, the concept of a coffer dam in the tailings impoundment will continue to provide a tailings beach along the entire crest length of the dam for future raises to closure. A coffer dam will be built over the tailings and the space between the main dam and coffer

dam will be filled with tailings to form a tailings beach. The benefits of a wider tailings beach will be balanced with other considerations to select optimal beach widths and coffer dam alignments for closure.

#### **4.0 FACTORS INFLUENCING STABILITY**

The stability of a dam is influenced by several factors including dam geometry, shear strength of the dam and foundation materials, external and seismic loadings, groundwater conditions and construction activity impacts. These factors must all be considered to achieve a safe and optimum design of a dam.

Geotechnical conditions are a crucial part of a dam design. Historic slope failures show that small weak zones in a competent soil or rock mass can cause instability. Seismic loads are critical to stability and often control slope designs in seismic areas. Groundwater and seepage conditions can impact stability in many ways. Pore pressures resulting from external forces and changes in seasonal, short-term or long-term groundwater flow can induce changes in shear strengths and increase driving forces that destabilize soil elements. Construction activities and their duration also impact stability.

URS identified the following seven major factors for detailed considerations in the stability analyses for the tailings main dam:

- Dam geometry
- Gouge zones
- Shear strengths
- Seismic loading
- Phreatic surface
- Construction impact
- Long-term stability

These factors on the stability of the tailings main dam are discussed in the following sections.

#### **4.1 DAM GEOMETRY**

The stability of the tailings dam at closure is impacted by its geometry, which is controlled by:

- Upstream slope of the dam
- Downstream slope of the dam
- Presence and size of berm on the downstream slope
- Elevation of tailings in the tailings impoundment

The tailings main dam would generally be more stable with flatter than steeper ones. However, flatter slopes require a larger dam footprint and increased material quantities. An increased footprint may require foundation construction on weaker materials and relocation of existing facilities. An increased quantity of materials will impact the availability of materials and construction time and cost.

The upstream slope of the existing Stage VII-B raise is 2.5H:1V (URS 2004a, 2005b, 2006, 2007a). A flatter upstream slope for future raises would require upstream raise construction and the future

raises founded on tailings. For the conceptual design, a downstream raise with the same upstream slope of 2.5H:1V was considered.

The downstream slope of the existing Stage VII-B raise is 4H:1V and 3H:1V, below and above, the hinge point at El 852.5, respectively. A downstream raise to a closure crest at El. 986 with minimal impact to existing seepage collection system is possible only with a steeper downstream slope. In order to identify a stable downstream slope that would minimally impact the seepage collection system, three different uniform downstream slopes were considered in the stability analysis as follows:

- 2.50H:1V
- 2.75H:1V
- 3.00H:1V

Figure 4-1 shows the dam footprint for these closure configurations. The effect of the different slope configurations on the seepage control structures is shown in the cross section of the dam in Figure 4-2.

The Stage VII-B geometry of the tailings main dam includes a berm at the downstream toe that is about 10 feet high and 80 feet wide. The presence of this berm improves the static and seismic stability of the dam. At closure, the berm width of this berm reduces with different downstream slopes:

- Downstream slope 2.50H:1V - Berm width is 70 feet or 90% of the existing berm width
- Downstream slope 2.75H:1V - Berm width is 35 feet or 45% of the existing berm width
- Downstream slope 3.00H:1V - No berm.

The tailings level will the stability and seepage through and under the dam. For the conceptual closure design, the tailings level was fixed at El 975 per the tailings storage needs at closure.

## 4.2 GOUGE ZONES

Highly fractured rock and gouge zones with large variations in bedding orientation were encountered in the bedrock under the tailings main dam during geotechnical investigations (Dames & Moore 1986; URS 2006). The bedding orientation variations are a result of intense folding and bending of bedrock

The presence of the gouge zones under the dam foundation could provide a sliding plane under the dam and therefore could adversely affect the stability of the dam. These zones are weaknesses in the bedrock that resulted from the rock having been sheared and broken. Such zones are often associated with potential critical surfaces in stability analyses. The critical surface is the weakest plane of a slope, so that if a slope is weak enough that it fails, the failure is along the critical surface.

The presence of gouge zones under the dam foundation affects stability of the dam. Gouge zones could either be continuous layers or isolated lenses. The impact of the gouge zones on the dam stability could be marginal if the zones are discontinuous, but could be significant if the zones are continuous.

### 4.2.1 Stability Analyses for Stages I to VI

The geotechnical data that was available for the original Stages I to VI design was inadequate to prove or disprove the presence of continuous gouge zones under the dam. Therefore, a 6-inch thick

weak gouge layer was assumed under the dam at the interface between ice-rich and ice-free bedrock 15 feet below the original ground surface, and with a downstream-sloping orientation to provide conservative results (Dames & Moore, 1986). The residual friction angle of the gouge material was chosen to be 24 degrees based on one consolidated direct shear test (Dames & Moore, 1986 and 1987b), and was used for the dam design up to Stage VI.

Dames & Moore (1986) computed the gouge shear strength required to obtain a seismic factor of safety (FOS) of 1.0 for the tailings main dam under the Maximum Design Earthquake (MDE) (referenced as Maximum Credible Earthquake) to be only 6 degrees (internal friction angle). Since the required friction angle was much smaller than the measured residual friction angle of the gouge material, additional shear strength tests of the gouge material were not considered necessary.

#### **4.2.2 Stability Analyses for Stages VII-A and B**

For the Stage VII-A and B stability analyses, URS (2002a and b) used a similar analysis approach and computed that gouge shear strength should correspond to an internal friction angle of 15 degrees to obtain a seismic factor of safety (FS) of 1.0 under the MDE. Again, the required internal friction value was significantly lower than the measured residual strength of 24 degrees. Therefore, it was concluded that the Stage VII dam and foundation were stable, and that it was not necessary to further investigate the weak pre-sheared zone under the Stage VII condition.

Based on the previous findings, it is clear that the gouge zone characteristics are among the main controlling factors for the stability design of the future raises to closure. As a result, it was considered that a re-evaluation of the strength characteristics of these gouge zones was prudent for the stability analysis due to the increased dam height, desire for a steeper slope, and long-term nature of the closure condition. Moreover, the dam at closure would be founded on an area beyond the current toe.

#### **4.2.3 Re-evaluation of Gouge Presence and Strength**

On the basis of a preliminary set of stability analyses (URS, 2005e), it was shown that the final dam with a steeper slope may be stable only if favorable foundation conditions exist. Therefore, the 2005 geotechnical investigation included borings to re-examine the possibility of continuous gouge zones under the dam foundation, and laboratory cyclic direct shear tests to obtain residual friction angles of the gouge samples collected from the site (URS 2005a, 2006 Section 4.3).

Highly fractured rock and gouge zones with large variations in bedding orientation were encountered in the bedrock under the dam by the geotechnical investigations (Dames & Moore, 1986 and URS, 2006). The variations of bedding orientation are a result of intense folding and bending of the bedrock. After reviewing the observation for the gouge zones that were encountered, URS concluded that the gouge zones observed are not continuous between the borings and under the dam (URS, 2006).

#### **4.2.4 Stability Analyses for Future Raises to Closure**

The presence of the gouge zones and their locations under the dam could result in potentially weak planes, even if the zones are not continuous. Therefore, for the stability analysis, 'layers' of continuous gouge zones were assumed to be present under the dam foundation. The estimated 'layers' are described in the subsurface profiles in the geotechnical report. Idealized gouge zones and the soil profile along the critical section (Section H-H') of the dam are shown on Figure 4-4.

### 4.3 SHEAR STRENGTH OF DAM AND FOUNDATION MATERIALS

The strength characteristics of the dam and foundation materials impact the stability of the tailings main dam. Geotechnical investigation data is presented in the 2005 geotechnical report (URS, 2006).

The subsurface condition at the dam site is overburden over bedrock. The overburden includes fill and native soil. Bedrock typically is shale and less typically siltstone. Typically, the upper part of the shale bedrock is very weathered and the weathering decreases with depth. The shale bedrock had gouge zones, where the rock had been sheared and broken, leaving a zone of clayey silt with rock fragments. The shear strength of the gouge material was investigated by laboratory cyclic direct shear tests on samples collected on the site (Dames & Moore, 1986; and URS, 2006). The test results are shown in the geotechnical report (URS, 2006) and summarized below.

#### 4.3.1 Stability Analysis for Stages I-VI

For the design of the original dam Stages I to VI, the residual shear strength of the gouge material was evaluated using one set of consolidated cyclic direct shear tests (Dames & Moore, 1986). The residual shear strength parameters of the gouge material obtained from the laboratory testing were:

- Friction angle            24 degrees
- Cohesion                 175 psf

For the design of Stages I through VI, the design residual strength parameters of the gouge material were established as:

- Friction angle            24 degrees
- Cohesion                 0 psf

Considering the seismic stability, Dames & Moore (1986) established that a minimum friction angle of 6 degrees was required for the gouge material to maintain seismic stability of Stages I to VI.

#### 4.3.2 Stability Analysis for Stages VII-A and B

For design of the Stage VII-A and VII-B raises, URS (2002a and 2002b) established that a minimum friction angle of 15 degrees was required for the gouge material to maintain seismic stability.

#### 4.3.3 Reevaluation of Gouge Strength

Realizing that future raises to closure of the tailings main dam will result in a higher dam and increased footprint, it is desired that the downstream slope at closure be steeper than the current downstream slope. Considering that the strength of the gouge material is critical for the stability of the higher and steeper dam, additional cyclic direct shear tests were on the gouge material were performed during the 2005 geotechnical investigation (URS, 2006).

The data points from both sets of direct shear test results (Dames & Moore, 1986; and URS, 2006) were considered together and residual shear strength parameters of the gouge material were estimated to using least-square best-fit approach. The residual shear strength parameters of the gouge material obtained from the laboratory testing were:

- Friction angle            19 degrees
- Cohesion                 400 psf

In order to be consistent with the design parameters established for the previous designs, the gouge material was also evaluated as a cohesionless material and the equivalent residual shear strength parameters were established for design of future raises, as follows:

- Friction angle            22 degrees
- Cohesion                    0 psf

#### 4.3.4 Stability Analysis for Stages for Future Raises to Closure

Based on the cyclic direct shear test results, URS (2006) selected the design residual shear strength of the gouge 'layers' to correspond a friction angle of 22 degrees and zero cohesion.

Primary materials comprising the tailings main dam and its foundation are shown on Figure 4-3. Shear strength parameters, consisting of internal friction angle and cohesion, and the unit weight of these materials for the stability analysis, are summarized in Table 4-1. These parameters were mostly chosen on the basis of triaxial and direct shear test results, supplemented by engineering judgment (Dames & Moore, 1986; URS, 2002a, 2002b, and 2006). These design material parameters were selected to be consistent with the previously-used design parameters (Dames & Moore, 1986).

**Table 4-1 - Material Unit Weight and Strength Parameters**

Material	Unit Weight (pcf)		Effective Stress Shear Strength Parameters		Source
	Moist	Saturated	Cohesion (psf)	Phi (deg)	
Tailings (Silt and Fine Sand)	120	120	0	30	URS, 2002a and 2002b
Buttress (Random Rockfill)	135	140	0	35	URS, 2002a and 2002b
Liner Bedding	125	138	0	35	URS, 2002a and 2002b
Liner	115	115	0	24	URS, 2002a and 2002b
Filter drain	125	138	0	35	URS, 2002a and 2002b
Transition Rockfill	125	138	0	35	URS, 2002a and 2002b
Random Rockfill	135	140	0	35	URS, 2002a and 2002b
Highly Weathered Shale	115	115	0	30	URS, 2002a and 2002b
Underdrain	115	115	0	30	URS, 2002a and 2002b
Moderately Weathered Shale	145	150	0	35	URS, 2002a and 2002b
Kivalina Shale Fill	112	112	250	11	URS, 2004b
Gouge 'Layer'	120	120	0	22	URS, 2006

#### 4.4 SEISMIC LOADING

The tailings main dam is located in a relatively low seismic region in Alaska. The following factors influence the seismic loading and the stability of the tailings main dam:

- Inertial forces due to horizontal and vertical ground accelerations
- Reduction in shear strength of materials due to excess pore pressure
- Possible liquefaction of tailings retained in the impoundment
- Magnitude of permanent deformations of the dam

The inertial forces due to horizontal and vertical accelerations cause an increasing of the driving forces and decrease of the resisting forces, which will result in reduced stability of the dam during the earthquake.

Any excess pore pressure generated during the earthquake within the dam and its foundation materials might result in reduced shear strength of those materials. Any possible reduction in shear strength of the dam and foundation materials would reduce the stability of the dam during the earthquake.

The tailings liquefaction potential will impact the dam stability. Liquefaction is a nearly complete loss of shear strength due to excess pore pressures generated during strong shaking events. Also, after the shaking, the tailings shear strength will be represented by a residual shear strength of the tailings, which will be lower. Alternately, densification of the tailings will likely occur immediately after liquefaction, which will improve the tailings shear strength.

The upstream stability of the tailings main dam would be greatly impacted if the tailings would liquefy. The impact would depend on the extent of the liquefaction. For the stability analyses of Stage I to VII-B designs, using the seismic criteria considered for those designs, the liquefaction potential of the tailings was evaluated and the tailings were found to be non-liquefiable.

Permanent vertical and horizontal deformations of the dam during a significant seismic event are anticipated. However, if the deformation is small enough then the stability of the dam is not adversely impacted. Alternately, large vertical and horizontal deformations could result in slope failures and crest depressions, which would lead to loss of freeboard.

Two levels of design earthquakes were considered in the seismic stability analyses for the original Stage I to VI raise, later Stages VII-A and VII-B raises, and future raises to closure.

#### **4.4.1 Seismic Design of Tailings Main Dam**

Section 6.3.2 of “Guidelines for Cooperation with the Alaska Dam Safety Program” dated June 2005, prepared by Dam Safety and Construction Unit, Water Resources Section, Division of Mining, Land and Water, Alaska Department of Natural Resource (ADNR, 2005). The definition of design earthquakes based on dam safety guidelines are as follows:

- **Operating Basis Earthquake (OBE)**: Represents the ground motions or fault movement from an earthquake considered to have a reasonable probability of occurring during the functional life-time of the project. All critical elements of the project (such as dam, appurtenant structures, reservoir rim, and equipment) should be designed to remain functional during the OBE, and any resulting damage should be easily repairable in a limited time. The OBE can be defined based on probabilistic evaluations, with the level of risk (probability that the magnitude of ground motion will be exceeded during a particular length of time) being determined relative to the hazard potential classification and location of the dam.
- **Maximum Design Earthquake (MDE)**: Represents the ground motions or fault movements from the most severe earthquake considered at the site, relative to the acceptable consequences of damage in terms of life and property. All critical elements of the dam and appurtenant structures for which the collapse or failure could result or precipitate an uncontrolled release of the reservoir must be designed to resist the MDE. In addition, the dam and appurtenances must be designed to resist the effects of the MDE on the reservoir and reservoir rim. The MDE may be defined based on either deterministic or probabilistic evaluations, or both.

The return period for the MDE is selected in direct correlation with the magnitude of the Maximum Credible Earthquake (MCE) for the known or suspected regional seismic sources and dam classification. Section 6.3.2 of the dam safety guidelines defines the MCE as the reasonably could be generated by a specific seismic source, based on seismological and geologic evidence and interpretations. This seismic hazard level is also referred to as the safety-level seismic hazard.

It is considered appropriate to consider different levels of seismic risk by considering the hazard potential of the structure. Section 2.4 of the dam safety guidelines define three different hazard classifications for dams based on potential impacts of failure and improper operation:

- Class I (high)
- Class II (significant)
- Class III (low).

The tailings main dam is now classified as a Class II (significant) hazard potential dam, but was earlier classified as a Class III (low) hazard potential dam (URS 2005c). The dam safety guidelines suggest a range of return periods for each class of dam for the OBE and MDE level hazards to define different levels of seismic risk.

Seismic design guidelines, requirements and hazard maps have changed over time. The following sections summarize the seismic criteria used in the original Stage I to-VI design and later Stage VII-A and B raises. The seismic criteria for the future raises to closure design are presented in Section 7.1.

#### **4.4.2 Seismic Criteria used for Stages I to VI**

The seismic criteria for the Stage I to VI design was established (Dames & Moore, 1986 and 1987b) based on the National Research Council (NRC 1983) seismic hazard map. At the time of design, the dam was rated as a Class III (low) hazard potential dam. The OBE and MDE levels of design earthquake were used. Peak ground accelerations (PGA) were obtained from the NRC map as follows:

- **OBE:** A 475-year seismic event with a 10% probability of being exceeded in 50 years was established as the OBE seismic hazard. The bedrock PGA for the OBE level seismic event was obtained from the hazard maps as 0.05g.
- **MDE:** The bedrock PGA corresponding to the MDE level seismic event was established as 0.10g. The MDE level event was taken as an earthquake with a return period of 10,000 years.

This MDE level earthquake has often been assumed to be the MCE (NRC, 1983), as this terminology was repeated in the Dames & Moore (1986) design report that presented the stability analysis of the original Stage I to VI dam design.

The amplification of the bedrock PGA was not considered and the PGA at the dam-ground interface was taken as the bedrock PGA.

The Dames & Moore (1986, 1987b and 1999) seismic stability analyses used a pseudo-static approach with reduced undrained shear strength and constant seismic lateral force associated with a horizontal seismic coefficient equal to the bedrock PGAs described above for the OBE and MDE. The seismic criteria used for the stability analysis and design of Stage I to VI are summarized in Table 4-2.

**Table 4-2 – Summary of Seismic Criteria for Stages I to VII-B**

Stage	PGA at Bedrock (g)		Seismic Coefficient		Source
	OBE	MDE	OBE	MDE	
I-VI	0.05	0.10	0.05	0.10	National Research Council (1983)
VII-A, VII-B	0.10	0.20	0.05	0.10	USGS (1999)

#### 4.4.3 Seismic Criteria used for Stages VII-A and B

Prior to the Stage VII-A and B raise design, the hazard potential of the dam was upgraded from low (Class III) to significant (Class II) hazard potential. URS (2002a and 2002b) updated the seismic criteria to reflect the newly applicable seismic requirements, hazard maps and codes. Bedrock PGA values were obtained from USGS hazard maps published for Alaska (Wesson et al, 1999), as follows:

- **OBE:** The dam safety guidelines (ADNR 2005) specify a return period for the OBE seismic hazard to range from 70 to 200 years. A 475-year seismic event with a 10% probability of being exceeded in 50 years was used as the OBE seismic hazard. The bedrock PGA for the OBE seismic event was obtained from the USGS seismic hazard maps (1999) as 0.10g.
- **MDE:** The dam safety guidelines (ADNR 2005) specify the return period for the MDE level seismic hazard to range from 1,000 to 2,500 years. A 2,475-year seismic event with a 2% probability of being exceeded in 50 years was used as the MDE seismic hazard. The bedrock PGA for the MDE level seismic event was obtained from the USGS seismic hazard maps (1999) as 0.20g.

The amplification of the bedrock PGA was not considered and the PGA at the dam-ground interface was taken as the bedrock PGA.

The seismic stability analyses for Stages VII-A and B (URS, 2002a and b) used a pseudo-static approach with reduced undrained shear strength and constant seismic lateral force associated with a horizontal seismic coefficient 50% of the PGAs described above for the OBE and MDE. This approach was based on studies that showed that earth dams with pseudo-static factors of safety greater than 1.0, obtained by using a seismic lateral force based on 50% of the PGA, will not develop large deformations (Hynes-Griffin and Franklin 1984, Kramer 1996, Washington State Department of Transportation (WSDOT) 2005). Seismic coefficients used for the stability analysis and design of Stages VII-A and B are summarized in Table 4-2.

#### 4.5 PHREATIC SURFACES

Phreatic surfaces within the tailings main dam and the tailings impoundment have a direct impact on stability analyses of the tailings main dam due to the following reasons:

- Effective stress is dependant on pore water pressure
- Unbalanced water pressures
- Impact on liquefaction potential of tailings

The drained shear strength of the soil and rock material is dependant on the effective stress, which reduces with a higher phreatic surface. Therefore, the stability of the tailings main dam would be adversely impacted with high phreatic surface within the dam.

Different water levels upstream and downstream of the dam result in unbalanced hydrostatic forces acting on the dam. Similarly, unbalanced hydrostatic forces will also act on the trial failure surfaces, resulting in lower a FS against instability of the dam.

The phreatic surface under the tailings beach upstream of the dam will directly impact the liquefaction potential of the tailings. Tailings above the phreatic surface would not be liquefiable, even if it meets other criteria for liquefaction. The liquefaction potential of the tailings is discussed in Section 7.2.

#### **4.5.1 Historical Records**

The phreatic surface in the protective rockfill part of the tailings main dam that is upstream of the liner and under the tailings is influenced by the presence and width of the tailings beach and water level in the impoundment. The tailings management practices and water levels have varied over time and are well documented. However, the changes in phreatic surface upstream of the liner have not been directly documented and have to be estimated from the seepage analysis models and piezometer data.

The phreatic surface conditions in and under the dam downstream of the liner have been documented by the underdrain piezometers P-8, P-9, and P-10 that are located along the critical section of the dam. The phreatic surface downstream of the liner was estimated from the historical data of underdrain piezometer readings collected and provided by TCAK as well as information presented in past reports (Dames & Moore 1987a and 1987b; URS 2005a; and Water Management Consultants 1999).

The highest piezometric water levels recorded along the critical cross section of the dam, downstream of the liner, are presented on Figure 4-5. The estimated phreatic surface along the Stage VI axis of the dam is presented on Figures 4-6 and 4-7, respectively.

#### **4.5.2 Phreatic Surface at Closure**

The historical records show that the phreatic surface in the dam and under the tailings beach depends on various conditions, of which the following are either controlled by design or operation of the dam at closure:

- Tailings impoundment level
- Tailings beach width
- Tail water conditions controlled by the pumpback system operations

Selection of the design phreatic surface for the final closure conditions should consider these factors along with the historical phreatic surface measurements in the dam. Selection of the design phreatic surface for the stability analyses of future raises to closure is presented in Section 7.3.

### **4.6 CONSTRUCTION IMPACT**

Stability of the tailings main dam might be impacted by construction activities at or near the dam. Activities such as fill placement, material hauling, compaction and blasting could generate excess pore pressures in the dam. Dissipation of excess pore water pressures in low permeability (hydraulic conductivity) materials will take longer than in high permeability materials. Such excess pore pressures reduce the shear strengths of the material because of lower effective stress, and thus impact the dam stability.

Generation of construction related excess pore pressures in the dam and foundation materials should be monitored and controlled to maintain dam stability during construction work. The excess pore pressure is dependant on the rate of fill (load) placement and rate at which the materials can dissipate the excess pore pressures. The pore pressure coefficient ( $R_u$ ) is the ratio of excess pore pressure to total overburden stress at a location to model pore pressure increases for use in the stability analysis.

The selection of representative pore pressure coefficient for the stability analysis of future raises to closure is presented in Section 7.4.

#### 4.7 LONG-TERM STABILITY

In developing the conceptual design, the closure condition is considered to last in perpetuity. In order to evaluate this long-term condition, a seepage sensitivity analysis was completed (URS 2007b), to consider an extreme worst case of the liner no longer functioning as an impervious barrier in the dam. This will result in a higher phreatic surface in the dam and reduced dam stability. Therefore, it may be necessary to increase the tailings beach width to improve the stability. The seepage analysis of this extreme case was completed with a 900-foot wide beach as described in Section 7.6.

### 5.0 ANALYSIS APPROACH

The objective of the stability analyses of the future raises to closure of the tailings main dam is to support the development of the closure plan and conceptual design of the raises. In order to accomplish this objective, three primary components of analyses are completed as follows:

- **Seismic Hazard Analysis:** A site specific probabilistic seismic hazard analysis (PSHA) was performed to define the seismic hazard at the dam and seismic criteria for future raises.
- **Stability Analysis:** A stability analysis was completed to determine the steepest stable downstream slope at closure that would ensure static and seismic stability of the dam.
- **Deformation Analysis:** A deformation analysis was completed to determine the maximum dam displacement due to a maximum seismic event that could reasonably be anticipated.

The analysis approach for each of these analyses is presented in the following subsections.

#### 5.1 SEISMIC HAZARD ANALYSIS

The site specific seismic hazards may be analyzed either deterministically or probabilistically to estimate the ground-shaking hazards at the site, as follows:

- **Deterministic Seismic Hazard Analysis (DSHA):** In a DSHA, the ground motion hazard evaluation is based on a particular earthquake scenario consisting of a postulated occurrence of an earthquake of a specified size occurring at a specified location (source). A typical DSHA includes the following four-step process.
  - Identify and characterize all seismic sources capable of producing significant ground motions at the site
  - Determine the distance from the source to the site (epicentral or hypocentral) for each source zone.
  - Select the controlling earthquake, expressed in terms of size and distance from the site.

- Define the seismic hazard in terms of ground motion (peak acceleration, peak velocity and response spectrum ordinates) produced at the site by the controlling earthquake.
- **Probabilistic Seismic Hazard Analysis (PSHA)**: In a PSHA, uncertainties in the size, location and rate of earthquake recurrence, and in the variation of ground motion characteristics with earthquake size and location are considered. A typical PSHA includes the following four-step process.
  - Identify and characterize all seismic sources capable of producing significant ground motions at the site
  - Characterize the earthquake recurrence relationships.
  - Determine the ground motion produced at the site using attenuation relationships.
  - Determine the probability of the ground motion parameter being exceeded during a particular time period, by combining the uncertainties in earthquake location, size, and ground motion parameter.

The use of DSHA was prevalent in the early years of geotechnical engineering. This approach presents a simple procedure to characterize the worst-case ground motions or largest magnitude at the closest distance, but provides no information on the likelihood of occurrence of the controlling earthquake. A significant advantage of DSHA is that it is not necessary to model every fault, earthquake, and ground motion record in detail. If an active fault crossed a site, a DSHA would be appropriate to examine the effect on the site due to fault movement.

A PSHA includes all deterministic events above a specified minimum magnitude with a finite probability of occurrence and provides a framework to identify and quantify uncertainties. The PSHA also provides a more complete picture of the seismic hazard through the integration of all identified uncertainties. Generally uncertainties are incorporated into a PSHA through probability distributions.

A PSHA is appropriate for the design of the future raises of the tailings main dam, which is located in a low seismic region. Specification of scenario earthquakes, as required in a DSHA, is arbitrary for regions where no active faults are identified, such as at the mine. Therefore, URS only performed a PSHA for the dam. Analysis details and results are presented in Section 6.0.

## 5.2 STABILITY ANALYSIS

The most commonly used slope stability analysis methods are based on a limit equilibrium approach. This approach was developed before the widespread use of computers, but with increased computer applications, it found wide use in analyzing slopes with complex geometry and characteristics such as, non-homogeneity, layered soils, various forms of external loads, and different groundwater conditions.

The limit equilibrium approach is primarily based on assumed failure surfaces. The stability of a slope along each assumed surface is evaluated by subdividing the failure mass into small slices. By satisfying equilibrium conditions along the edges of each slice, summations of driving and resisting forces are computed to obtain a FS.

A commercial two-dimensional (2D) slope stability analysis software, SLOPE/W, was used for the calculations based on a specific assumed failure surface. The approach assumes that mobilized shear strength at each slice along the failure surface is on the verge of failure at the same time. Several variations of this approach and varied assumptions are used to derive the slice equilibrium forces. The Modified Bishop, Simplified Janbu, and Spencer methods are more widely used and accepted.

More sophisticated stability analysis involves the use of 2D or 3D finite element (FEA) or finite difference (FDA) analysis approaches. These approaches are typically warranted when:

- The failure mechanisms are not well modeled by limit equilibrium techniques
- A detailed deformation analysis of the slope is required.

Slope failure mechanisms consist of circular, block or irregular failure surfaces. The weak gouge zones under the tailings main dam are a major factor in controlling critical failure surfaces for the dam stability. Hence, circular and block failure surfaces were considered for evaluating the dam stability by limit equilibrium analysis. The analyses were performed by the Spencer method using the commercially available software, "SLOPE/W", by GEO-SLOPE International Ltd., Calgary, Alberta.

The sensitivity of the FS for slope stability resulting from the factors outlined in Section 4 was reviewed. Analyses were conducted assuming block and circular failure surfaces under both static and seismic conditions.

The seismic stability was analyzed by a pseudo-static approach, in which the effect of seismic loading was represented by constant horizontal and vertical seismic coefficients. The seismic coefficients were selected as a fraction of the peak ground accelerations corresponding to the seismic hazard to represent the inertial forces resulting from horizontal and vertical accelerations caused by the design earthquake. The seismic criteria, selection of coefficients, and stability analysis are presented in Section 7.0.

### 5.3 DEFORMATION ANALYSIS

Excessive deformation in an embankment dam could result in either failure of the dam or one of its key components, and prevent it from performing its original functions after the seismic event. Therefore, seismically induced deformations of a dam are completed to ensure dam stability. Acceptable methods of estimating seismically induced embankment deformation include:

- **Newmark sliding block analysis:** Newmark (1965) sliding block analysis provided a simple approach to estimate seismic deformation of slopes and embankments. In this approach, the unstable soil mass is treated as a rigid block. The procedure for the Newmark sliding block analysis consists of the following three steps:
  - Identify the yield acceleration of the slope by completing limit equilibrium stability analysis. The yield acceleration is the horizontal seismic (pseudo-static) coefficient required to for a FOS of unity.
  - Select an earthquake time history representative of the design earthquake
  - Double integrate the difference in acceleration (acceleration time history and yield acceleration) that would cause permanent deformation.
- **Simplified charts approach based on Newmark Analysis:** Based on the Newmark sliding block analysis approach, simplified charts (Makdisi and Seed, 1978; Franklin and Chang, 1977; Martin and Qiu, 1994; Bray and Rathje, 1998) are used to estimate seismic deformation of slopes and embankments. These approaches estimate a range of permanent seismically induced embankment deformation and are widely used.
- **Dynamic stress-deformation models:** Dynamic stress-deformation computer models utilizing finite element or finite difference analysis tools (e.g., FLAC, PLAXIS, and DYNFLOW) are also used to estimate seismic deformation of slopes and embankments. This approach is typically used for complex projects and where an understanding of the mechanism of deformation is needed and a detailed deformation analysis is warranted.

This approach requires a constitutive model capable of modeling dynamic stress-deformation characteristics of soils.

Although a detailed dynamic stress-deformation model would provide a better and problem specific estimate for the tailings main dam, the use of simplified charts was considered adequate for the following reasons:

- The dam is located within a low seismic region
- The dam is constructed of highly permeable materials
- Excess pore-pressures generated during an earthquake will dissipate quickly.

URS completed the deformation analysis of the tailings main dam using a simplified charts based approach. Different chart approaches (Makdisi and Seed, 1978; Franklin and Chang, 1977; Martin and Qiu, 1994; Bray and Rathje, 1998) were used and the results were compared in selecting a reasonable permanent seismic deformation for the design of the future raises of the dam. The details of the deformation analysis are presented in Section 8.0.

## 6.0 SEISMIC HAZARD ANALYSIS

A site-specific PSHA was performed for the Red Dog Mine site, located at approximately 68.128°N and 162.944°W. The objective of the PSHA was to compute site ground motions that had 10% and 2% probabilities of being exceeded in 50 years. These ground motions have corresponding average return periods of 475 years and 2,475 years, respectively.

URS conducted the PSHA for the tailings main dam by building off a seismic hazard analysis that was completed in 2002 for a confidential project in Alaska, for which URS developed a PSHA model for the entire state of Alaska. The 2002 PSHA model was updated by completing the following:

- Review of the seismicity recorded in the mine site region since the 2002 study
- Determination of whether the seismic activity rate had changed significantly
- Review and update of the attenuation equations used by URS in 2002.

Using the updated PSHA model for Alaska, a seismic hazard analysis was completed for the tailings main dam site. Details of the model, analysis and results are described in the following sections. Three earthquake magnitude symbols are used:

- $M$  – generic magnitude that encompasses the various magnitude scales.
- $M_w$  - moment magnitude scale.
- $M_s$  – surface wave magnitude scale.

The  $M_w$  scale is used in the PSHA because the attenuation equations, key inputs to this analysis, were developed for  $M_w$ . This magnitude is more indicative of the actual physical size of the earthquake, and it is computed from the formula,  $M_w = (2/3) (\log M_o - 16.05)$ , where  $M_o$  is the seismic moment of the earthquake in dyne-cm. The seismic moment is given by  $M_o = \mu A s$ , where  $\mu$  is the fault rigidity (dyne/cm<sup>2</sup>),  $A$  is the fault-rupture area (cm<sup>2</sup>), and  $s$  is the average slip displacement (cm) on the fault.

The  $M_s$  is a magnitude scale based on the amplitude of Rayleigh waves with a period of about 20 seconds. This scale was developed during the early part of the 20th Century and predates the  $M_w$  scale, which was developed in 1979. Thus, magnitudes of large earthquakes occurring prior to 1979

were often reported as  $M_s$ , but for many of these events, the  $M_s$  values were converted to  $M_w$  by seismologists, who also developed empirical formulas to convert various other magnitudes, such as  $M_L$  (local) and  $m_b$  (body-wave), to  $M_w$ .

## 6.1 REGIONAL TECTONIC SETTING

The major tectonic features of central and southern Alaska are the strike-slip Denali fault which generated a moment magnitude  $M_w$  7.9 earthquake in November 2002, and the Aleutian megathrust, which generated an  $M_w$  9.2 earthquake in March 1964. However, in northern Alaska, most tectonic activity is inferred to have occurred during the accretion of terranes comprising the region, and most do not exhibit evidence of Quaternary-age displacement (Plafker et al., 1994).

Active faults are not known to exist in the Red Dog site region, and the seismicity rates are fairly low.

## 6.2 REGIONAL SEISMICITY

Maps of the regional seismicity are shown in Figures 6-1, 6-2 and 6-3. These maps were taken from the 2002 URS study which was completed before the  $M_w$  7.9 earthquake in November 2002:

- Figure 6-1 shows the epicenters (color circles) of earthquakes in the state. The size of the circle is proportional to magnitude and the color code indicates the magnitude range.
- Figure 6-2 contains the same epicenters color coded by focal depth
- Figure 6-3 resents the subset of events from Figure 6-1 of magnitude,  $M \geq 6$ .

These three epicenter maps reveal that the Red Dog region is characterized by relatively small ( $M < 6$ ) infrequent earthquakes of shallow focal depth. The largest  $M \geq 6$  event closest to the mine was an  $M_w$  6.1 earthquake on May 13, 1971, that occurred approximately 155 miles south of Red Dog. The closest event of  $M \geq 7$  occurred on April 7, 1958, as an  $M_s$  7.3 with an epicenter approximately 250 miles southeast of Red Dog near the east-west trending, late Quaternary Kobuk fault.

## 6.3 SIGNIFICANT SEISMIC SOURCES

The seismic sources that URS developed for the 2002 project are shown in Figure 6-4. Of these sources, only the Brooks Range is significant to Red Dog because it is considered capable of generating site ground motions at levels of engineering interest. The Brooks Range is characterized by low historical seismicity and lack of late Pleistocene or Holocene age tectonic structures (Page et al., 1991; Plafker et al., 1994). However this region contains numerous east-west trending reverse faults favorably oriented relative to the north-south compressive stress regime of the region.

Therefore, these faults, and perhaps others that may exist in the Red Dog area, could generate significant but relatively infrequent strong ground motion at the dam site. Because of the faulting within this zone, the Brooks Range is distinguished as a separate zone from the North Slope with a potential for a slightly higher maximum moment magnitude,  $M_{MAX}$ , which was selected as 6.5.

## 6.4 SITE GEOTECHNICAL CONDITIONS

Geotechnical conditions at the tailings main dam are described in the URS (2006) geotechnical investigation report. The general subsurface conditions are fill and native soil overburden over shale and siltstone bedrock. Native soils include up to several feet of near-surface peat and organics, till,

alluvium, and/or colluvium. In some locations, the native soil is overlain by fill. The bedrock typically is highly to moderately weathered shale, which becomes more competent with depth.

The “Site Class” for the tailings main dam site was established based on the average soil properties in the top 100 feet of the soil profile (Section 1615.1.5, IBC 2003). In accordance with the definitions presented in Table 1615.1.1, IBC 2003, a “Site Class C, Very Dense Soil and Soft Rock Profile” represents the subsurface conditions at the tailings dam site.

## 6.5 PROBABILISTIC SEISMIC HAZARD ANALYSIS

The analytical model used for the PSHA is based on probabilistic models developed by Cornell (1968) and Der Kiureghian and Ang (1975), and is consistent with those used by the U.S. Geological Survey (USGS). The basic assumption of these models is that the occurrence of earthquakes in space and time within a particular seismic zone is completely random (i.e., a Poisson process). This type of model is used worldwide for seismic hazard analyses of important facilities and is used by URS for seismic studies in Alaska.

### 6.5.1 Probabilistic Hazard Model

The two basic components of the probabilistic hazard model are:

- **Seismic source models:** These models specify spatial, temporal, and magnitude distributions of earthquake occurrences expected in each of the seismic sources.
- **Ground-motion attenuation models:** These models determine the distribution of ground motions expected at a site for a potential earthquake occurrence (characterized by magnitude and location, and other factors) on a seismic source.

These components comprised the inputs to the PSHA. Probability-of-exceedance rates were computed for a range of horizontal ground motions, which were expressed in terms of peak ground acceleration (PGA) and 5 percent-damped pseudo absolute spectral accelerations (PSA) at 9 oscillator periods (T) of 0.00, 0.05, 0.10, 0.20, 0.30, 0.50, 0.75, 1.0, and 2.0 seconds.

Uniform probability spectra corresponding to probabilities of exceedance of 10% in 50 years and 2% in 50 years (or equivalently, average return periods of 475 years and 2,475 years) were then computed. Computation details, results and comparisons with USGS results are provided in Sections 6.6 to 6.8.

### 6.5.2 Seismic Source Models

The following three types of seismic sources were included in the URS 2002 PSHA model for Alaska:

- Aleutian and Yakataga Gap Megathrust Interplate subduction zones
- Aleutian Megathrust and Wrangell Intraplate subduction zones
- Shallow crustal faults and seismic zones.

Subduction sources locations are shown as dashed lines in Figure 6-4, and shallow crustal source locations are shown as solid lines. A planar representation of the Aleutian Megathrust Interplate source placed at a depth of 12.5 miles (20 km) was selected as an approximation of this source for the PSHA. This smaller depth is inconsequential to the PSHA. The distance measure used in the probability calculation for the greatest earthquake on this source is the closest distance to the site.

The Aleutian Intraplate zone in Figure 6-4 dips down to the northwest to approximate the dip of the Wadati-Benioff zone. The east edge of the zone is approximately 22 miles (35 km) deep, and the west edge is approximately 94 miles (150 km) deep. The Wrangell Intraplate zone dips down to the northeast. The south edge of the zone is approximately 25 miles (40 km) deep, and the north edge is approximately 67 miles (100 km) deep. For simplicity in the PSHA model, both the Aleutian and Wrangell Intraplate zones are modeled as dipping rectangles.

The shallow crustal faults in the URS Alaskan PSHA model include the Tintina, Kaltag, Denali, Castle Mountain, and Montague Island-Rude River. These faults were modeled as line sources capable of generating characteristic maximum moment magnitude earthquakes at specified annual recurrence rates.

The areal seismic zones are also in the shallow crust, and are shown in Figure 6-4. Three of these zones are relatively narrow and contain the Kaltag, Tintina, and Denali faults. Because of the similar rates of seismicity in the Cook Inlet-Kenai-Talkeetna Mountains zone and Prince William Sound-Chugach Mountains-Copper River Basin zone, these two zones were combined into one areal seismic zone for the PSHA, as shown in Figure 6-4.

The Brooks Range areal seismic zone is the only significant source to the seismic hazard at the Red Dog Mine site. Nevertheless, all sources were retained in the model for completeness.

#### *6.5.2.1 Earthquake Recurrence Models*

Earthquake recurrence equations for the seismic source zones were derived from either the historical seismicity or geologic data, whichever was considered more appropriate. The recurrence equation for the Aleutian Megathrust was based on the historical seismicity still remaining in the Interplate and Intraplate portions of this source zone after exclusion of the 1964  $M_w$  9.2 event, and its aftershocks from the database. The reasons for excluding these events from the analysis are explained below.

Geologic studies of the Copper River delta area (Plafker et al., 1992; Dames & Moore, 1991a) indicate that the recurrence time of great megathrust earthquakes in the Prince William Sound region is  $720 \pm 200$  years. Analyses by Donovan, Tang, and Wen and Tang (in Dames & Moore, 1991b) showed that the likelihood of a repeat event similar to the 1964 earthquake is very small (probability  $< < 10^{-4}$ /year in the next 100 years). Therefore, it is not necessary to include this type of event in the hazard analysis for computing ground motions with annual probabilities of  $10^{-4}$  or greater (Dames & Moore, 1991b).

The smallest annual ground-motion probability of interest for the tailings main dam is  $4 \times 10^{-4}$ . Therefore, the possible but extremely unlikely recurrence of a great earthquake on the Aleutian megathrust was not included in the seismic source model for the dam because it would have no effect on the ground-motion results.

The foreshocks and aftershocks of the  $M_w$  9.2 event were excluded because of their association with this earthquake. The remaining seismicity within the Aleutian Megathrust was used to develop the recurrence curves for the Interplate and Intraplate regions. In developing this recurrence equation (as well as recurrence equations for other sources) from the historical seismicity, the following completeness intervals were selected (Mueller et al., 1997).

<u>Time Interval</u>	<u>Moment Magnitude Interval</u>
1964 – 2000	$4.5 \leq M_w < 6.0$
1930 – 2000	$6.0 \leq M_w < 7.0$
1897 – 2000	$7.0 \leq M_w < 8.0$

Within these time intervals, the recording of earthquakes in the associated moment magnitude intervals is considered complete. The recurrence equation based on the historical seismicity, and data to which the equation is fit, are plotted in Figure 6-5 for the Brooks Range, which is the key seismic source for the tailings main dam. The lack of seismicity in the Brooks Range since 2000 indicates that the straight-line recurrence curve for this zone in Figure 6-5 is sufficient. The vertical axis in Figure 6-5 is the annual number of events (N) of moment magnitude  $\geq M_w$  in the Brooks Range on Figure 6-4.

**Table 6-1: Seismicity-based Recurrence Equations in PSHA**

Source Zone	Modeled Area-km <sup>2</sup>	Recurrence Equation Parameters		Maximum Moment Magnitude, $M_{MAX}$
		a	b	
North Slope	28,750	2.081	1.000	6.25
Brooks Range	70,200	4.450	1.164	6.50
Kobuk-Koyukuk	16,500	3.458	1.000	7.00
Dall Mtn.-Rampart	10,125	2.234	0.667	6.75
Kaltag	4,000	3.703	1.000	6.50
Minto	9,900	3.286	0.862	6.25
Fairbanks	6,000	2.511	0.731	6.00
Salcha	6,750	2.952	0.882	6.00
Tintina	8,100	2.265	0.823	6.50
Yukon Flats	16,800	3.193	1.002	6.25
Canning-Camden-Bay	1,5000	3.233	1.000	7.00
Kuskokwim	8,500	2.388	0.879	7.25
Denali	22,425	1.881	0.723	7.00
Yukon-Tanana Upland	45,825	3.421	1.000	7.25
CI, K, TM, PWS, CM, CRB	111,300	2.805	0.676	7.50
Aleutian Interplate Megathrust	120,000	3.103	0.672	7.75
Aleutian Intraplate Megathrust	15,285	4.476	0.980	7.50
Wrangell Intraplate	28,311	4.301	1.134	7.25

CI = Cook Inlet, K = Kenai, TM = Talkeetna Mountains, PWS = Prince William Sound, CM = Chugach Mountains, CRB = Copper River Basin

The recurrence equations for this and the other areal seismic sources are given by the formula:

$$\log(N) = a - bM_w \quad (6-1)$$

where  $a$  and  $b$  are constants. The actual source zone areas modeled in the PSHA are different from the areas in Figure 6-4 due to the rectilinear shape of the modeled areas. For some larger zones, the model areas were reduced to exclude areas that do not contribute to the ground-motion hazard and reduce the run time of the PSHA program. The  $a$  values were modified to reflect the actual area for each zone in the model. The recurrence curves based on the historical seismicity are summarized in Table 6-1.

A recurrence equation was not developed for the intracycle seismicity associated with the Yakataga Gap megathrust because of the low rate of activity in this zone and the large distance from the zone to Red Dog. A large characteristic earthquake was assumed as described in Dames & Moore (1991a, b).

Recurrence rates for the characteristic magnitudes of discrete faults (Castle Mountain, Denali, Kaltag, Tintina, Montague Island-Rude River), and the Minto, Fairbanks, and Salcha faults, are summarized in Table 6-2.

**Table 6-2: Annual Recurrence of Characteristic Earthquakes**

Source	Maximum Moment Magnitude ( $M_{MAX}$ )	Annual Recurrence
Kaltag Fault	7.5	0.00020 (= 1/5000 yrs)
Tintina Fault	7.5	0.00020 (= 1/5000 yrs)
Denali Fault	8.0	0.00143 (= 1/700 yrs)
Montague Is. – Rude R. Fault Zone	7.75	0.00057 (= 1/1750 yrs)
Castle Mountain Fault	7.5	0.00077 (= 1/1300 yrs)
Minto Zone	7.5	0.00083 (= 1/1200 yrs)
Fairbanks Zone	7.25	0.00083 (= 1/1200 yrs)
Salcha Zone	7.25	0.00083 (= 1/1200 yrs)

The maximum moment magnitudes in Tables 6-1 and 6-2 were estimated, except for the great earthquake in the Yakataga Gap, based on the historic seismicity and the lengths of faults. The maximum moment magnitude for the Yakataga Gap was based on the area of the source zone.

### 6.5.3 Attenuation Equations

In the PSHA for the B/C boundary (bedrock), the attenuation equations and associated parameter values and weights (Table 6-3) were incorporated into the computational model.

**Table 6-3: Attenuation Equations for PSHA**

Source-type	Equations	Parameters	Wt.
Subduction Interplate	Youngs et al. (1997) - rock	$Z_T = 0$	1.0
Subduction Intraplate	Youngs et al. (1997) - rock	$Z_T = 1$	1.0
Shallow Crustal Area and Fault Sources	Abrahamson & Silva (1997)	$S = 0; F = 0, 0.5, \text{ or } 1; HW = 0$	1/3
	Campbell & Bozorgnia (2003)	$S_{VFS} = 0; S_{SR} = S_{FR} = 0.5; F_{RV} \text{ and } F_{TH} = 0, 0.25, \text{ or } 0.5; \delta = 45 \text{ or } 90 \text{ km}$	1/3
	Boore et al. (1994)	$V_s = 760 \text{ m/s}; G_{SS} = 0 \text{ or } 1; G_{RS} = 0 \text{ or } 1$	1/3

The parameter definitions for each equation are given Subsections 6.5.3.1 through 6.5.3.4.

#### 6.5.3.1 Abrahamson and Silva (1997)

The basic form of the attenuation equations derived by Abrahamson and Silva is:

$$\ln Y = f_1(M_w, r) + Ff_3(M_w) + HWf_4(M_w, r) + Sf_5(\overline{pga}_{rock}) \quad (6-2)$$

where:	$Y$	=	5% damped spectral acceleration in g
	$M_w$	=	moment magnitude
	$r$	=	closest distance from site to fault rupture in km
	$F$	=	fault type (1 for reverse, 0.5 for reverse/oblique, and 0 otherwise)
	$HW$	=	dummy variable for hanging wall sites (1 for sites over wall, 0 otherwise)
	$S$	=	dummy variable for site class (0 for rock or shallow soil, 1 for deep soil)
	$\overline{pga}_{rock}$	=	expected value of peak ground acceleration on rock
	$f_i$	=	functions given in Abrahamson and Silva (1997)

### 6.5.3.2 Campbell and Bozorgnia (2003)

The form of the Campbell and Bozorgnia equations for horizontal and vertical components is

$$\ln(Y) = c_1 + f_1(M_w) + c_4 \ln \sqrt{f_2(M_w, R, S)} + f_3(F) + f_4(S) + f_5(HW, F, M_w, R) \quad (6-3a)$$

$$f_1(M_w) = c_2 M_w + c_3 (8.5 - M_w)^2 \quad (6-3b)$$

$$f_2(M_w, R, S) = R^2 + [c_5 + c_6 (S_{VFS} + S_{SR}) + c_7 S_{FR}]^2 \cdot (\exp[c_8 M_w + c_9 (8.5 - M_w)])^2 \quad (6-3c)$$

$$f_3(F) = c_{10} F_{RV} + c_{11} F_{TH} \quad (6-3d)$$

$$f_4(S) = c_{12} S_{VFS} + c_{13} S_{SR} + c_{14} S_{FR} \quad (6-3e)$$

$$f_5(HW, F, M_w, R) = HW \cdot f_3(F) f_{HW}(M_w) f_{HW}(R) \quad (6-3f)$$

where:	$Y$	=	5% damped pseudo absolute spectral acceleration for horizontal or vertical components in g
	$M_w$	=	moment magnitude
	$R$	=	closest distance in km from site to seismogenic portion of the rupture
	$S_{VFS}$	=	index site geologic variable (1 for very firm soil, 0 otherwise)
	$S_{SR}$	=	index site geologic variable (1 for soft rock, 0 otherwise)
	$S_{HR}$	=	index site geologic variable (1 for hard rock, 0 otherwise)
			( $S_{VFS} = S_{SR} = S_{HR} = 0$ signifies firm soil)
	$F_{RV}$	=	index fault-type variable (1 for reverse, 0 otherwise)
	$F_{TH}$	=	index fault-type variable (1 for thrust faulting, 0 otherwise)
			( $F_{TH} = F_{RV} = 0$ for strike-slip and normal faulting)
	$HW$	=	0, for $r_{jb} \geq 5.0$ km and $\delta > 70^\circ$

$$\begin{aligned}
& (S_{VFS} + S_{SR} + S_{HR})(5 - r_{jb}), \quad \text{for } r_{jb} < 5.0 \text{ km and } \delta \leq 70^\circ \\
f_{HW}(M_w) &= 0, \text{ for } M_w < 5.5 \\
& M_w^{-5.5}, \quad \text{for } 5.5 \leq M_w \leq 6.5 \\
& 1, \quad \text{for } M_w > 6.5 \\
f_{HW}(R) &= c_{15}(R/8), \quad \text{for } R < 8.0 \text{ km} \\
& c_{15}, \quad \text{for } R \geq 8.0 \text{ km} \\
f_i &= \text{functions given in Campbell and Bozorgnia (2003)} \\
c_i &= \text{coefficients from regression analysis}
\end{aligned}$$

### 6.5.3.3 Boore et al. (1994)

The Boore et al. equations for horizontal components only were derived mostly from California strong motion data recorded from 1940 through 1992. Their database is provided in Boore et al. (1993). The Boore et al. (1994) equations are given by

$$\log(Y) = b_{ss} G_{ss} + b_{rs} G_{rs} + b_2 (M_w - 6) + b_3 (M_w - 6)^2 + b_4 r + b_5 \log(r) + b_v \log(V_s / V_A) \quad (6-4a)$$

$$r = \sqrt{(r_o^2 + h^2)} \quad (6-4b)$$

where:

$Y$	=	peak ground acceleration - PGA, or 5% damped pseudo-velocity response spectra – PSV
$G_{SS}$ and $G_{RS}$	=	fault type (for strike slip faults, $G_{SS} = 1$ and $G_{RS} = 0$ ; for reverse slip faults, $G_{SS} = 0$ and $G_{RS} = 1$ )
$M_w$	=	moment magnitude
$r_o$	=	the shortest distance (km) from the recording site to the vertical projection of the earthquake fault rupture on the surface of the earth
$V_A$	=	reference shear-wave velocity in Boore et al. (1994)
$V_s$	=	site shear-wave velocity
$b_{SS}, b_{RS}, b_i, h$	=	coefficients from regression analysis

### 6.5.3.4 Youngs et al. (1997)

The Youngs et al. rock equations have the following form:

$$\ln(Y) = a_1 + f_1(M_w) + a_2 \ln(r + a_1 \exp(a_4 M_w)) + a_5 H + a_6 Z_T \quad (6-5)$$

where:

$Y$	=	peak ground acceleration or 5% damped spectral acceleration in g
$M_w$	=	moment magnitude
$r$	=	closest distance to source rupture in km
$H$	=	focal depth in km
$Z_T$	=	source-type index variable (0 for interface or interplate, 1 for intraslab or intraplate)

$f_l(M_w)$  = function of moment magnitude given in Youngs et al. (1997)  
 $a_i$  = coefficients from regression analysis

## 6.6 COMPUTATIONS OF MEAN GROUND MOTION

For each shallow crustal area and fault source, the PSHA code computes a hazard curve that is a weighted average of curves computed for each of the three selected attenuation equations (Abrahamson and Silva, Campbell and Bozorgnia, and Boore et al.). The averages are computed for ground-motion levels specified in the input file. The last column of Table 6-3 lists 1/3 as the weight applied to each of the three equations, so that each equation was considered equally valid. Averaging is reasonable for the subduction sources because only one attenuation equation (Youngs, et al.) is used.

The lognormal distribution about the median values predicted by each attenuation equation was included in the computation. This distribution was not truncated at any standard deviation level above the median level, as is sometimes done in PSHA determinations.

The effect of fault-rupture size on the calculation of exceedance probabilities was included in the PSHA. Invoking this option within the PSHA program results in the measurement of source-to-site distances to the point on the rupture that is closest to the site, which is consistent with the definition of the distance term in the attenuation equations.

## 6.7 RESULTS

The PSHA outputs for the tailings main dam site were 475-year and 2,475-year horizontal-component response spectra at 5% damping ratio as summarized in Table 6-4. The response spectrum describes the maximum response of a single degree of freedom (SDOF) system to a particular input motion as a function of the natural frequency and damping ratio of the SDOF system. The zero-period ordinates of these spectra are the PGA values. The Table 6-4 response spectra apply to a generic bedrock, defined as the boundary between Site Classes B and C (B/C boundary). The bedrock response spectra results are shown in Figure 6-6.

Section 6.4 describes how the “Site Class” for the tailings main dam was established as “Site Class C, Very Dense Soil and Soft Rock Profile”. Factors to convert the bedrock spectra to spectra corresponding to Site Class C were computed from the  $F_a$  and  $F_v$  factors in Tables 1615.1.2 (1) and (2) of IBC (2003). The product of these factors and the B/C boundary spectra yielded the response spectra (Table 6-5) for Site Class C. The response spectra for the tailings dam site are in Figure 6-7.

**Table 6-4: Five Percent Damped Uniform Probability Spectral Accelerations in g for Bedrock**

Period, T (sec)	10% in 50 yrs. (g)	2% in 50 yrs. (g)
0.00	0.077	0.182
0.05	0.098	0.250
0.10	0.136	0.368
0.20	0.165	0.413
0.30	0.141	0.338
0.50	0.096	0.212
0.75	0.067	0.137
1.00	0.053	0.105
2.00	0.030	0.059

**Table 6-5: Five Percent Damped Response Spectral Accelerations in g for Site Class C**

Period, T (sec)	10% in 50 yrs. (g)	2% in 50 yrs. (g)
0.00	0.084	0.198
0.05	0.107	0.273
0.10	0.148	0.401
0.20	0.179	0.451
0.30	0.154	0.369
0.50	0.113	0.249
0.75	0.084	0.172
1.00	0.066	0.132
2.00	0.038	0.074

## 6.8 COMPARISON WITH USGS VALUES

The 2% in 50 year PSHA results of this study for PGA were compared with the corresponding USGS values that were computed by Wesson et al. (2005), which is yet to be adopted by national and local codes. The comparison is provided in Table 6-6.

**Table 6-6: Comparison of Bedrock PGA (g) Results from This Study and USGS**

Probability Level	This Study	USGS
10% in 50 years	0.077	0.10
2% in 50 years	0.18	0.23

The reason that the results of this study are lower than those of the USGS is believed to be primarily due to the following differences:

- The historical seismicity are treated differently
- $M_{MAX}$  values are different.

USGS did not delineate shallow crustal areal source zones as URS did for the tailings main dam. USGS assumed that the seismic activity in a region was similar to the spatial density of seismicity defined by the historical record. Some spatial smoothing of the seismicity was employed by USGS to

reduce the impact on their PSHA of concentrations or absence of seismicity in certain areas. However, the resulting spatial density of epicenters in the site region was still higher than the average for the Brooks Range. The USGS also used a  $M_{MAX}$  of 7.3 for the region (Wesson et al, 2005).

On the other hand, the URS study for the tailings main dam assumed that the activity rate was uniform within a given areal seismic source zone. This rate was determined from historical seismicity within the zone, and thus the activity rates among the various zones varied according to each zone's historical seismicity record. The  $M_{MAX}$  used in this study varied depending on the seismic source. In the Brooks Range seismic source zone, where the site is located, the  $M_{MAX}$  was selected as 6.5 (Table 6-1).

## 7.0 STABILITY ANALYSIS

URS completed a 2D pseudo-static stability analysis of the tailings main dam to evaluate the feasibility of future raises to closure and to determine the steepest stable downstream slope for the raises assuming that they are built by downstream construction methods. The seismic criteria, liquefaction potential, phreatic surface, pore-pressure coefficient, stability analyses and special sensitivity analyses are discussed in the following sections.

### 7.1 SEISMIC CRITERIA

The hazard potential of the tailings main dam for the future raises to closure remains at the increased hazard level, significant hazard potential (Class II). The design level earthquakes defined in Section 4.4.1 were selected based on the Alaska dam safety guidelines (ADNR, 2005) as follows:

- **OBE:** An earthquake with 10% probability of exceedance in 50 years (i.e. return period of 475 years).
- **MDE:** An earthquake with 2% probability of exceedance in 50 years (i.e. return period of 2475 years).

ADNR (2005) defines the MDE as “represents the ground motions or fault movements from the most severe earthquake considered at the site, relative to the acceptable consequences of damage in terms of life and property”. The MCE is defined as “the greatest earthquake that reasonably could be generated by a specific seismic source, based on seismological and geologic evidence and interpretations”. The return period selected for the MDE should correlate with the magnitude of the MCE for the known or suspected regional sources, dam type, size and geometry, and impoundment capacity.

ADNR (2005) provides a 1,000 to 2,500-year range for return periods of 70 to 200 years for a Class II dam. Therefore, the selection of a 2,475 year return period seismic event for MDE is conservative.

Bedrock (Site Class B/C interface) and ground (Site Class C) PGA values for OBEs and MDEs from the USGS (2005) hazard map and URS PSHA are summarized in Table 7-1. The conversion of USGS bedrock PGA values (Site Class B/C) to surface PGA values (Site Class C) was computed as 1.09 from the  $F_a$  factors in Table 1615.1.2 (1) of the International Building Code (IBC, 2003).

**Table 7-1 – Seismic Hazard for Tailings Main Dam**

Source	Peak Bedrock Acceleration (g) <sup>1</sup>		Peak Ground Acceleration (g) <sup>1</sup>	
	OBE	MDE	OBE	MDE
USGS (2005)	0.10	0.23	0.11	0.25
URS PSHA	0.077	0.18	0.084	0.20

**Note:**<sup>1</sup> Acceleration values rounded to two significant digits

Figures 7-1 and 7-2 show the 2005 USGS seismic hazard maps for Alaska. The PGAs from the 2005 USGS hazard maps are higher, and were conservatively selected for the stability analysis as follows:

- **OBE:** The PGA corresponding to OBE level seismic event is 0.11 g.
- **MDE:** The PGA corresponding to MDE level seismic event is 0.25 g.

The prevailing practice (WSDOT 2005) for pseudo-static stability analyses is based on studies that show that earth dams with pseudo-static FS greater than 1.0, obtained by using a seismic lateral force with 50% of the PGA, will not develop large deformations (Hynes-Griffin et. al, 1984; Kramer, 1996).

Hynes-Griffin et. al provided amplification factors for considering dam crests compared to input accelerations at the base, to identify dams that could have unacceptable deformations. They suggested using one-half the bedrock acceleration applied to the dam crest with an acceptable FS greater than 1.0 and up to 20% reduction on material strengths to account for pore pressure generation. The assessment was limited to earthquakes of M less than 8.0 with non-liquefiable materials in the dam embankment.

Based on the standard of practice for pseudo-static stability analysis, the seismic coefficients for the future raises to closure design were taken as 50% of the surface PGA values in Table 7-1, as follows:

- **OBE:** The seismic coefficient corresponding to OBE level seismic event is 0.055.
- **MDE:** The seismic coefficient corresponding to MDE level seismic event is 0.125.

## 7.2 LIQUEFACTION POTENTIAL OF TAILINGS

The liquefaction potential of the tailings was evaluated using the cone penetration tests performed on the tailings (ConeTec, 2000), tailings properties summarized in the geotechnical reports (Dames & Moore, 1986 and 1987b; Golder, 2003; and URS, 2006) and the updated seismic criteria presented in Section 7.1, for the future raises to closure.

### 7.2.1 Selection of Earthquake Magnitude

The earthquake magnitude was estimated using probabilistic seismic hazard deaggregation maps for Alaska, developed by USGS (1996) from the 1996 USGS seismic hazard map. Deaggregation maps for OBE and MDE hazard levels at the tailings main dam site are on Figures 7-3 and 7-4. The modal magnitude of the deaggregation model is considered as the most probable earthquake magnitude. The most probable moment magnitude for OBE and MDE hazards is estimated to be 5.23. The corresponding Magnitude Scaling Factor (MSF) is 2.5 based on revised Idriss values in Youd et al. (2001).

## 7.2.2 Liquefaction Evaluation

The liquefaction evaluation of the tailings was performed by using commercially available LiquefyPro software. The evaluation was completed using the data collected from two CPT tests (ConeTec, 2000) on tailings. The CPT tests were completed to depths of 79.15 and 59.55 feet. Estimated depths of ground water at these locations were 13 and 15 feet, respectively.

The liquefaction evaluation was completed based on the modified Robertson approach (1997) using the CPT data. The evaluation was also repeated using the Youd et al. (2001) approach based on equivalent  $(N1)_{60}$  reported by Conetec, Inc (2000).

The results from the liquefaction evaluation indicate that the tailings will not liquefy for the OBE and MDE seismic levels. The evaluation was repeated for  $M_w$  6.0, the approximate mean value from the deaggregation plots. For  $M_w$  6.0, the tailings were found to be non-liquefiable for the OBE level. For the MDE, a relatively thin (less than 3 to 4-foot thick) layer of tailings was found to be liquefiable.

The liquefaction evaluation was completed for the water table conditions found by the CPT tests. For the closure condition, a wide tailings beach is being planned to reduce the seepage and improve stability. The phreatic surface under such a beach would be much lower at the upstream face of the dam. Since soil above the phreatic surface would not liquefy, a wide tailings beach reduces any zones of potential liquefaction in the tailings.

Based on the liquefaction analysis results and observations noted, URS concludes that the liquefaction potential of the tailings is low.

## 7.3 DESIGN PHREATIC SURFACE FOR CLOSURE

The phreatic surface in the tailings main dam is discontinuous due to the presence of the geomembrane part of the liner system that provides a seepage barrier parallel to the upstream slope of the dam. The phreatic surface, upstream and downstream of the liner, influences the dam stability.

In ideal conditions, the seepage analysis results can be used to estimate this upstream phreatic surface. However, the seepage analysis (URS, 2007b) models were developed based on simplified assumptions and the results reflect unique and average conditions that exist or were assumed. It is prudent to use a reasonable but worst case phreatic surface for the stability analyses of the future raises. Although future conditions could not be predicted with certainty, the design phreatic surface was estimated based on engineering judgment and review of the following information:

- Historical instrumentation data from piezometers, thermistors and pumpback.
- Dam configuration at closure
- Impoundment water level at closure
- Presence of a tailings beach and its width at closure.

The selections of upstream and downstream phreatic surfaces are presented in the following sections.

### 7.3.1 Upstream Phreatic Surface

The upstream phreatic surface will significantly impact the stability of the upstream slope of the dam and the liquefaction potential of the tailings. The upstream phreatic surface is primarily dependant on the tailings impoundment water level and width of the tailings beach.

The conceptual design being considered includes a tailing beach wider than 600 feet alongside the dam crest. The presence of this beach will lower the phreatic surface upstream of the liner as shown by the seepage analysis (URS, 2007c). However, the design upstream phreatic surface was conservatively selected as El 980.2 to correspond to the maximum tailings water elevation for the following reasons:

- For the future raises to closure dam configurations and tailings levels, the upstream slope of the dam is more stable than for configurations through Stage VII-B.
- The beach effect could be somewhat compromised because of preferential seepage paths in the tailings and surface soils under the impoundment and beach.
- This simplification eliminates uncertainties associated with predicting a reasonably accurate phreatic surface resulting from the beach effect.

### 7.3.2 Downstream Phreatic Surface

The downstream phreatic surface would have a significant impact on the stability of the upstream and downstream slopes of the dam. The downstream phreatic surface is complex due to characteristics of the dam and its surroundings as described in the seepage analysis report (URS, 2007c). For the 2D slope stability analyses, the downstream phreatic surface along the critical section of the dam was established, based on a review of the historical data, closure conditions, and engineering judgment.

Piezometer, thermistor and pumpback data along with tailings management practices from 1997 to 2006 were reviewed for the selection of the design phreatic surface. Thermistor records along with piezometer records were used to confirm that rock in the vicinity of these piezometers remained above freezing (32°F), and groundwater level readings could be relied upon.

Dam instrumentation (URS, 2007a) consists of several piezometers to monitor the phreatic surface changes within the dam and its foundation. Since the underdrain piezometers, P-8A, P-8B, P-9A, P-9B, P-10A and P-10B, are most relevant to establish the phreatic surface downstream of liner along the critical section of the dam, the data from these are discussed in detail.

Piezometers P-8A, P-9A, and P-10A were located in the underdrain, about 5 feet above the original ground surface. They monitor the piezometric head at various points in the underdrain under the dam. Piezometers P-8B, P-9B, and P-10B are seated about 20 feet below the original ground surface to monitor the piezometric head at corresponding points in the foundation rock. Figure 4-5 shows a cross section of the dam through the lowest downstream toe of the dam, approximate piezometer locations, and maximum recorded phreatic levels. The highest piezometric water levels and the historical permafrost degradation recorded along the Stage VI axis of the dam are presented on Figure 4-6.

The head difference between readings from the piezometers in the underdrain and corresponding piezometers in the underlying dam foundation material has typically been about 3 feet. This head difference was ignored in the selection of design phreatic surface and the higher water level at each location was conservatively used.

Before 2004, the highest downstream phreatic surface in the underdrain piezometers was recorded in 1998. Significant increases in phreatic water levels in underdrain piezometers were noted during 2004 and 2005, except in P-10A and P-10B, which are likely influenced by the tail water conditions at the seepage collection pond. The water level in the seepage collection pond is controlled by the pumpback system (URS, 2005c). The highest downstream piezometric levels shown on Figure 4-5 for P-8 and P-9 (both A and B) were recorded between June and August of 2005.

In general, the downstream phreatic surface fluctuated almost in direct correlation with the pumpback data, which is assumed to be total seepage. The pumpback data has varied with factors such as:

- Tailings management (beach width)
- Tailings impoundment water level
- Depth to frozen ground

Table 7-2 provides summarizes the representative piezometer records along with seepage pumpback rate, impoundment water levels, and tailings beach conditions to illustrate the above impact of these factors. The following subsections discuss how the above factors impact the downstream phreatic surface and the selection of the design downstream phreatic surface for closure.

### *7.3.2.1 Tailings Management*

The tailings management practices (TCAK, 2002; and Swendseid, 2005) have varied over the years as described in the tailings main dam history report (URS 2007a). The effectiveness of the tailings beach to control seepage is discussed in the seepage report (URS, 2007b). The historical effectiveness of the tailings beach due to varying tailings management practices are shown along with the pumpback data in Figure 7-7. The presence of effective tailings beach conditions is summarized as follows:

- No beach condition:
  - Before May 1998
  - May 2003 to July 2005
- Partially effective beach condition:
  - June 1998 to August 1999
  - September 2002 to May 2003
- Fully effective 600-foot wide beach condition:
  - August 1999 to September 2002
- Fully effective 300-foot wide beach condition:
  - August 2005 to date

As shown on Table 7.2, the presence of the tailings beach results in a lower phreatic surface downstream of the liner and reduced total seepage. A lower phreatic surface would result in more stable slopes; therefore the presence of the tailings beach improves the stability of the dam.

Recognizing the benefits of a wider tailings beach to reduce the seepage rate and lower the phreatic surface in the tailings main dam, a coffer dam in the tailings impoundment will continue to provide a tailings beach alongside the dam crest for future raises to closure. Following the current practices, the coffer dam will be built over the tailings and the space between the main dam and coffer dam will be filled with tailings to form a tailings beach.

The benefits of a wider tailings beach will need to be balanced with other closure considerations in selecting an optimal beach width and thus locating coffer dam alignments for closure.

**Table 7-2: Representative Underdrain Piezometer and Pumpback Rate Records**

Condition	Width of Beach (feet)	Date	Water Level (feet)	Seepage Rate (gpm)	Piezometer P-8B		Piezometer P-9A		Piezometer P-10A		Comments
					Water El. (feet)	N <sup>(1)</sup>	Water El. (feet)	N <sup>(1)</sup>	Water El. (feet)	N <sup>(1)</sup>	
No Beach	0	7/16/1998	932.2	673.93	816.4	0.23	809.8	0.19	805.4	0.16	
		8/22/1998	935.2	2558.8	821.6	0.26	814.3	0.22	808.5	0.18	possible permafrost degradation
		9/28/1998	935	2129.1	818.6	0.24	811.7	0.2	806.9	0.17	possible permafrost degradation
		11/3/1998	934.4	1711.6 <sup>2</sup>	816.4	0.23	810.1	0.19	806	0.16	
		5/31/2004	944.3	1299.5	819.6	0.24	813.1	0.2	809.1	0.17	
		7/23/2004	943.2	1045	819.6	0.24	813.1	0.2	808.3	0.17	
		8/20/2004	944.2	1451.5	821.1	0.25	814.5	0.2	809.2	0.17	possible permafrost degradation
		9/12/2004	944	1258.4	818.9	0.23	812.6	0.19	808	0.17	
		11/5/2004	944.7	1353.5	818.5	0.23	812.2	0.19	807.8	0.16	
		3/21/2005	946.9	832.5	819.5	0.23	812.9	0.19	808.2	0.16	
		4/23/2005	947.1	977.1	819.8	0.23	813.3	0.19	808.4	0.16	
		5/3/2005	947.5	1414.6	821.3	0.24	814.4	0.2	809.1	0.17	possible permafrost degradation
6/5/2005	948.7	1403.4	821.9	0.24	815.2	0.2	809.6	0.17	possible permafrost degradation		
7/12/2005	947.6	1003.5	815.4	0.21	810.3	0.18	806.4	0.15			
Beach	600	1/25/2001	935.4	455.2	805.9	0.16	800.4	0.12	797.9	0.11	
		7/27/2001	935.2	477.9	806.5	0.16	800.8	0.13	798.5	0.11	
		8/21/2001	935	612.7	808	0.17	802.1	0.14	799.7	0.12	possible permafrost degradation
		8/28/2001	934.6	518.8	806.5	0.17	801.4	0.13	799	0.12	
		12/14/2001	934.4	251.6	804	0.15	798.7	0.11	796.7	0.1	
		2/9/2002	934.9	277.6	803.5	0.15	798.5	0.11	796.4	0.1	
		5/21/2002	937.4	113.5	804.6	0.15	799.7	0.12	797.4	0.1	
		8/28/2002	936.9	439.3	806.8	0.16	801.9	0.13	799.4	0.12	
		9/17/2002	937.7	671	809.6	0.18	804.1	0.15	801.3	0.13	possible permafrost degradation
10/16/2002	937.8	594.3 <sup>2</sup>	809.4	0.18	803.9	0.15	801.2	0.13			
Beach	300	11/5/2005	947.7	700.5	813.1	0.19	806.5	0.15	803.3	0.13	
		12/10/2005	947.9	774.9	811.4	0.18	805.9	0.15	802.7	0.13	

**Note:**<sup>1</sup> - N - Normalized Total Head (Ht - 781.2) / (P - 781.2), where Ht is total water head and P is impoundment water level, where El 781.2 is the impoundment bottom at the low point of the pumpback system

<sup>2</sup> - Interpolated value

*7.3.2.2 Tailings Impoundment Water Level*

The phreatic surface in the tailings dam fluctuates almost in correlation with the water level in the tailings impoundment. As part of the tailings dam operation and maintenance (URS, 2005d), a normalized total head (N) parameter is calculated and tracked for each piezometer. The normalized total head encapsulates the piezometric head fluctuations due to changes in the impoundment water level, and is defined as follows:

Y:\Red Dog Mine\Mine Closure & Reclamation\Tailings Main Dam\Stability Analyses\Stability Analysis Report(Current Report in Progress)\TD Stability Analysis Rpt.doc

$$N = (H_t - 781.2) / (P - 781.2)$$

where,  $H_t$  is total head in feet,

$P$  is pond water surface elevation in feet, and

the pond bottom is considered as the datum elevation of 781.2 feet.

Table 7.2 shows normalized total heads of piezometers P-8B, P-9A, and P-10A for representative beach conditions. The selected data shows that the normalized total head of each piezometer varies within a narrow range for a select beach width. With increasing beach width, the normalized total head decreases, indicating a lower phreatic surface under similar impoundment water levels. However, for the same beach width, the downstream phreatic surface rises with increased impoundment water level.

### 7.3.2.3 Depth to Frozen Ground

The review of the thermister and seepage pumpback records indicates that the changes in depth to the frozen ground, either permafrost degradation and aggradation, or the freezing and thawing of active layer above the permafrost, affect the total seepage and the downstream phreatic surface. The changes in depth to frozen ground will result in short and long-term seepage rate and phreatic surface changes.

The permafrost depth in both abutments and thaw bulb width has changed since the construction of the dam and development of the impoundment. The permafrost conditions were estimated from thermal and water level data from thermistors and piezometers, past studies (Dames & Moore, 1987a and 1987b; Water Management Consultants, 1999; and URS, January 2005a), TCAK annual inspection reports (TCAK, 2007), and communications on permafrost research at the mine (Weaver, 2005). The seepage analysis report (URS, 2007c) describes the permafrost degradation and its impact on seepage.

Figure 4-7 summarizes the historical permafrost degradation along the Stage VI dam axis and the thaw bulb widening at the creek bed. Thermistor TDAM-T-1 and TDAM-T-15 records on Figures 7-5 and 7-6 show representative permafrost degradation recorded at the west and east abutments of the dam. The records show that when there was a major permafrost degradation, the pumpback rate increased and the downstream phreatic surface rose. Table 7-2 shows how the normalized total head for these piezometers also increased, reflecting a higher than normal downstream phreatic surface.

### 7.3.2.4 Selection of Downstream Phreatic Surface

The review of the instrumentation records and tailings management practices revealed the following:

- The underdrain piezometer readings fluctuate in direct correlation with the pumpback data
- The presence of a tailings beach results in a lower phreatic surface downstream of the liner.
- The downstream phreatic surface and normalized total head decrease with a wider beach.
- The downstream phreatic surface rises with increasing impoundment water level.
- Depth changes to frozen ground impact the downstream phreatic surface.
- The downstream phreatic surface rises as the permafrost degrades or active layer thaws.
- The downstream phreatic surface lowers as the permafrost aggrades or active layer freezes.

The changes in normalized total head as a result of variation in depth to the frozen surface have been impacted by tailings management practices. Possible permafrost degradation was identified as shown

in Table 7-2 by reviewing the historical seepage rates and thermistor data. The maximum variations in normalized total head associated with possible permafrost degradation (or aggradation) were then identified. The variation in normalized total head due to permafrost degradation is high for the no-beach condition and low for the 600 feet-wide beach condition.

The normalized total head has varied by as much as 0.03 (July 16, 1998 to August 22, 1998 and June 5, 2005 to July 12, 2005) for the no-beach condition. The variation has reduced to 0.02 (August 28, 2002 to September 17, 2002) for 600-foot beach conditions.

A higher variation in normalized head that is attributable to possible permafrost degradation was observed in underdrain piezometer P-8 than in underdrain piezometer P-10. This could be because the piezometer P10 levels are controlled mainly by tailwater conditions at the pumpback wells. In order to establish the cause-effect relationships, trend lines of seepage versus normalized head relationship were developed for the following conditions:

- No beach - summer
- No beach - winter
- No beach - possible permafrost degradation
- 600-foot beach - summer
- 600-foot beach - winter
- Partially effective beach

Using these trend lines, the downstream design phreatic surface of the future closure condition was obtained corresponding to anticipated maximum seepage at closure. The calculated summer seepage rate at closure corresponding to 600-foot wide beach is 600 gpm (URS, 2007b). Allowing for uncertainties in this approach and possible variations in the seepage estimate, the anticipated maximum seepage was conservatively estimated to be 2,000 gpm. The 600-foot wide beach summer trend was used to obtain the calculated the normalized total head value.

The calculated normalized total head value was then increased by a minimum value of 0.02 to obtain the design normalized total head to account for permafrost degradation based on the historical data. Using this normalized total head value and design impoundment water level at El. 980.2, the design downstream phreatic surface levels were computed. The design piezometric head at the seepage collection pond location was conservatively selected as El. 795 by considering the following:

- Seepage dam crest at El. 800 and spillway at El. 795.
- Seepage pond water levels to activate pumps range from El 772 to 790 (URS, 2005d).

Table 7-3 presents the design phreatic surface elevations for the stability analyses, at the underdrain piezometer locations, upstream of liner and at the seepage collection pond. The maximum piezometric heads recorded on the underdrain piezometers and their tip elevations are also presented in Table 7-3.

#### **7.4 PORE PRESSURE COEFFICIENT**

As discussed in Section 4.6, a temporary increase in pore pressure occurs in saturated non-free draining materials in response to the increases in overburden pressure. This increase in pore water pressure in the tailings main can be modeled either by considering total stress parameters or effective stress parameters with appropriate pore pressure coefficient,  $R_u$ .

**Table 7-3: Design Downstream Piezometric Heads**

Piezometer Identification	Elevation of Piezometer tip (ft.)	Max Piezometric Head to date (ft.)	Design Normalized Total Head <sup>(1)</sup> (ft.)	Design Piezometric Head (ft.)
P-08A	798	821.9	0.32	845.0
P-08B	773	823.3	0.32	845.0
P-09A	792	815.24	0.25	830.0
P-09B	767	810.62	0.25	830.0
P-10A	790	809.58	0.17	815.0
P-10B	765	803.9	0.17	815.0
Upstream	N/A	N/A	N/A	980.2
Seepage pond	N/A	N/A	N/A	795.0

Notes: 1 -  $N = \frac{H_t - 781.2}{P - 781.2}$ , where  $H_t$  is total water head and  $P$  is impoundment water elevation, where El 781.2 is the elevation of the impoundment bottom at the low point of the pumpback system

The excess pore pressure generated by the introduction of more fill will vary. It was estimated that an average value of  $R_u$  would be between 0.1 and 0.2 in the highly weathered shale, gouge layers, and any less pervious fills such as Kivalina shale in the dam. This range of  $R_u$  was estimated based on the assumption that the future raises will be built in the three interim stages VIII, IX, and X.

The excess pore pressure generation within these layers could be monitored and controlled by controlling the construction pace and stages. Therefore, an average pore pressure coefficient value,  $R_u$ , of 0.1 was selected for the conceptual design of the future raises.

## 7.5 STABILITY ANALYSES

Stability analyses of the tailings dam future raises to closure were completed using 2D limit equilibrium approach in accordance with the analysis approach summarized in Section 5.2. A 2D slope stability analysis software, SLOPE/W, was used to perform the calculations using the Spencer method of slices. The critical cross section for the analyses (Section H-H'), shown on Figure 4-4, was chosen through the seepage collection pond and through the lowest ground elevation along the toe of the dam.

The geological settings at this section as well as the presence of weak gouge zones beneath the dam foundation were reviewed from the available geotechnical data (URS, 2006). The effective strength parameters were used for the various materials.

Randomly selected circular failure surfaces and pre-specified block failure surfaces through the potentially weak gouge zones were considered. Static and seismic stability analyses were performed. The following two basic design conditions were analyzed:

- End of construction
- Long term condition

For end-of-construction conditions, the excess pore water pressures generated during fill placement are expected to remain for considerable time in saturated slow-draining low permeable material. The stability analyses were performed for a range of pore pressure coefficient,  $R_u$ , ranging from 0.1 to 0.3.

For long-term conditions, all excess pore pressures are assumed to have dissipated and effective stress parameters are expected to govern the behavior of all materials. Static and seismic loading conditions were considered for long term stability analyses with pore pressure coefficient,  $R_u$  equal to zero.

For static loading, minimum static FS values of 1.3 and 1.5 are commonly acceptable for end-of-construction and long term conditions, respectively. For seismic loading, a pseudo-static FS ranging from 1.0 to 1.2 is used, depending on the earthquake loading criteria. In this design, a minimum required FS of 1.0 is considered acceptable for the MDE, given its longer recurrence interval.

The strength parameters of the dam and foundation materials are summarized in Table 4-1 and Section 4.3. These parameters are applicable for the stability analyses of the dam under static loading. As summarized in Section 7.1, it is appropriate to reduce the shear strength of the less permeable materials by up to 20 % to account for the pore pressure generation within these materials during the seismic shaking (Hynes-Griffin and Franklin 1984, Kramer 1996, WSDOT 2005).

Considering the relatively small thickness of the less permeable and highly weathered shale and gouge layers in the foundation and the Kivalina shale in the dam, and the higher permeability of the surrounding materials, a 10 % reduction in shear strength is considered adequate. The material strength parameters used in the static and seismic stability analyses are summarized in Table 7-4.

**Table 7-4 - Material Parameters for Stability Analyses**

Material	Unit Weight (pcf)		Shear Strength Parameters (Effective Stress)			
	Moist	Saturated	Static		Seismic	
			Cohesion (psf)	Phi (deg)	Cohesion (psf)	Phi (deg)
Tailings (Silt and Fine Sand)	120	120	0	30	0	30
Buttress (Random Rockfill)	135	140	0	35	0	35
Liner Bedding	125	138	0	35	0	35
Liner	115	115	0	24	0	24
Filter drain	125	138	0	35	0	35
Transition Rockfill	125	138	0	35	0	35
Random Rockfill	135	140	0	35	0	35
Highly Weathered Shale	115	115	0	30	0	27
Underdrain	115	115	0	30	0	30
Moderately Weathered Shale	145	150	0	35	0	35
Kivalina Shale Fill	112	112	250	11	225	9.9
Gouge 'Layer'	120	120	0	22	0	19.8
<b>Sensitivity Analysis</b>						
Gouge 'Layer'	120	120	0	19	0	17.1

**Table 7-5: Summary of Stability Analysis Results**

Design Condition	Loading Conditions	Minimum Required FS	Computed FS (for gouge friction angle 22 deg. & 0 cohesion)						
			2.75H:1V				3H:1V		
			Stage VIII	Stage IX	Closure		Stage VIII	Stage IX	Closure
with berm	without berm								
End-of-Construction Ru =0.1	Static, Block	1.3	1.46	1.44	1.45	1.35	1.54	1.50	1.53
	Static, Circular	1.3	1.73	1.68	1.65	1.45	1.88	1.70	1.58
Long Term Condition	Static, Block	1.5	1.61	1.58	1.59	1.52	1.70	1.65	1.67
	Static, Circular	1.5	1.81	1.77	1.74	1.59	1.96	1.82	1.71
	Seismic (OBE) Block	1.2	1.23	1.23	1.23	1.18*	1.27	1.27	1.29
	Seismic (OBE) Circular	1.2	1.47	1.46	1.39	1.26	1.55	1.42	1.38
	Seismic (MDE) Block	1.0	0.98*	0.98*	1.00	0.96*	1.01	1.02	1.06
	Seismic (MDE) Circular	1.0	1.22	1.18	1.14	1.04	1.23	1.15	1.14

\* Does not meet minimum FS criteria

Several tailings main dam were conditions were investigated to determine the steepest possible downstream slope for future Stages VIII, IX and X at closure. Table 7-5 presents the FS results for design and loading conditions analyzed for downstream slopes of 2.75H:1V and 3H:1V. Results for the 2.5H: 1V slope are not shown because they do not meet the long-term stability criteria. The end-of-construction results in Table 7-5 correspond to a pore pressure coefficient of 0.1 in the less pervious foundation and gouge materials. The results of the stability analyses in the Table 7-5 show:

- For the end-of-construction condition with a pore pressure coefficient of 0.1, the tailings dam will be stable with a FS greater than 1.3 for Stages VIII, IX, and X at closure with both downstream slopes, 2.75H:1V and 3H:1V.
- For the long term condition, the tailings dam with a downstream slope of 2.75H: 1V will not be stable for Stages VIII, IX, and X at closure, based on the minimum required FOS of 1.0 for the seismic-MDE case.
- For the long term condition, the tailings dam with a downstream slope of 3H:1V, will be stable for Stages VIII, IX, and X at closure, based on the minimum required FOS of 1.5, 1.2, and 1.0 for the static, seismic-OBE, and seismic-MDE, respectively.

Block failure surfaces though the weaker ‘gouge zones’ yield lower FS values than for corresponding circular failure surfaces. In order to investigate the effect of the berm at the downstream toe, two set of analyses with and without berm were carried out for the 2.75H: 1V geometry. The critical block failure surfaces with and without berm are shown in Figures 7-8 and 7-9, respectively, for the long term condition under the MDE. For comparison, the critical circular failure surfaces for the corresponding cases are also shown in Figures 7-10 and 7-11. Figure 7-12 shows the critical block failure surface for the Stage VIII configuration of the dam with a 3H: 1V slope under MDE level seismic loading.

It is evident that that the presence of a berm helps increase the dam stability. However, due to the presence of the seepage collection pond there is no room for a berm at the toe of the 3H:1V

downstream slope. Thus, the beneficial effect from the toe berm diminishes for the 3H:1V slope configuration at closure.

## 7.6 SENSITIVITY ANALYSES

Material strength parameters and assumptions used in the stability analyses are justified by laboratory strength test data and engineering judgment. Of the material strength parameters, the stability results are highly sensitive to the residual shear strength of the gouge material. Of the assumptions, the pore pressure coefficient and effectiveness of the liner are of major importance. Therefore, sensitivity analyses were completed to evaluate the impact from three key parameters for the dam at closure:

- Pore pressure coefficient
- Shear strength of gouge material
- Condition of ‘No-Liner’ in the dam

The sensitivity analyses and results obtained are described in the following sections.

### 7.6.1 Pore Pressure Coefficient

The excess pore pressure generated by construction activities can vary depending on factors that may be difficult to control. As discussed in Section 7.4, the pore pressure coefficient is estimated to range from 0.1 to 0.2 at the end of construction. However, in order to evaluate its sensitivity, the stability analyses were performed for the end-of-construction static loading condition with pore pressure coefficients ranging from 0.1 to 0.3. The computed FS from the stability analyses are summarized in Table 7-6. Figures 7-13 and 7-14 show the critical block failure surface of the dam with a downstream face slope of 2.75H: 1V at closure under end-of-construction static loading.

**Table 7-6: Factor of Safety Values for Different Values of  $R_u$**

Design Condition	Loading Conditions	Minimum Required FS	Computed FS for different downstream slopes						
			Slope =2.75 H:1 V			Slope =3 H:1 V			
			$R_u=.1$	$R_u=.15$	$R_u=.2$	$R_u=.1$	$R_u=.2$	$R_u=.25$	$R_u=.3$
End Of Construction	Static, Block	1.3	1.45	1.38	1.29*	1.53	1.37	1.30	1.24*
	Static, Circular	1.3	1.65	1.60	1.56	1.58	1.45	1.39	1.32

\* Does not meet minimum FS criteria

The end-of construction condition stability analyses results summarized in Table 7-6 show that the tailings dam with downstream face slopes of 2.75H: 1V and 3H: 1V will be stable with FS greater than the minimum required value of 1.3 for pore pressure coefficient values of up to about 0.2.

### 7.6.2 Shear Strength of Gouge Material

The possible presence of a continuous gouge layer under the tailings main dam and its residual shear strength values are the most important factors that affect the stability of the dam at closure. In order to evaluate the sensitivity of the residual shear strength, the analyses were repeated with a gouge internal friction angle (residual) value of 19 degrees and no cohesion. As summarized in Table 7-4, the internal friction angle of the gouge zone for under seismic loading was taken as 17.1 degrees with no cohesion to account for pore pressure increases during seismic shaking. The stability analyses results for end-of-construction and long-term conditions are summarized in Table 7-7.

Table 7-7 shows that both tailings dam downstream face slopes do not meet the minimum FS requirements with a residual shear strength of 19 degrees for the gouge zone. The stability analyses for the 3H: 1V case were repeated with both site specific PSHA and USGS seismic coefficients shown in Table 7-1. The seismic FS are in Table 7-8, and show that the dam would marginally meet the minimum FS requirements when evaluated with the site-specific seismic loading from the PSHA.

**Table 7-7: Factor of Safety Values with Gouge Friction Angle of 19 degrees**

Design Condition	Loading Conditions	Minimum Required FS	Computed FS for different stages					
			2.75H:1V			3H:1V		
			Stage VIII	Stage IX	Stage X Closure	Stage VIII	Stage IX	Stage X Closure
End-of-Construction, Ru =0.1	Static, Block	1.3	1.34	1.32	1.34	1.41	1.37	1.40
	Static, Circular	1.3	1.71	1.66	1.63	1.86	1.67	1.55
Long Term Condition	Static, Block	1.5	1.47*	1.45*	1.46*	1.55	1.52	1.54
	Static, Circular	1.5	1.79	1.75	1.71	1.94	1.79	1.67
	Seismic (OBE), Block	1.2	1.13*	1.13*	1.13*	1.16*	1.16*	1.19*
	Seismic (OBE), Circular	1.2	1.46	1.45	1.37	1.53	1.39	1.35
	Seismic (MDE), Block	1.0	0.89*	0.90*	0.92*	0.92*	0.93*	0.97*
	Seismic (MDE), Circular	1.0	1.21	1.16	1.12	1.21	1.13	1.13

\* Does not meet minimum FS criteria

### 7.6.3 Sensitivity to No Liner in Dam

The stability of the tailings main dam will be lower when the phreatic surface in the dam is higher. Among the factors presented in Section 4.5 that impact the phreatic surface, the tailings beach width has the greatest impact. In addition, the effectiveness of the HDPE geomembrane in the liner system must be considered because it is assumed that it will continue to function as designed. However, the geomembrane will degrade over time. Therefore, the geomembrane longevity was investigated and its life expectancy was found to range from 500 to 1600 years (URS 2007d).

**Table 7-8: Summary of Stability Sensitivity Analysis Results for Seismic Loading Condition**

Seismic Loading Conditions	Minimum Required FS	FS Values for 3H:1V Configuration					
		USGS			PSHA		
		Stage VIII	Stage IX	Stage X Closure	Stage VIII	Stage IX	Stage X Closure
OBE, Block	1.2	1.16*	1.16*	1.19*	1.22	1.22	1.25
OBE, Circular	1.2	1.53	1.39	1.35	1.61	1.46	1.43
MDE, Block	1.0	.92*	0.93*	.97*	1.0	1.0	1.04
MDE, Circular	1.0	1.21	1.13	1.13	1.31	1.21	1.21

\* Does not meet minimum FOS criteria

Considering the life expectancy of the geomembrane, it is possible to have a long-term condition with the liner being ineffective. In order to evaluate this possible condition, a “no liner” sensitivity analysis was performed with no geomembrane in the liner and cutoff systems. With no liner, the phreatic surface in the dam would rise, which could be lowered by increasing the tailings beach width. A 900-foot-wide tailings beach was selected for the sensitivity evaluation. The down stream phreatic surface for this case was obtained from 3D seepage analysis results and is shown in Figure 7-15.

Figure 7-16 shows the critical block failure surface of the dam at closure under long term static loading. The dam is found to be stable with a FS of 1.36, which does not meet the minimum required FS of 1.5. However, this can be mitigated by further widening the beach to lower the phreatic surface in the dam and improve the dam stability.

Therefore, it will be necessary that the dam instrumentation be regularly monitored and maintained to detect possible degradation of the liner system in time to plan and take whatever corrective measures may be needed to improve the dam stability.

## 8.0 DEFORMATION ANALYSIS

A simplified, chart-based, deformation analysis of the tailings main dam was completed to estimate the possible permanent deformation of the dam that would be caused by the maximum seismic event that could be reasonably anticipated at the site. The simplified deformation analyses and permanent deformation estimates that were obtained are described in the following sections.

### 8.1 SIMPLIFIED DEFORMATION ANALYSIS

Simplified chart-based deformation analysis methods (Makdisi and Seed 1978, Franklin and Chang 1977, Martin and Qiu 1994, and Bray and Rathje, 1998) were developed based on Newmark sliding block analysis methods to estimate earthquake-induced deformations. These methods provide a simple yet rational approach to supplement pseudo-static stability analyses with deformation estimates.

The Newmark sliding block analysis assumes that the sliding mass is a rigid body. A big improvement of chart-based approaches is the ability to account for dynamic response, rather than rigid body behavior, of an embankment or dam. This is important because observations, model tests,

and dynamic analyses of existing dams indicate that horizontal accelerations due to earthquakes vary along the height of the dam. Without using realistic dynamic analyses in the design, several major slides had resulted in dams for which the pseudo-static approach with a constant horizontal seismic coefficient had predicted a safe condition.

For the tailings main dam deformation analysis, the following chart-based approaches were used:

- Makdisi and Seed (1978)
- Franklin and Chang (1977)
- Martin and Qiu (1994)
- Bray and Rathje (1998)

The Makdisi and Seed (1978) and Bray and Rathje (1998) methods have similar approaches that were developed for dams and landfills, respectively. Both methods relate displacement to the ratio of yield acceleration to average acceleration of the potential sliding mass. The earthquake magnitude is a parameter in Makdisi and Seed charts for estimating earthquake-induced permanent displacements. Confidence levels such as 95%, 84%, and 50%, are included in charts prepared by Bray and Rathje.

The Martin and Qiu (1994) approach relates the displacement to ratio of yield acceleration to peak ground acceleration at the base of the sliding mass. The method does not include earthquake magnitude. Martin and Qiu note that magnitude is not a key parameter for the range of magnitudes (M6 to M7.5) used in their evaluation. However, this approach considered the ratio of peak ground acceleration to peak ground velocity as an additional regression parameter.

The Franklin and Chang (1977) approach relates the displacement to ratio of yield acceleration to peak earthquake acceleration. This approach is known to yield very large, unreasonably conservative, deformation estimates (ATC/MCEER, 2003). Use of the Franklin and Chang approach in AASHTO standards has been discontinued (WSDOT, 2005).

All of these approaches assume that failure occurs on a well-defined slip surface and the soil behaves elastically at stress levels below failure but is perfectly plastic at and above its yield strength. These approaches require the following three determinations:

- Yield acceleration,  $k_y$
- Earthquake-induced acceleration of the sliding mass
- Permanent displacement

The following subsections discuss the above steps for each of the above approaches.

### **8.1.1 Determination of Yield Acceleration, $k_y$**

Yield acceleration is defined as an average acceleration at which a potential sliding surface would develop a FS of unity and cause the sliding mass to begin to experience permanent displacements. For slopes in which large deformations are not expected during a seismic event, the stability analyses based on limit equilibrium method can provide a reasonable estimate of the yield acceleration. This step is common for all chart-based deformation analyses used in this study.

It is important to note that due to the difference in soil behavior under cyclic and static loadings, the cyclic yield strength is defined as the stress level above which the material behaves plastically and below which the material behaves elastically. Experimental data and earthquake response analyses

reported in the literatures suggest that cyclic yield strength for a clayey material is 80% or more of the static undrained strength.

Makdisi and Seed (1978) reported several finite element response analyses to compute maximum shear strains for different earthquake magnitudes and embankment characteristics. They showed that the maximum earthquake-induced shear strains ranged between 0.1 to 1.0% in strong earthquakes. Alternately, the static failure strain for compacted clayey material normally ranges from 3 to 10%. Since the ratio of cyclic strain to static failure strain is small (0.5 or less), earthquake loadings are expected to cause very little strength reduction for compacted clayey material.

For the deformation analysis for the tailings main dam, the internal friction angle values of the highly weathered shale, gouge and Kivalina shale fill materials were conservatively reduced by 20% from the Table 4-1 values. By performing pseudo-static stability analyses using reduced strength parameters, the yield acceleration,  $k_y$ , at which a potential sliding surface would develop a FS of unity, was found to be 0.095g and 0.115g for the 2.75H:1V and 3H:1V slopes, respectively. These values were based on the critical block failure surfaces under MDE loading. The yield acceleration was selected as 0.095 g.

### **8.1.2 Determination of Earthquake Induced Acceleration, $k_{max}$**

In general, the maximum horizontal average acceleration ( $k_{max}$ ) for the time histories of a sliding mass is determined by performing a dynamic response analysis, using a finite element analysis or a simple 1D technique. The following sections present the approximate methods provided in each of the above chart based approaches to calculate the maximum horizontal average acceleration.

#### *8.1.2.1 Makdisi and Seed (1978)*

A simplified method to estimate the maximum earthquake-induced crest acceleration in embankments is presented in Maksidi and Seed (1977). Using empirical graphs relating  $G/G_{max}$ , shear strain and damping, the maximum induced crest acceleration was computed iteratively. An initial  $G/G_{max}$  value was assumed where  $G$  is the shear modulus of the material. The shear modulus, shear wave velocity and period of the first three vibration modes of the dam were computed conventional mechanics. The maximum induced crest acceleration was computed based on spectral accelerations corresponding to the periods of the first three modes of the dam. The average shear strain was calculated and checked with that corresponding to the assumed  $G/G_{max}$  ratio. The iterative procedure was continued until a shear strain match was achieved to obtain the maximum induced acceleration at the crest of the dam.

Makdisi and Seed present a normalized chart for the estimation of maximum average acceleration with depth of potential failure for embankments and dams, which was developed based on the results from several dynamic finite element analyses and previous investigations. This normalized chart was used to obtain the maximum average earthquake induced acceleration for the tailings main dam.

#### *8.1.2.2 Franklin and Chang (1977)*

The Franklin and Chang charts use the ratio of yield acceleration ( $k_y$ ) to the peak ground acceleration ( $k_{max}$ ) at the base of the sliding mass. Since the critical failure surface of the tailings dam essentially passes through the base of the dam, the peak ground acceleration ( $k_{max}$ ) at the base of the sliding mass was assumed to be the PGA estimated from the PSHA corresponding to Site Class C.

### 8.1.2.3 Bray and Rathje (1998)

Bray and Rathje (1998) provide a chart to estimate the maximum average earthquake-induced acceleration of the sliding mass, and use nonlinear dynamic analysis results to develop the normalized chart for estimating maximum horizontal average accelerations. The approach needs estimates of mean period of earthquake motion, fundamental period of the dam, nonlinear response factor (NRF) or ratio of maximum horizontal accelerations at the crest and rock, and maximum horizontal rock acceleration.

Based on the PSHA results in section 6.7, the predominant period of the site was estimated as 0.2 sec. According to Rathje et al. (1998), the mean period of earthquake motion is twice the predominant period. In order to accommodate variation of mean periods for possible earthquake motion at the dam site, a range of mean period values, 0.2 to 0.6 seconds, were used. The fundamental period of the dam was estimated from Maksidi and Seed (1977). The NRF factor was estimated using the Harder (1991) relationship for earth dams. A bedrock PGA from the Red Dog PSHA was used. The Bray and Rathje chart was used to obtain the maximum horizontal average acceleration for the tailings main dam.

### 8.1.2.4 Martin and Qiu, 1994

Martin and Qiu charts use the ratio of yield acceleration ( $k_y$ ) to the peak ground acceleration ( $k_{max}$ ) at the base of the sliding mass. Since the critical failure surface of the tailings main dam essentially passes through the base of the dam, the peak ground acceleration ( $k_{max}$ ) at the base of the sliding mass was assumed to be the PGA estimated from the PSHA corresponding to Site Class C.

## 8.1.3 Estimation of Permanent Displacement

Using the values estimated for yield acceleration,  $k_y$  and maximum horizontal average acceleration,  $k_{max}$ , the permanent displacement of the tailings main dam due to maximum conceivable seismic event at the site is estimated for each of the above approaches.

The Makdisi and Seed (1978) dimensionless chart presents the normalized displacement versus ratio of  $k_y/k_{max}$  for different earthquake magnitudes. The Bray and Rathje (1998) chart presents the normalized displacement versus the  $k_y/k_{max}$  ratio for different confidence levels or probability of exceedance. Earthquake durations of 4 to 20 seconds were considered to estimate permanent displacement using the Bray and Rathje chart. The Martin and Qiu (1994) chart presents permanent earthquake-induced displacement versus the  $k_y/k_{max}$  ratio for different velocity to acceleration ratios, which depend on the epicentral distance. The Franklin and Chang (1977) chart presents permanent earthquake induced displacement against the  $k_y/k_{max}$  ratio for natural and synthetic records studied.

## 8.2 DEFORMATION ANALYSIS RESULTS

The simplified deformation analyses and results are described in the following sections.

### 8.2.1 Makdisi and Seed (1978)

Using the iterative procedure outlined in Section 8.1.2.1, the fundamental period of the dam ( $T_0$ ) and maximum crest acceleration ( $a_{max}$ ) for the design earthquake were computed to be 1.23 seconds and 0.76g, respectively. Using the Makdisi and Seed (1978) chart, the earthquake-induced average acceleration corresponding to the critical failure surface was obtained from the normalized curves and a range of maximum horizontal average accelerations were obtained: 0.266g (average) to 0.357g (maximum). The range of permanent earthquake induced displacement values, corresponding to an

earthquake of magnitude 6.5, was calculated using the Makdisi and Seed (1978) chart. The results are summarized in Table 8-1. The estimated maximum shear strain within the dam is 0.19%.

### 8.2.2 Franklin and Chang (1977)

Using the approach outlined in Section 8.1.2.2, the ratio of yield acceleration and the peak ground acceleration was calculated for the tailings main dam. The permanent ground displacement of the tailings dam was calculated with the aid of the Franklin and Chang (1977) chart. The range of the estimated earthquake-induced permanent displacement is tabulated in Table 8-1. As described in section 8.1, this method yields overly conservative results (ATC/MCEER, 2003). Therefore, URS did not use this result to make the conclusion of the maximum permanent horizontal crest displacement of the dam during the maximum anticipated earthquake at the Red Dog Mine site

### 8.2.3 Bray and Rathje (1998)

Using the approach outlined in Section 8.2.1.3, the permanent displacement of the tailings main dam was estimated using the Bray and Rathje (1998) approach. The NRF was estimated as 2.63 based on Harder’s (1991) relationship for earth dams, using the PGA (0.2 g) obtained from PSHA for Site Class C. A range of maximum horizontal average acceleration for the sliding mass was obtained from the Bray and Rathje (1998) normalized chart using the fundamental period estimate and considered mean period earthquake range of 0.2 to 0.6 seconds. The maximum horizontal average acceleration range was calculated from the rock site best fit curve as from 0.105g to 0.237g.

The maximum permanent earthquake induced displacements were calculated using Bray and Rathje (1998) chart. A range of significant time duration of 4 to 20 seconds was considered for estimating the earthquake-induced permanent displacement. The range of estimated earthquake induced permanent displacements with a 5% probability of exceedance is in Table 8-1.

### 8.2.4 Martin and Qiu (1994)

Using the approach outlined in Section 8.1.2.4, the ratio of yield to peak ground accelerations was calculated. Martin and Qiu (1994) provide two charts based on epicentral distances of less than 15 km (9.4 miles) and greater than 9.4 miles. Conservatively, URS used the chart for epicentral distances less than 9.4 miles. The estimated earthquake-induced permanent displacements are tabulated in Table 8-1.

**Table 8-1: Summary of Deformation Analysis Results**

Approach	Permanent Displacement (inches)
Makdisi and Seed, 1978	6 to 14
Franklin and Chang <sup>1</sup> , 1977	52 to 85
Bray and Rathje, 1998	2.5 to 20.5
Martin and Qiu, 1994	2.5 to 21

<sup>1</sup> The Franklin and Chang method yields overly conservative results

## 9.0 CONCLUSIONS AND RECOMMENDATIONS

### 9.1 CONCLUSIONS

On the basis of the results of the stability analyses, URS developed the following conclusions:

- Red Dog Mine is located in a region that has low seismicity and no known active faults.
- Two design-level earthquakes for dam designs in Alaska are defined by ADNR (2005) as:
  - Operating Basis Earthquake (OBE): 10% probability of exceedance in 50 years (return period of 475 years)
  - Maximum Design Earthquake (MDE): 2 % probability of exceedance in 50 years (return period of 2,475 years).
- The following seismic hazard was interpolated at the mine site from a 2005 USGS seismic hazard map for Alaska, which was developed by means of a PSHA at nodal points of a grid:
  - OBE - PGA is 0.10 g for bedrock and 0.11 g for Site Class C
  - MDE - PGA is 0.23 g for bedrock and 0.25 g for Site Class C
- A site specific seismic hazard analysis was performed based on a site specific PSHA for the mine site , and the following seismic hazard was obtained:
  - OBE - PGA is 0.077 g for bedrock and 0.084 g for Site Class C
  - MDE - PGA is 0.18 g for bedrock and 0.20 g for Site Class C
- Seismic criteria for the dam future raises to closure were established to be as follows:
  - OBE - conceptual design PGA is 0.11 g
  - MDE - conceptual design PGA is 0.25 g
- Seismic coefficients for pseudo-static stability analyses of the dam were selected to be:
  - OBE - seismic coefficient is 0.055
  - MDE - seismic coefficient is 0.125
- For the seismic criteria established for closure, the predominant moment magnitude of earthquake for both OBE and MDE events is 5.23.
- The liquefaction potential of the tailings is low for ground shaking induced by the OBE and MDE events.
- The shear strength of the gouge zones under the dam is the most critical parameter for designing a stable downstream slope of the dam. From the geotechnical data, it is estimated that the gouge zones have a shear strength corresponding to an internal friction angle of 22 degrees and zero cohesion.
- With an internal friction angle of 22 degrees and zero cohesion for the gouge material, the steepest stable downstream slope of the Stage X dam and interim Stage VII and IX raises is 3.0H: 1V. The final dam would be stable during the MDE.
- For the extreme “no liner” case of a failed geomembrane, the dam will be stable with a factor of safety (FS) of 1.36, which is less than the required minimum FS of 1.5. The FS could be increased by further widening the beach to lower the phreatic surface in the dam.

- The deformation analyses show that a maximum permanent horizontal crest displacement of the dam during the maximum anticipated earthquake at the site will be up to 21 inches, which is not a dam safety concern because of the adequate freeboard that will be in place.
- Using the simplified approach of deformation analysis, it is estimated that the maximum shear strain in the dam during the maximum anticipated earthquake at the site would be about 0.19%.
- With an internal friction angle of 19 degrees and zero cohesion for the gouge material, the downstream slope of 3.0H: 1V will be stable for static and OBE seismic conditions, but will not be stable under MDE seismic loading and will likely deform under this loading.

## 9.2 RECOMMENDATIONS

From the stability analysis results and conclusions, URS has developed the following recommendations:

- A downstream slope of 3.0H:1V is recommended for the tailings main dam future raises to closure, and would provide a stable embankment with required long-term factors of safety
- During construction of the future raises, the pore pressure coefficient in the foundation materials should be maintained less than 0.2.

## 10.0 REFERENCES

- Abrahamson, N., and Silva, W., 1997, "Empirical response spectral attenuation relations for shallow crustal earthquakes", *Seismological Research Letters*, vol. 68, no. 1, Seismological Society of America, p. 94-127.
- Alaska Department of Natural Resources, Division of Mining, Land and Water, Water Resources Section, Dam Safety and Construction Unit, 2005, "Guidelines for Cooperation with the Alaska Dam Safety Program", June 30, 2005a.
- Alaska Department of Natural Resources, Division of Mining, Land and Water, Water Resources Section, Dam Safety and Construction Unit, 2005b, "Multiple Accounts Analysis for Red Dog Tailings Disposal", letter to Teck Cominco Alaska Inc., June 2, 2005
- ATC/MCEER, 2003, "Recommended LRFD guidelines for the seismic design of highway bridges, Part II: Commentary and Appendices," MCEER/ATC-49 Report, ATC/MCEER Joint Venture, a partnership of the Applied Technology Council and the Multidisciplinary Center for Earthquake Engineering, Redwood City, California.
- Boore, D.M., Joyner, W.B., and Fumal, T.E., 1994, "Estimation of Response Spectra and Peak Accelerations from Western North American Earthquakes: an Interim Report, Part 2", U.S. Geological Survey Open-File Report. 94-127, 40 p.
- Boore, D.M., Joyner, W.B., and Fumal, T.E., 1993, "Estimation of Response Spectra and Peak Accelerations from Western North American Earthquakes, an Interim Report", U.S. Geological Survey Open-File Report 93-509.
- Bray, J.D. and Rathje, E. M., 1998, "Earthquake Induced Displacements of Solid-Waste Landfills" *Journal of Geotechnical and Geoenvironmental Engineering*, Volume 124, No 3.

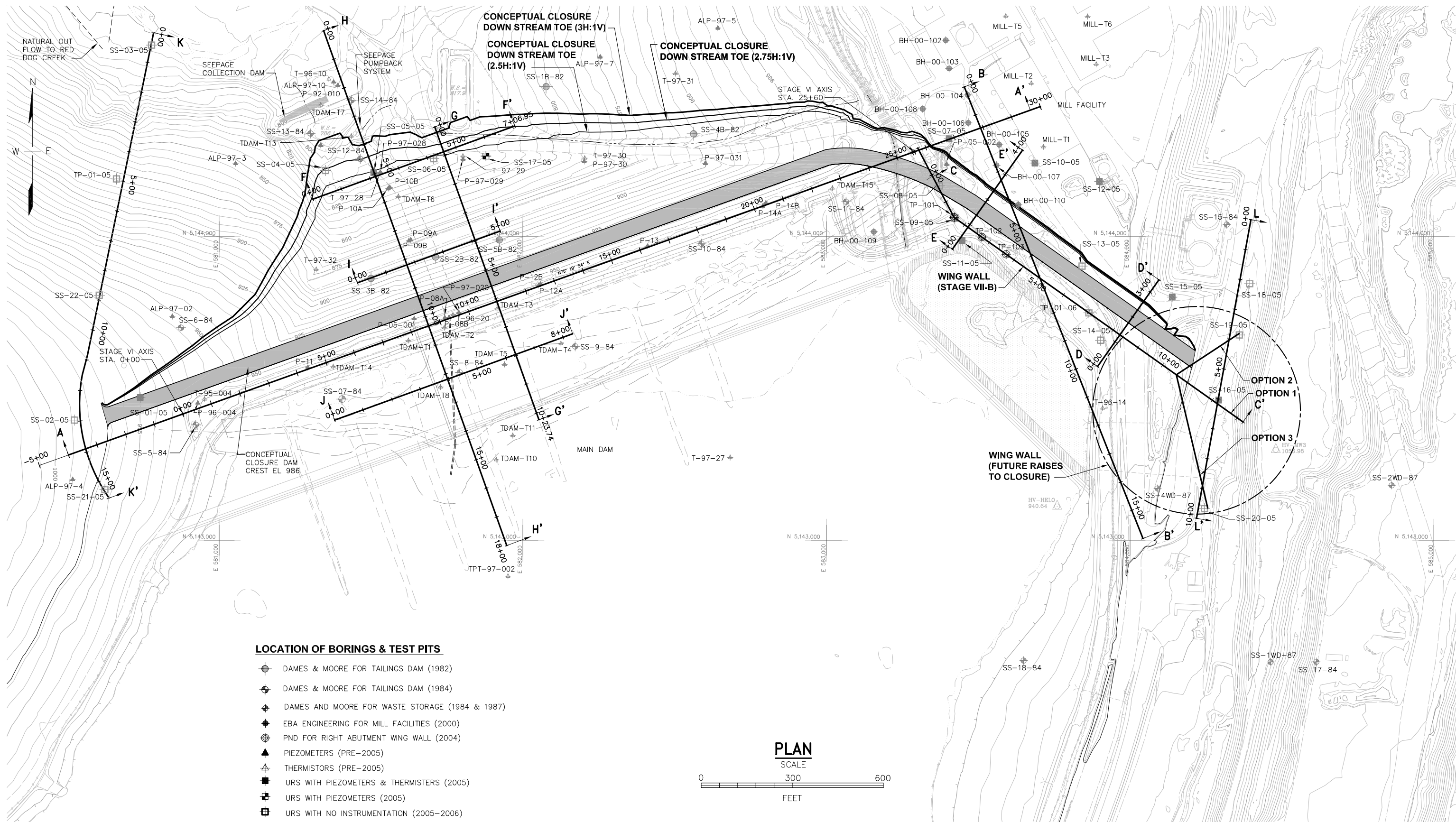
- Campbell, K.W. and Bozorgnia, Y., 2003, "Updated near-source ground-motion (attenuation) relations for the horizontal and vertical components of peak ground acceleration and acceleration response spectra:" Bull. Seis. Soc. Am., v. 93, no. 1, p. 314-331.
- Conetec, Inc. (Shawn Steiner), 2000, "CPT Results, Tailings Impoundment, Red Dog Mine, Alaska", March 21, 2000
- Cornell, C.A., 1968, "Engineering seismic risk analysis", Bulletin of the Seismological Society America v. 58, p. 1583-1605.
- Dames & Moore, 1986, "Design Report, Proposed Tailings Dam, Red Dog Mine Development", for Cominco Alaska, Inc., June 6, 1986.
- Dames & Moore, 1987a, "Construction Drawings, Tailings Impoundment Dam, Red Dog Project, Alaska, Revision 1", for Cominco Alaska, Inc., January 27, 1987.
- Dames & Moore, 1987b, "Waste Storage Areas Geotechnical Design Report", for Cominco Alaska, Inc., July 16, 1987.
- Dames & Moore, 1991a, "Geologic and Seismic Studies, Trans-Alaska Gas System, Anderson Bay LNG Terminal, Port Valdez, Alaska", for Yukon-Pacific Corporation, D&M Job No. 14930-018-128, 2 volumes, July 1991.
- Dames & Moore, 1991b, "Seismic Hazard Studies for the Anderson Bay Terminal of the Trans Alaska Gas System", for Yukon Pacific Corporation, July 1991.
- Dames & Moore, 1999, "Pipe Bench Stability Evaluation, Red Dog Tailings Dam", for Cominco Alaska, Inc., August 1999.
- Der Kuireghian, A., and Ang, A. H-S. ,1975, A fault rupture model for seismic risk analysis, Civil Engineering Studies, Structural Research Series No. 419, University of Illinois, Urbana.
- Franklin, A. G. and Chang, F.K., 1977, "Earthquake Resistance of Earth and Rock-Fill Dams: Permanent Displacement of Earth Embankments by Newmark Sliding Block Analysis, Miscellaneous Paper S-71-17, Report 5, U.S. Army Waterways Experiment Station, CE, Vicksburg, Mississippi.
- Golder Associates, 2003, "Detailed design, Tailings Impoundment -Back Dam, Red Dog Mine, Alaska, USA.", for Teck Cominco Alaska Incorporated, June 27, 2003.
- Harder, L. S. Jr., 1991, "Performance of earth dams during the Loma Prieta earthquake," Proc., 2nd Int. Conf. on Recent Adv. In Geotech. Earthquake Engineering and Soil Dynamics, University of Missouri, Rolla, Missouri.
- Hynes-Griffin, M.E., and Franklin, A.G.,1984, "Rationalizing the Seismic Coefficient Method", Miscellaneous Paper GL-84,-13, U.S. Army Corps of Engineers, Waterways Experiment Station, Vicksburg, Mississippi.
- Kramer, Steven. L., 1996, "Geotechnical Earthquake Engineering", Pearson Education, Inc.
- Makdisi, A.M., and Seed, H.B., 1977, "A Simplified Procedure for Computing Maximum Crest Acceleration and Natural Period for Embankments," Report No. UCB/EERC-77/19, Earthquake Engineering Research Center, University of California, Berkeley, California.
- Makdisi, A.M., and Seed, H.B., 1978, "Simplified Procedure for Estimating Dam and Embankment Earthquake-Induced Deformations," Journal of the Geotechnical Engineering Division, ASCE, Vol. 104, No. GT7, July, 1978, pp. 849-867.

- Martin, G. R. and Qiu, P., 1994, "Effects of Liquefaction Vulnerability Assessment," NCEER Highway Project on Seismic Vulnerability of New and Existing Highway Construction, Year one Research Tasks-Technical Research papers.
- Mueller, C., Frankel, A., Lahr, J, and Wyss, M., 1997, "Preparation of earthquake catalogs for the national seismic hazard maps: Alaska", USGS Draft Paper.
- National Research Council, 1983, "Safety of Existing Dams: Evaluation and Improvement.
- Newmark, N.M., 1965, "Effects of Earthquakes on Dams and Embankments", *Geotechnique*, 15(2), pp.139-160.
- Page, R.A., Biswas, N.N., Lahr, J.C., and Pulpan, H., 1991, "Seismicity of continental Alaska," in *Neotectonics of North America*, Geological Society of America, D.B. Slemmons (ed), p. 47-68.
- Plafker, G., Gilpin, L.M., and Lahr, J.C., 1994, "Neotectonic Map of Alaska," in G. Plafker and H.C. Berg (ed.), *The Geology of Alaska*, Geological Society of America, DNAG Volume G-1, Plate 12.
- Plafker, G., Lajoie, K.R. and Rubin, M., 1992, "Determining the recurrence intervals of great subduction zone earth-quakes in southern Alaska by radiocarbon dating, in Taylor, R.E., et. al., eds., *Radiocarbon after four decades*", An interdisciplinary perspective, New York, Springer Verlag, pp. 436-453.
- Rathje, E. M., Abrahamson, N. A., and Bray, J. D., 1998, "Simplified Frequency Content Estimates of Earthquake Ground Motions," *Journal of Geotechnical and Geoenvironmental Engineering*, Volume 124, No 2.
- Robertson, P. K, and Wride, C. E., 1997, "Cyclic liquefaction and its evaluation based on the SPT and CPT, "Proc. NCEER work shop on evaluation of liquefaction resistance of soils, Youd, T.L., NCEER 97-0022, pp. 41-88.
- SRK Consulting (Canada) Inc., 2006, "Red Dog Mine Closure Options, Volume 1 – Tailings," for Teck Cominco Alaska, March 20, 2006.
- SRK Consulting (Canada) Inc., 2005. "Tailings Closure Options, Red Dog Mine", for Teck Cominco Alaska, August 11, 2005.
- Swendseid, J., 2005 to 2007, "Personal communications regarding tailings discharge, instrumentation, inspections, maintenance and pumpback operations", Teck Cominco Alaska (TCAK).
- Teck Cominco Alaska, Inc, 2005, "Annual Instrumentation Report, Red Dog Tailings Dam, Red Dog Mine, to Alaska Department of Natural Resources", January 10, 2007 and previous editions.
- Teck Cominco Alaska, Inc.,, 2004, "Contour Drawings showing Cominco Topography", September 16, 2004.
- Teck Cominco Alaska Inc., 2002, "Red Dog Mine: Site Current Conditions", December 5, 2002
- URS Corporation, 2007a, "Dam History Report: Tailings Main Dam, Future Raises to Closure, Red Dog Mine, Alaska", for Teck Cominco Alaska Inc., February 26, 2007.
- URS Corporation, 2007b, "Seepage Analysis Report: Tailings Main Dam, Future Raises to Closure, Red Dog Mine, Alaska", for Teck Cominco Alaska Inc., February 26, 2007.
- URS Corporation, 2007c, "Conceptual Design Report: Tailings Main Dam, Future Raises to Closure, Red Dog Mine, Alaska", for Teck Cominco Alaska, Inc., 2007 (under completion).

- URS Corporation, 2006, “Geotechnical Investigation Report, Red Dog Tailings Main Dam, Future Raises to Closure”, Red Dog Mine, for Teck Cominco Alaska Inc., July 28, 2006.
- URS Corporation, 2005a, “Foundation Report, Red Dog Tailings Main Dam, Stage VII Raise, Red Dog Mine, Alaska” for Teck Cominco Alaska Inc., Red Dog Mine, Alaska, January 2005.
- URS Corporation, 2005b, “Construction Drawings, Tailings Dam, Stages VII-B”, for Teck Cominco Alaska Inc., Red Dog Mine, Alaska, May 2005.
- URS Corporation, 2005c, “Dam Periodic Safety Inspection (PSI) Report, Tailings Main Dam, Red Dog Mine, Alaska”, for Teck Cominco Alaska Inc., May 25, 2005.
- URS Corporation, 2005d, “Operations and Maintenance Manual Revision 4, Red Dog Tailings Dam, Red Dog Mine, Alaska”, for Teck Cominco Alaska, Inc., August 5, 2005.
- URS Corporation, 2005e, “Technical Memorandum: Conceptual Design of Tailings Main Dam and Back Dam at Closure”, for Teck Cominco Alaska Inc., April 8, 2005.
- URS Corporation, 2004a, “Construction Completion Report, Stage VII-A Raise, Red Dog Tailings Dam”, for Teck Cominco Alaska Inc., Red Dog Mine, Alaska, March 10, 2004.
- URS Corporation, 2004b, “Technical Memorandum: Review of Kivalina Shale Historic Permeability Test Data from Dames & Moore Reports”, for Teck Cominco Alaska Inc., December 13, 2004.
- URS Corporation, 2002a, “Stability Analysis Report, Stage VII Widening, Red Dog Tailings Dam”, for Teck Cominco Alaska Inc., Red Dog Mine, Alaska, December 19, 2002.
- URS Corporation, 2002b, “Stability Analysis Report, Stage VII Raise, Red Dog Tailings Dam”, for Teck Cominco Alaska Inc., Red Dog Mine, Alaska, December 19, 2002.
- URS Corporation, 2001, “Slope Stability Evaluation Report, Tailings Dam and Tailings, Beach Dust Control Structure, Red Dog Tailings Dam”, for Teck Cominco Alaska Inc., Red Dog Mine, Alaska, August 7, 2001.
- United States Geologic Survey, 2005, “Revision of time- independent probabilistic seismic hazard maps for Alaska” retrieved from [ftp://hazards.cr.usgs.gov/web/nshm/alaska\\_ti/](ftp://hazards.cr.usgs.gov/web/nshm/alaska_ti/).
- United States Geologic Survey, 1999, “Probabilistic seismic hazard maps for Alaska” retrieved from [http://earthquake.usgs.gov/hazmaps/products\\_data/Alaska/aks/pga1050.asc](http://earthquake.usgs.gov/hazmaps/products_data/Alaska/aks/pga1050.asc) and [http://earthquake.usgs.gov/hazmaps/products\\_data/Alaska/aks/pga0250.asc](http://earthquake.usgs.gov/hazmaps/products_data/Alaska/aks/pga0250.asc).
- United States Geologic Survey, 1996, “Interactive Deaggregations” retrieved from <http://eqint.cr.usgs.gov/eq-men/html/deaggint-06.html>.
- Washington State Department of Transportation, 2005, “Geotechnical Design Manual”, M46-03, September 2005.
- Water Management Consultants, 1999, “Report, Phase II Field work and Data Collection”, for Teck Cominco Alaska, March 1999.
- Weaver, J., 2005 to 2007, “Personal communications regarding groundwater and permafrost investigations and dam instrumentation, Geomatrix Consultants.
- Wesson, R.L., Frankel, A.D., Mueller, C.S., and Harmsen, S.C., 1999, “Probabilistic Seismic Hazard Maps of Alaska”.
- Wesson, R.L., Boyd, O.S., Mueller, C.S., Buff, C.G., Frankel, A.D., and Peterson, M.D., 2005, “Revision of Time-Independent Probabilistic Seismic Hazard Maps for Alaska,” USGS.

- Youd, T. L., Idriss, I. M., Andrus, R. D., Arango, I., Castro, G., Christian, J. T., Dobry, R., Finn, W. D. L., Harder, L. F. Jr., Hynes, M. E., Ishihara, K., Koester, J. P., Liao, S. S. C., Marcuson III, W. F., Martin, G. R., Mitchell, J. K., Moriwaki, Y., Power, M. S., Robertson, P. K., Seed, R. B., and Stokoe II, K. H., 2001, "Liquefaction Resistance of Soils: Summary Report from the 1996 NCEER and 1998 NCEER/NSF Workshops on Evaluation of Liquefaction Resistance of Soils", Journal of Geotechnical and Geoenvironmental Engineering, October 2001.
- Youngs, R.R., Chiou, S.J., Silva, W.J., and Humphrey, J.R., 1997, Strong ground motion attenuation relationships for subduction zone earthquakes: Seismological Research Letters, vol. 68, no. 1, Seismological Society of America, p.58-73.

# FIGURES



**LOCATION OF BORINGS & TEST PITS**

- DAMES & MOORE FOR TAILINGS DAM (1982)
- DAMES & MOORE FOR TAILINGS DAM (1984)
- DAMES AND MOORE FOR WASTE STORAGE (1984 & 1987)
- EBA ENGINEERING FOR MILL FACILITIES (2000)
- PND FOR RIGHT ABUTMENT WING WALL (2004)
- ▲ PIEZOMETERS (PRE-2005)
- ▲ THERMISTORS (PRE-2005)
- URS WITH PIEZOMETERS & THERMISTERS (2005)
- URS WITH PIEZOMETERS (2005)
- URS WITH NO INSTRUMENTATION (2005-2006)

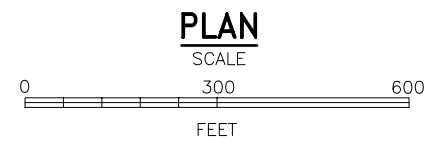
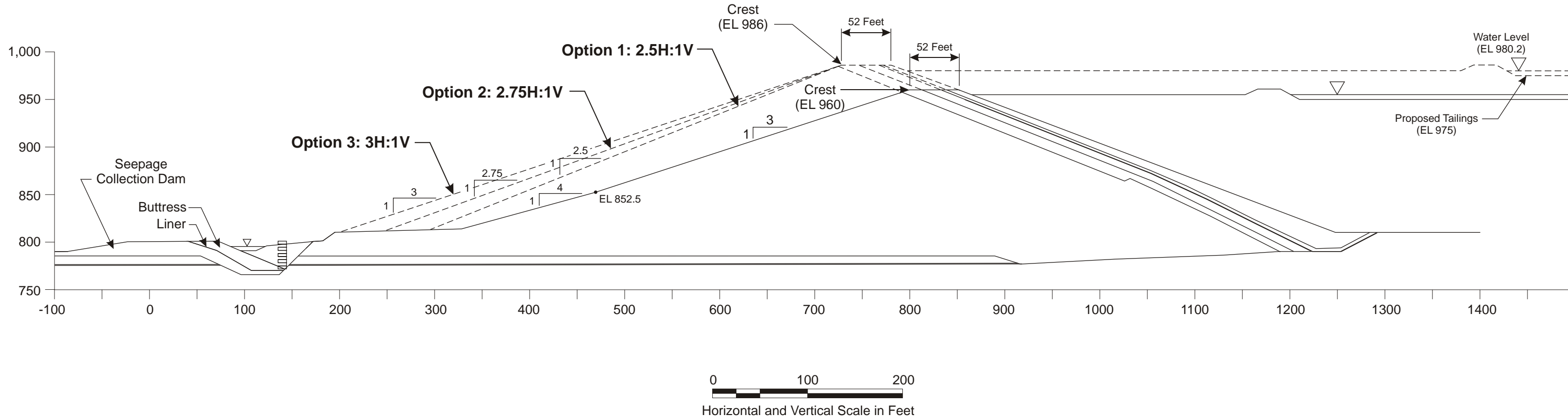
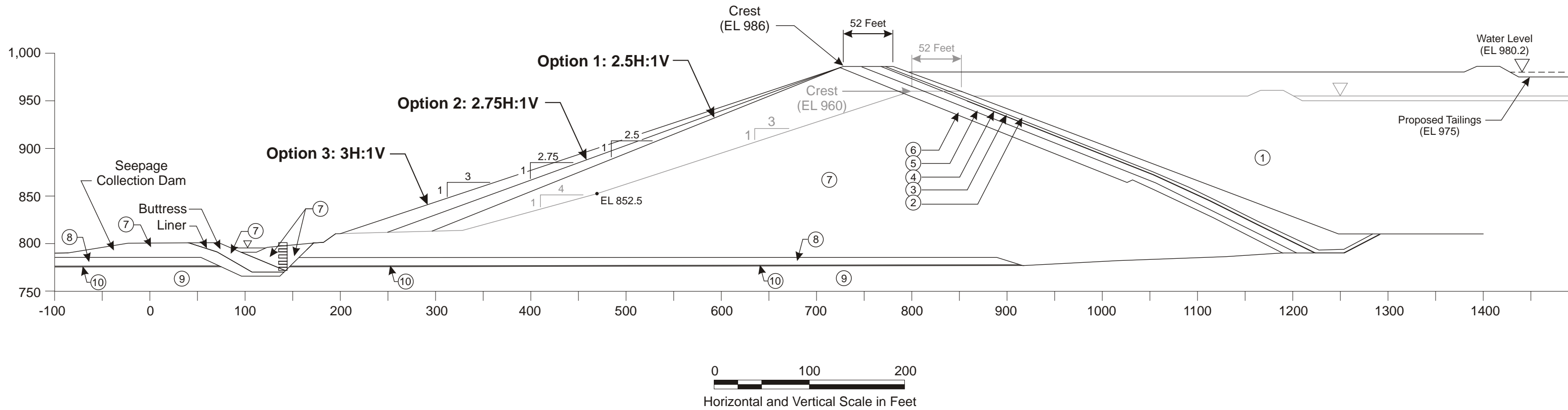


Figure 4-1  
**Site Plan and Location of Soil Profiles  
(Conceptual Design)**

Stability Analysis of Tailings Main Dam  
Future Raises to Closure  
Red Dog Mine, Alaska







Material Types and Parameters				
Material	Density		Effective Shear Strength Parameters	
	Moist (pcf)	Sat (pcf)	Cohesion c(pcf)	Friction Angle
1. Tailings Beach	120	120	0	30
2. Buttress	135	140	0	35
3. Liner Bedding	125	138	0	35
4. Liner	115	115	0	24
5. Filter Drain	125	138	0	35
6. Transition Rockfill	125	138	0	35
7. Random Rockfill	135	140	0	35
8. Highly Weathered Shale	115	115	0	30
9. Shale	145	150	0	35
10. Gouge	120	120	0	22

P:\ACAD\PROJECT\TechComincoAlaska\Stability Report\Figures\Figure-4-4.dwg Sep 08, 2006 - 1:58pm

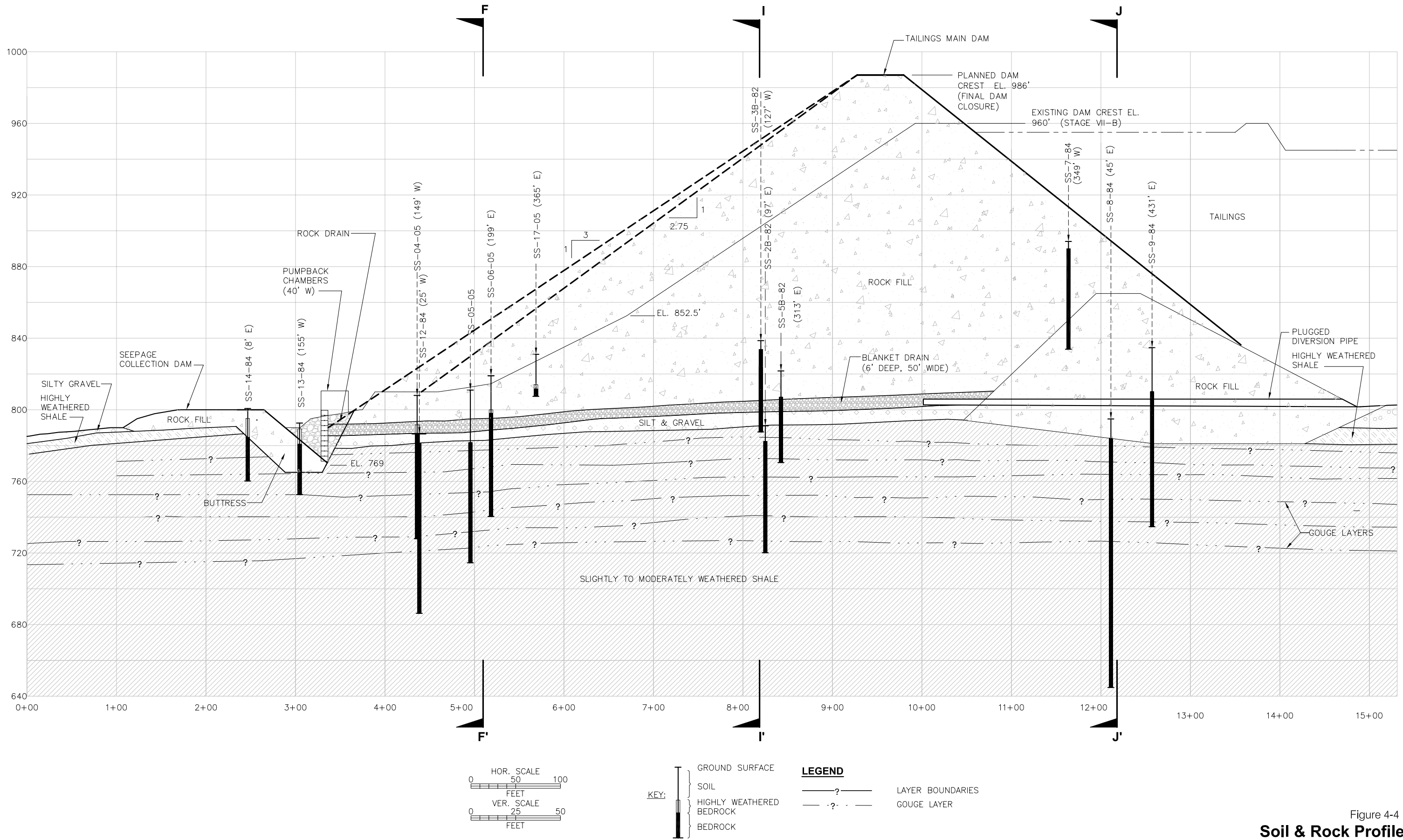
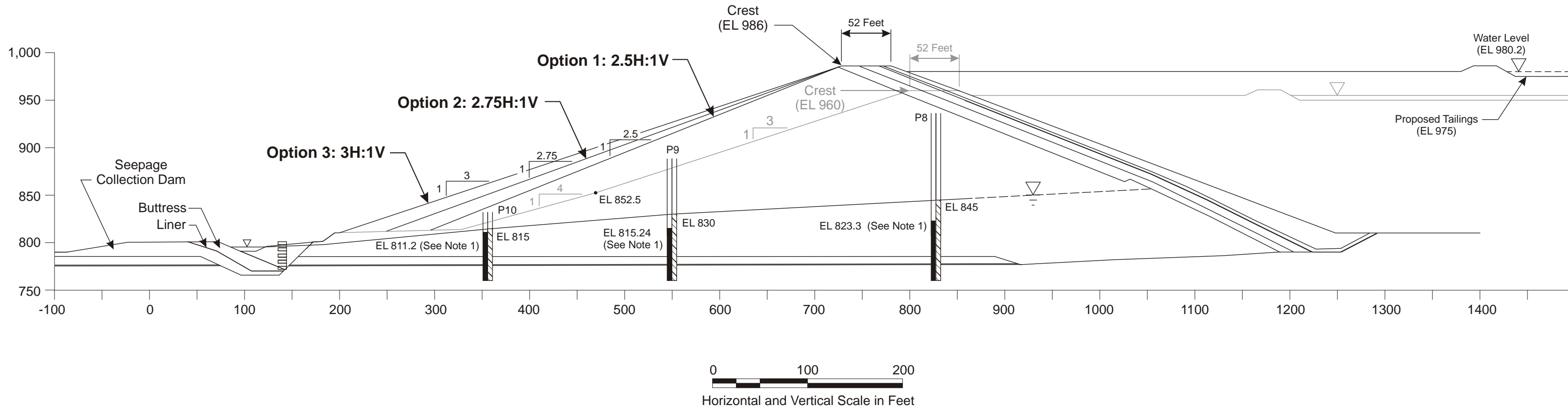


Figure 4-4  
**Soil & Rock Profile  
 (Cross Section H-H')**

Stability Analysis of Tailings Main Dam  
 Future Raises to Closure  
 Red Dog Mine, Alaska

Job Number: 33757098.00001





**LEGEND**

- Maximum recorded water level (Stage VII-B)
- Design water level (closure)

**NOTE**

1. Maximum recorded phreatic levels shown correspond to operational conditions and dam configuration present till 2005 and do not reflect the potential phreatic surfaces for closure configuration and operations.

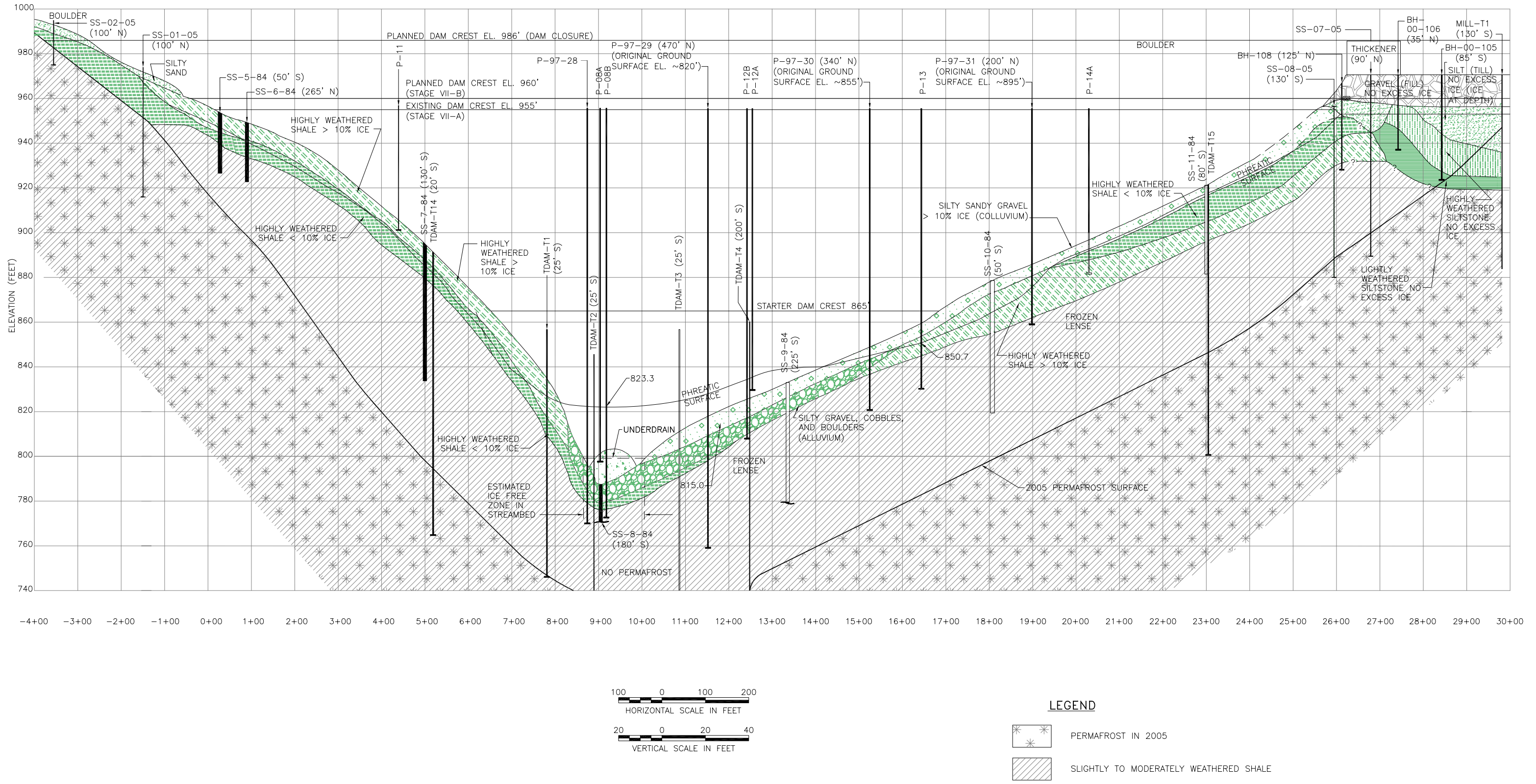


Figure 4-6  
**Permafrost and Phreatic Profile along Dam Crest**

Stability Analysis of Tailings Main Dam  
Future Raises to Closure  
Red Dog Mine, Alaska



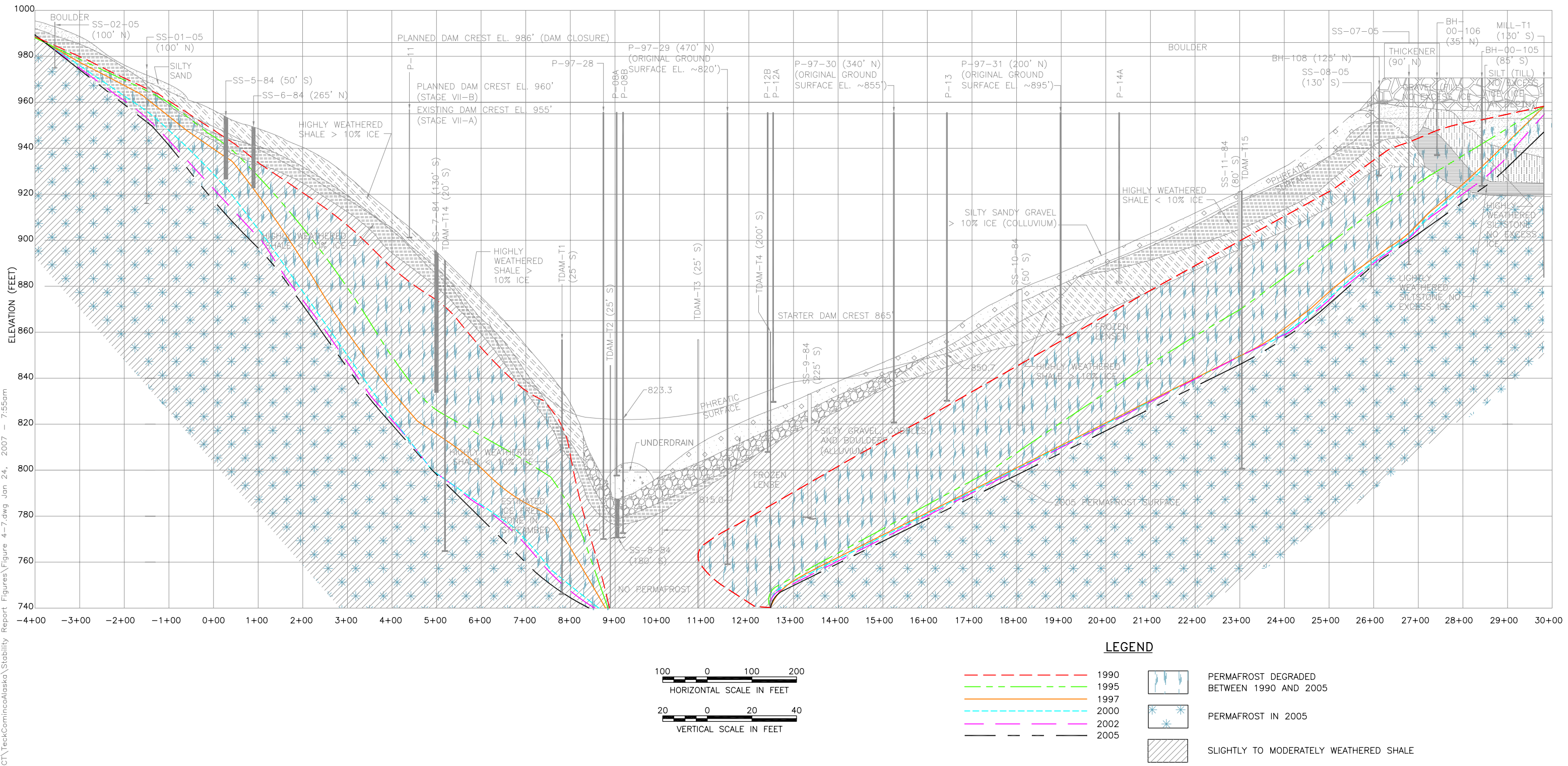
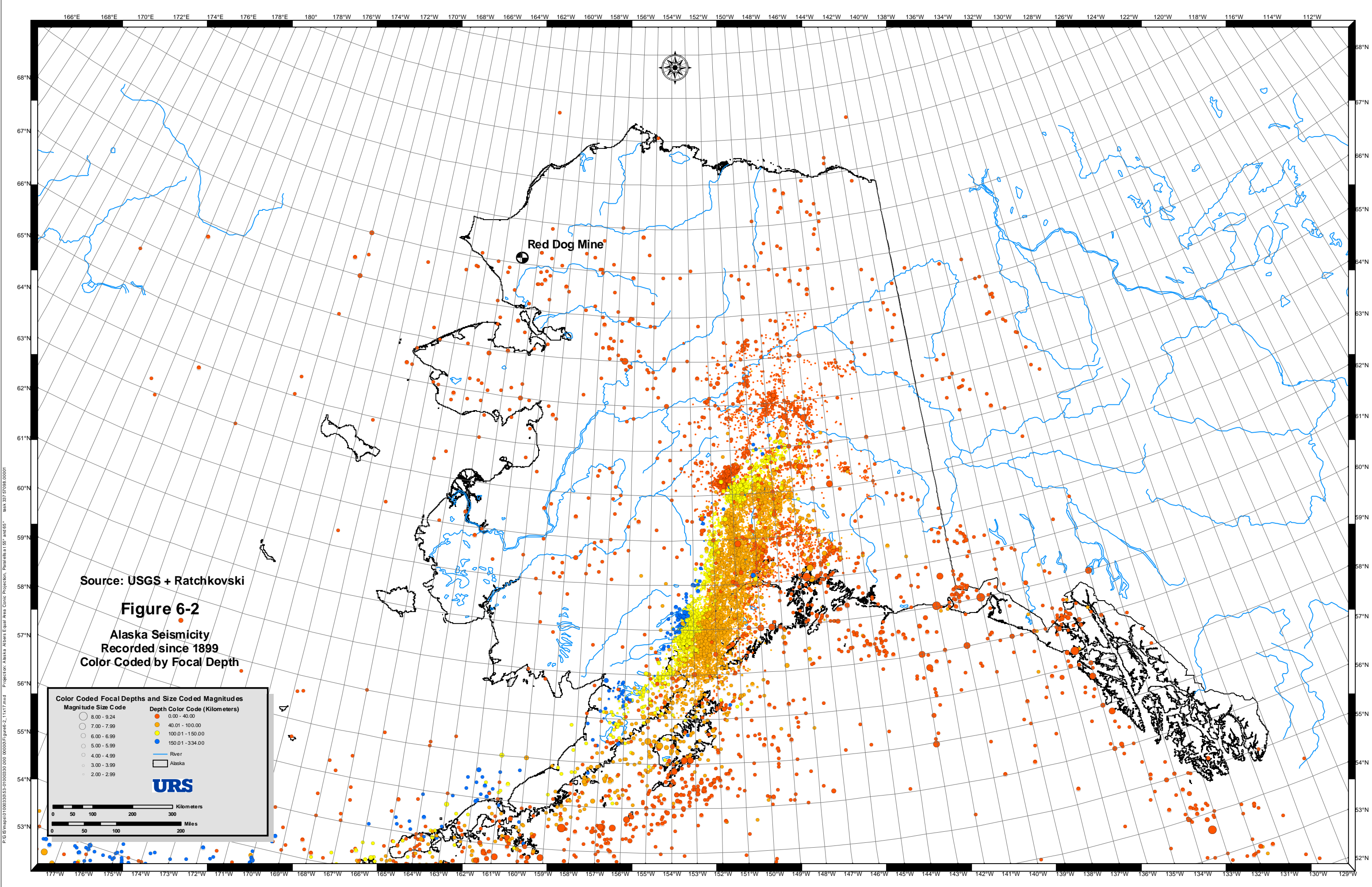


Figure 4-7  
**Historical Permafrost Degradation along Dam Crest**  
 Stability Analysis of Tailings Main Dam  
 Future Raises to Closure  
 Red Dog Mine, Alaska







Source: USGS + Ratchkovski

**Figure 6-2**  
**Alaska Seismicity**  
**Recorded since 1899**  
**Color Coded by Focal Depth**

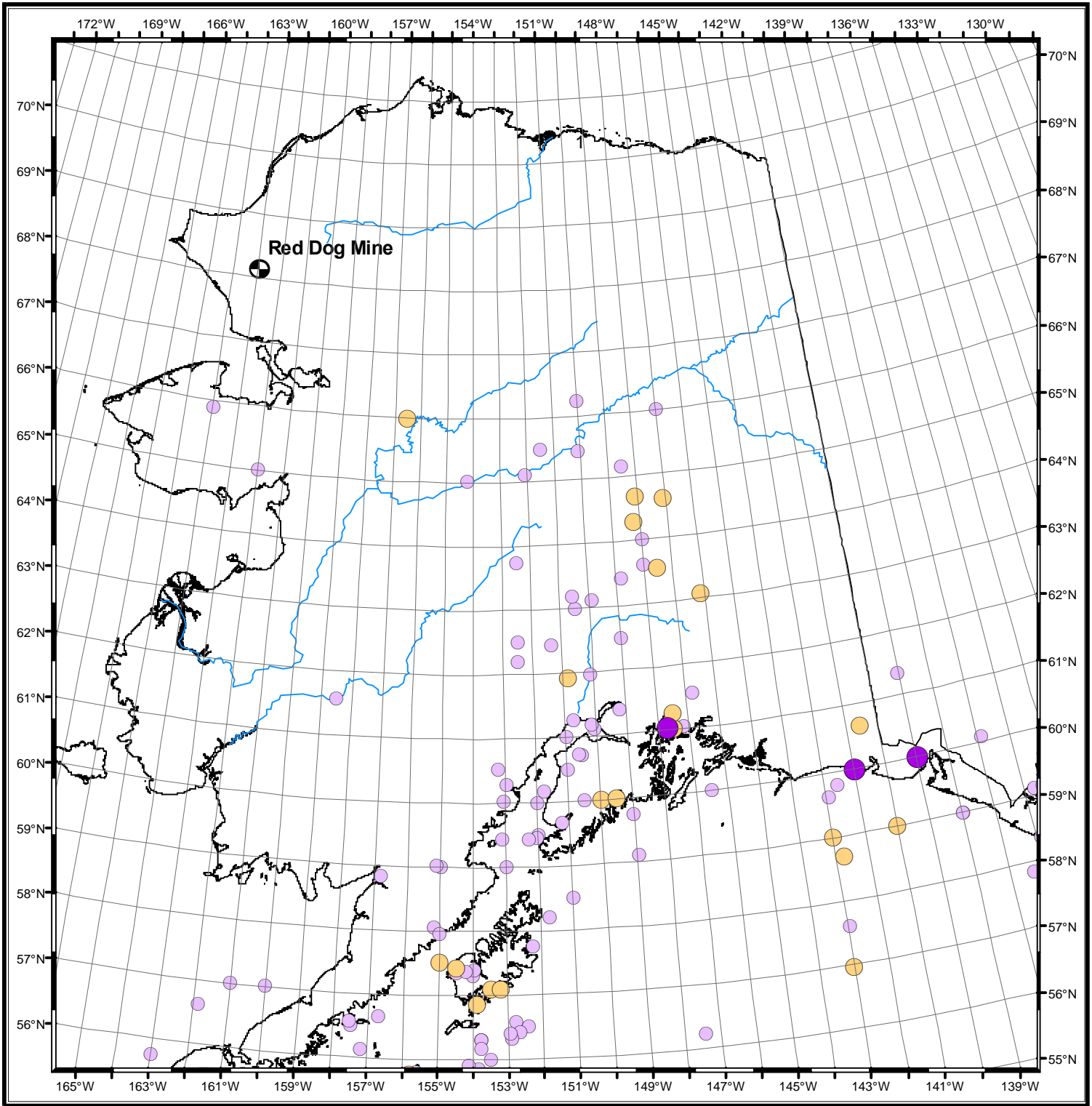
**Color Coded Focal Depths and Size Coded Magnitudes**

Magnitude Size Code	Depth Color Code (Kilometers)
○ 8.00 - 9.24	● 0.00 - 40.00
○ 7.00 - 7.99	● 40.01 - 100.00
○ 6.00 - 6.99	● 100.01 - 150.00
○ 5.00 - 5.99	● 150.01 - 334.00
○ 4.00 - 4.99	— River
○ 3.00 - 3.99	▭ Alaska
○ 2.00 - 2.99	

**URS**

0 50 100 200 300 Kilometers  
 0 50 100 200 Miles

P:\GIS\maps\010003303-01000330 0000000\Figures\2\_11x17.mxd Projection: Alaska Albers Equal Area Conic Projection, Pseudo at 15° and 65° task:33757098.00001



Projection: Alaska - Albers Equal Area Conic Projection, Parallels at 55° and 65°

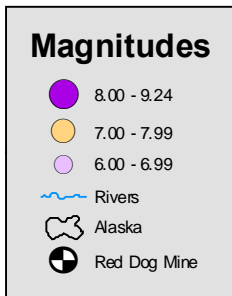
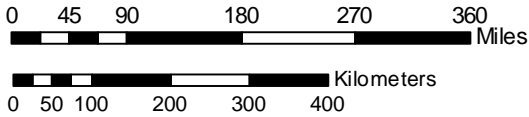


Figure 6-3

## Alaska Seismicity, $M \geq 6$

Job No. 33757098



P:\GIS\mapas\01000033\03-0100 0330\_000 000000\fig ure 6-3\_AK\_S seismicity.mxd

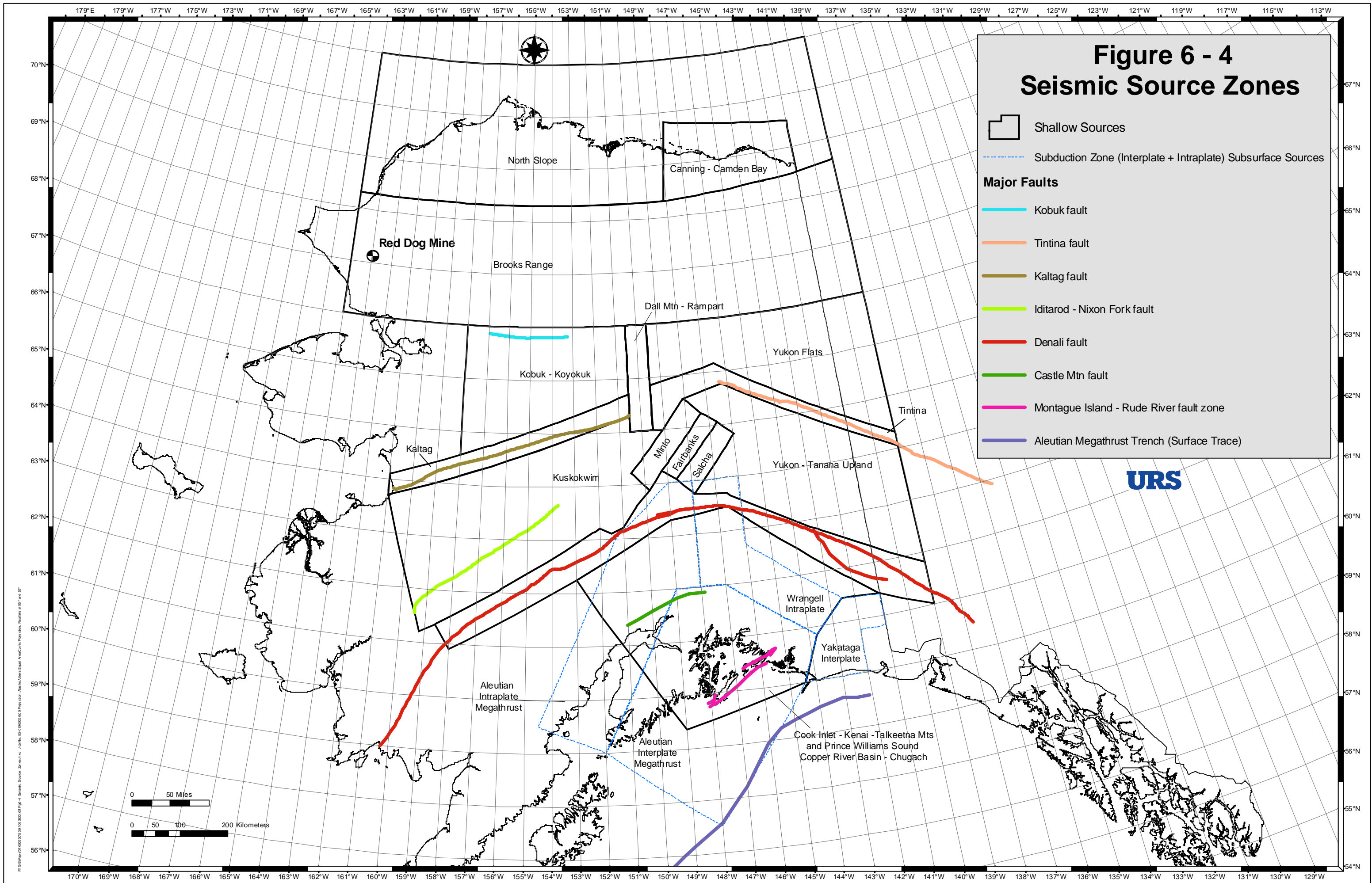
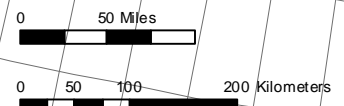


**Figure 6 - 4  
Seismic Source Zones**

- Shallow Sources
- Subduction Zone (Interplate + Intraplate) Subsurface Sources
- Major Faults**
- Kobuk fault
- Tintina fault
- Kaltag fault
- Iditarod - Nixon Fork fault
- Denali fault
- Castle Mtn fault
- Montague Island - Rude River fault zone
- Aleutian Megathrust Trench (Surface Trace)



**URS**

P:\GIS\Map\1000000000\1000000000\_001\Fig-4\_Seismic\_Sources\_Zones.mxd J:\Info\_03\1000000000\Fig-4\_Seismic\_Sources\_Zones.mxd, Resolved at 05/11/07

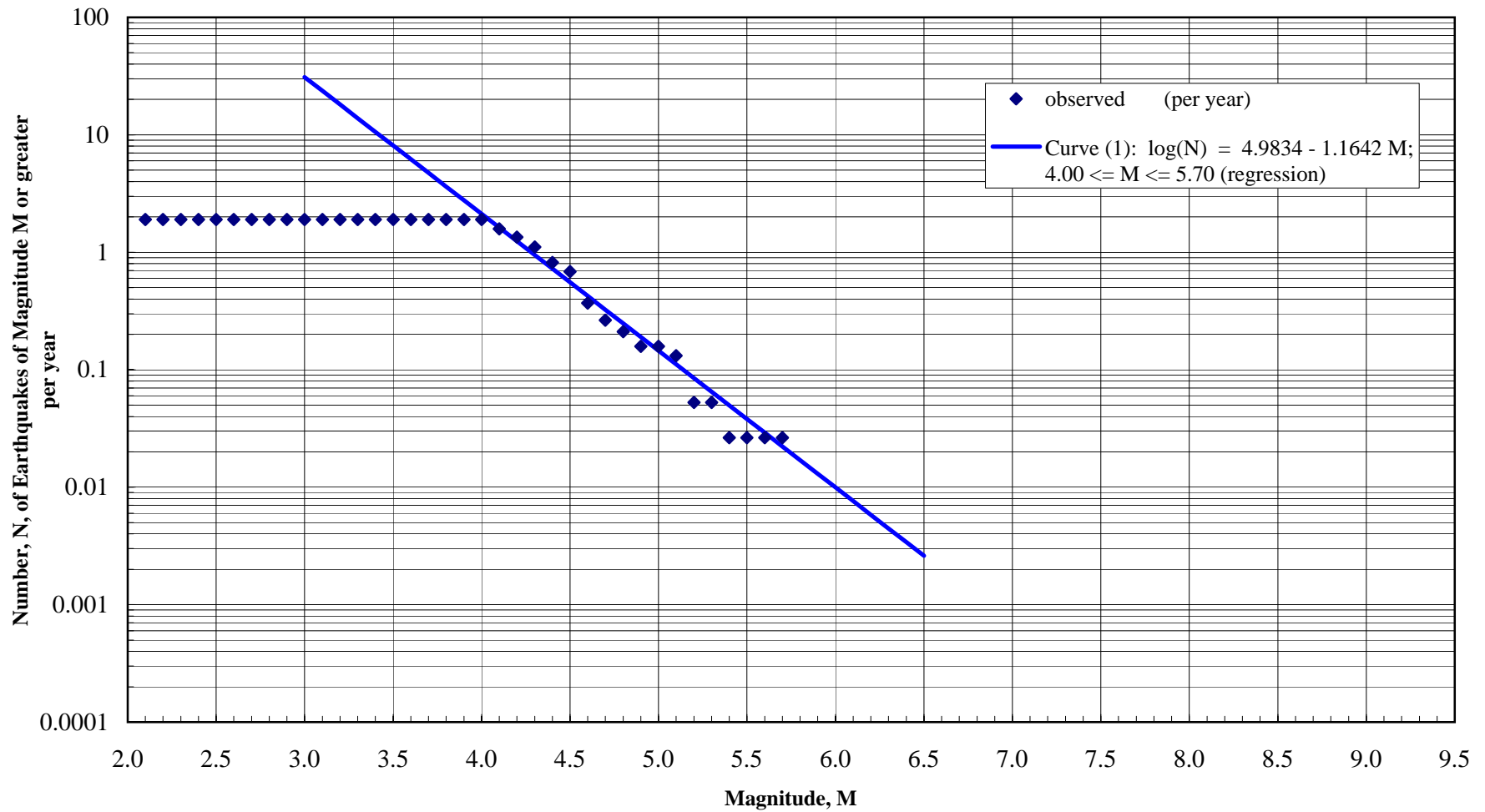


Figure 6-5

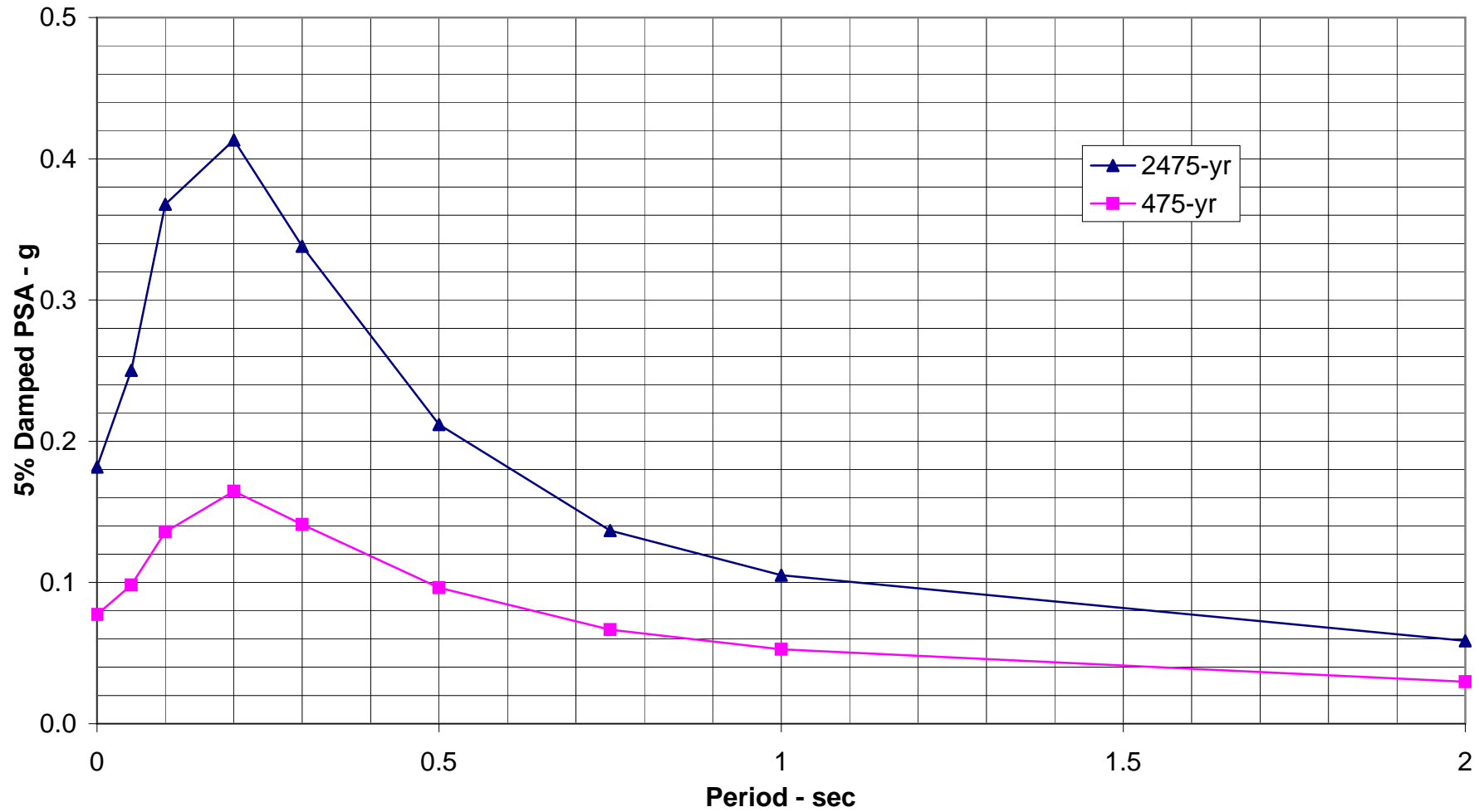


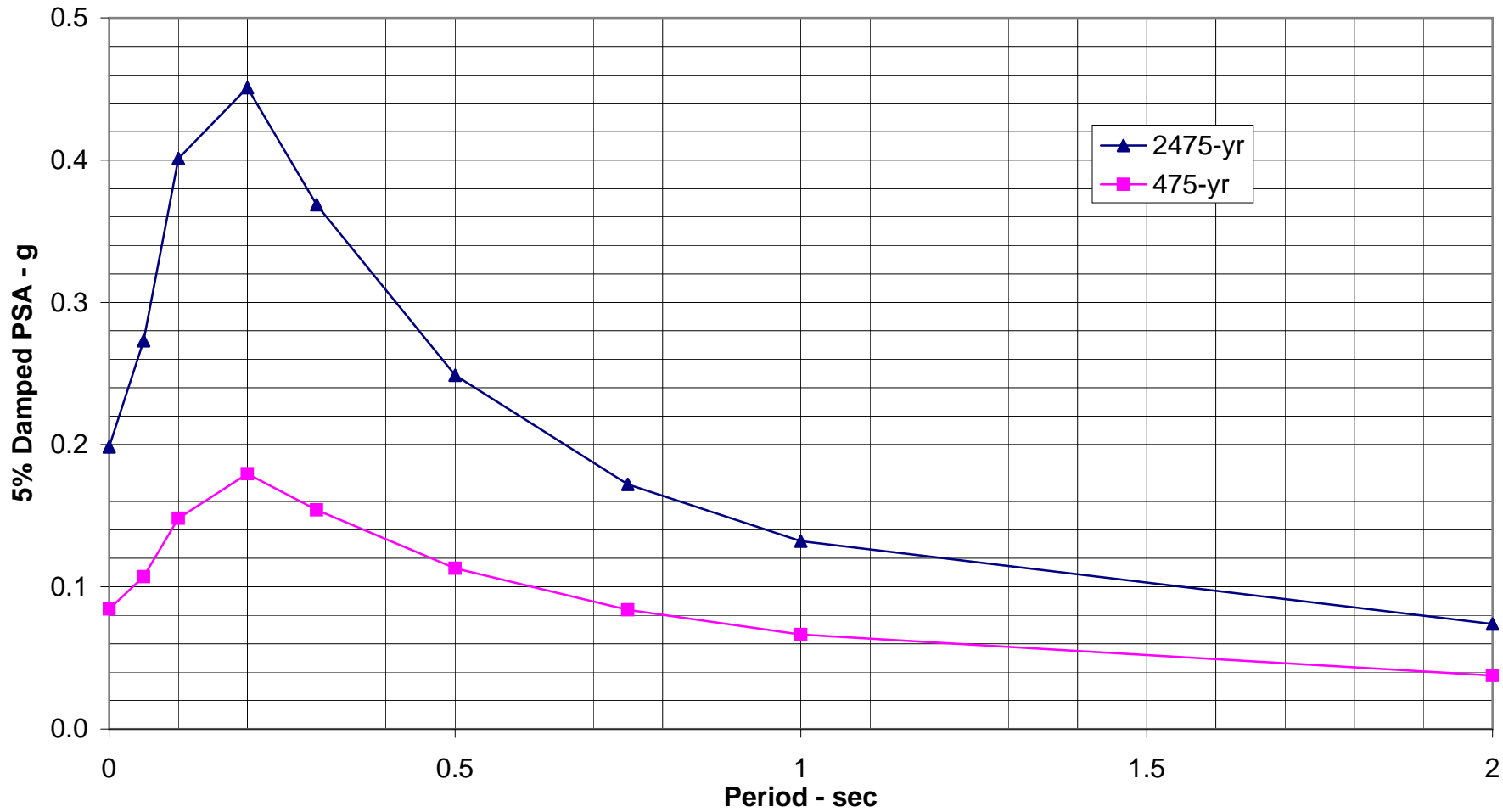
Figure 6-6

**Site-Specific Bedrock Response Spectra**

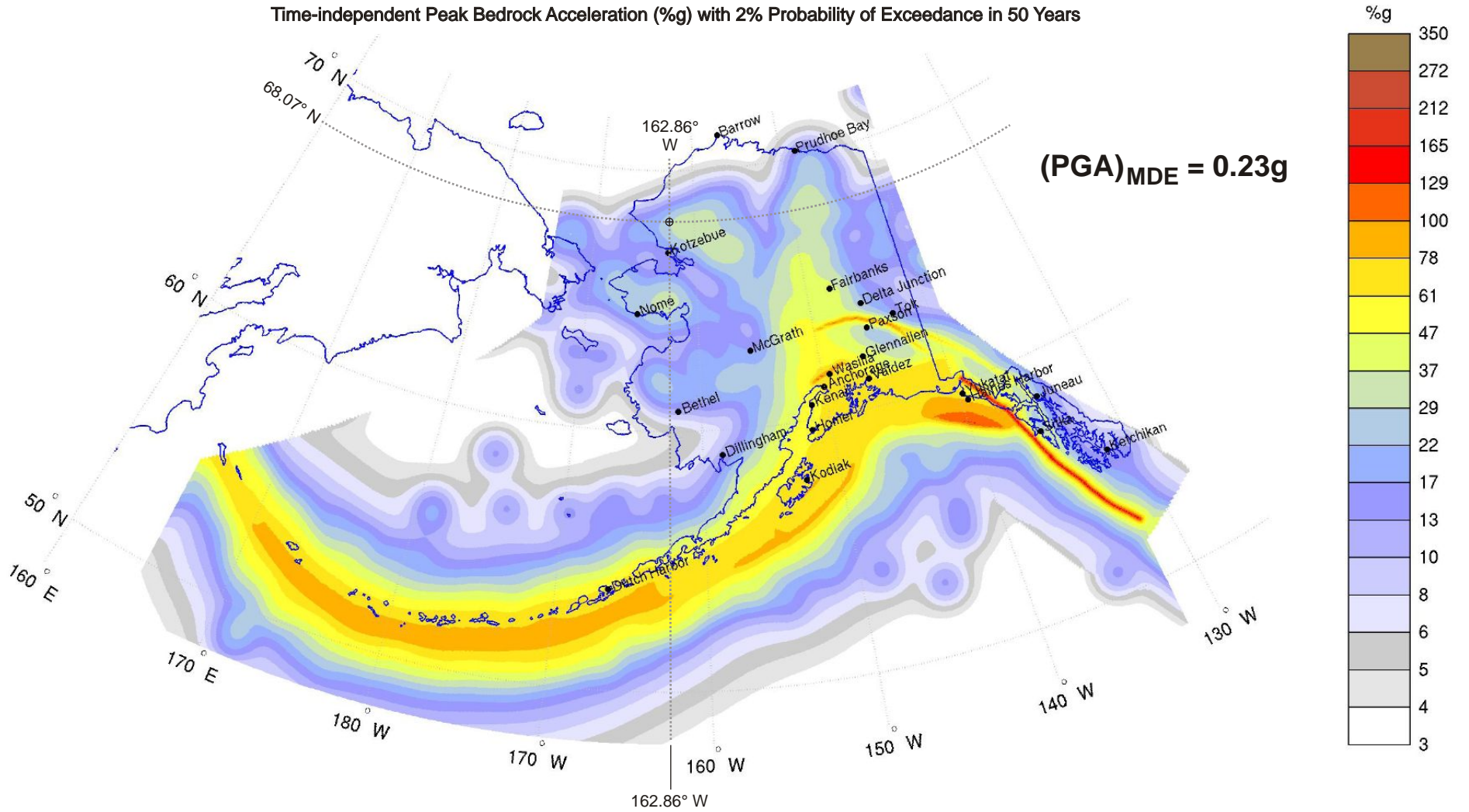
Stability Analysis of Tailings Main Dam

Future Raises to Closure

Red Dog Mine, Alaska





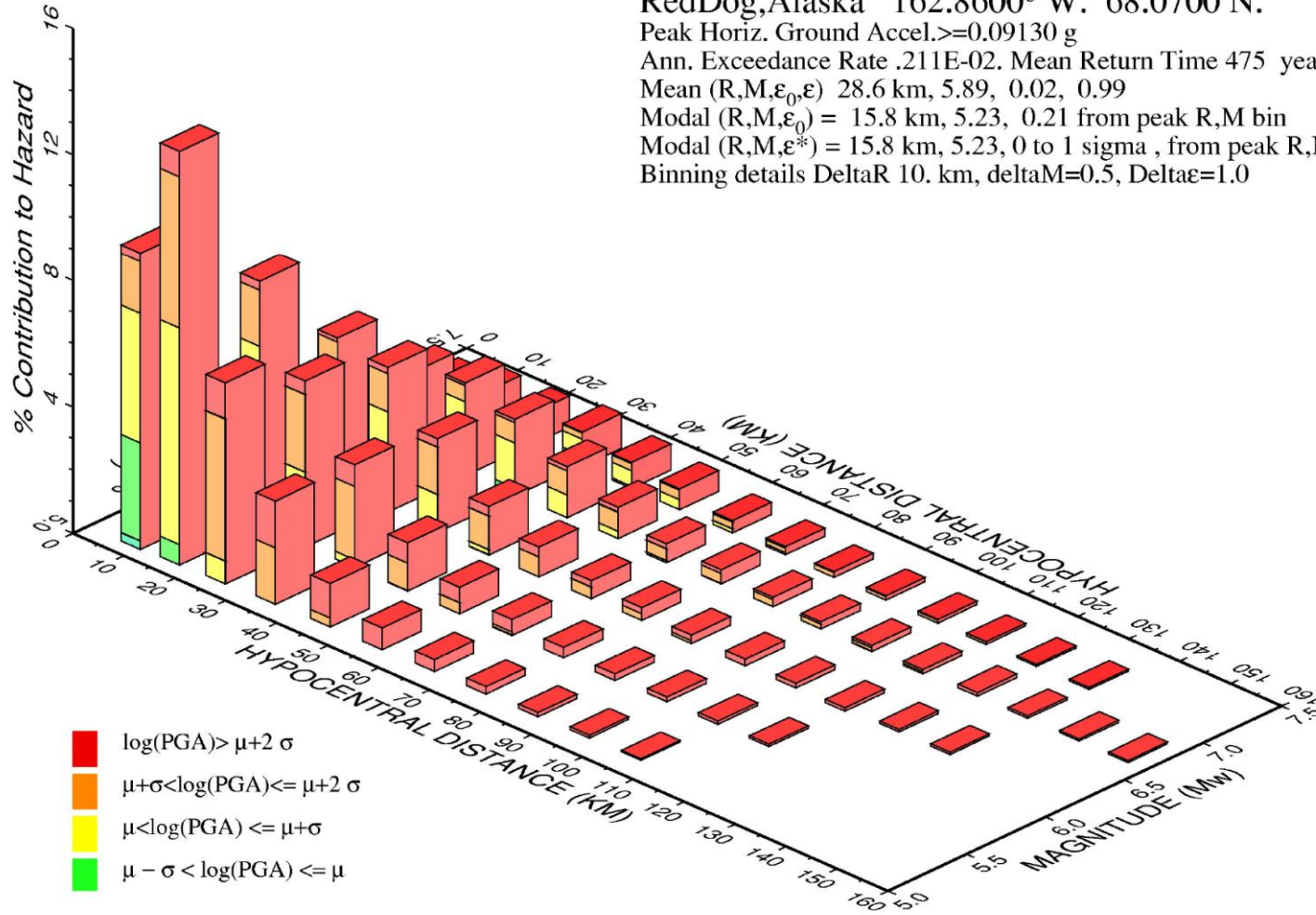


SOURCE:  
USGS Seismic Hazard Maps for Alaska, Draft 2005 for Comment  
(Wesson, R.L. et al., Revision of Time-Independent Probabilistic  
Seismic Hazard Maps for Alaska, 2005)

Job No. 33757098

Figure 7-2  
**Seismic Hazard Map for MDE**

**Prob. Seismic Hazard Deaggregation**  
**RedDog, Alaska 162.8600° W. 68.0700 N.**  
 Peak Horiz. Ground Accel.  $\geq 0.09130$  g  
 Ann. Exceedance Rate .211E-02. Mean Return Time 475 years  
 Mean (R,M, $\epsilon_0$ , $\epsilon$ ) 28.6 km, 5.89, 0.02, 0.99  
 Modal (R,M, $\epsilon_0$ ) = 15.8 km, 5.23, 0.21 from peak R,M bin  
 Modal (R,M, $\epsilon^*$ ) = 15.8 km, 5.23, 0 to 1 sigma, from peak R,M, $\epsilon$   
 Binning details DeltaR 10. km, deltaM=0.5, Delta $\epsilon$ =1.0



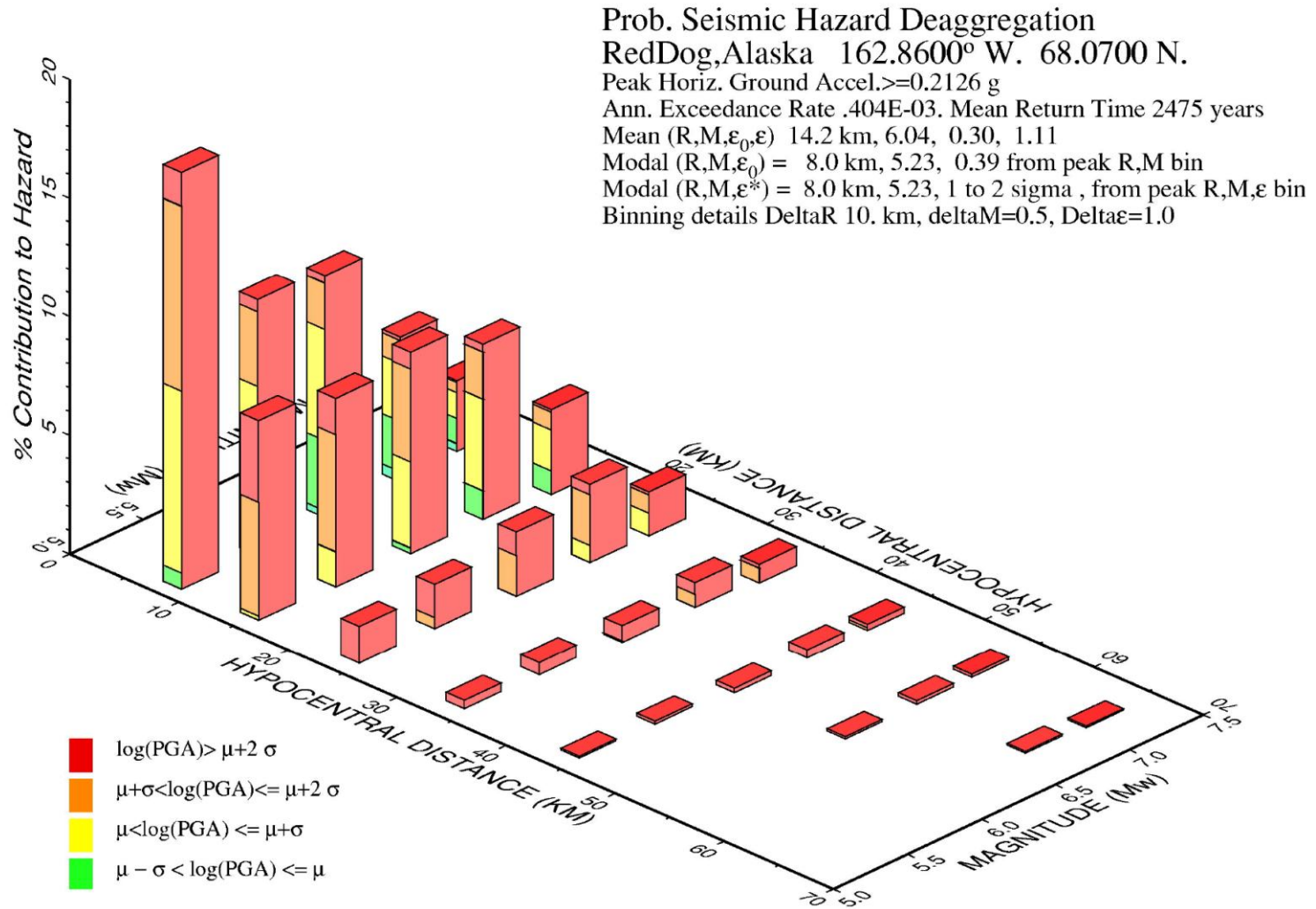
GMT Feb 16 10:46 Distance (R), magnitude (M), epsilon (E0,E) deaggregation for a site on rock with average vs=760m/s top 30 m. USGS CGHT PSHA From OFR 99-36. Bins with lt 0.05% contrib. omitted

SOURCE:  
 USGS Web Page, Interactive Deaggregations, 1996

Job No. 33757098

Figure 7-3  
**Probabilistic Seismic Hazard Deaggregation for OBE**





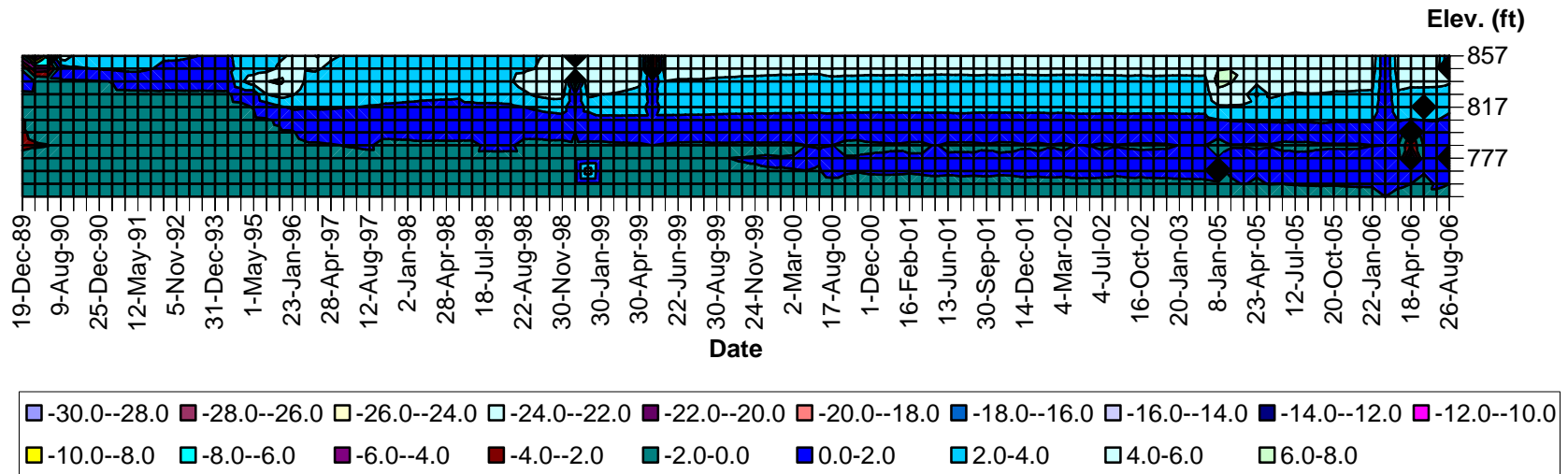
**GMT** Feb 16 10:45 Distance (R), magnitude (M), epsilon (E0,E) deaggregation for a site on rock with average vs=760m/s top 30 m. USGS CGHT PSHA From OFR 99-36. Bins with lt 0.05% contrib. omitted

SOURCE:  
 USGS Web Page, Interactive Deaggregations, 1996

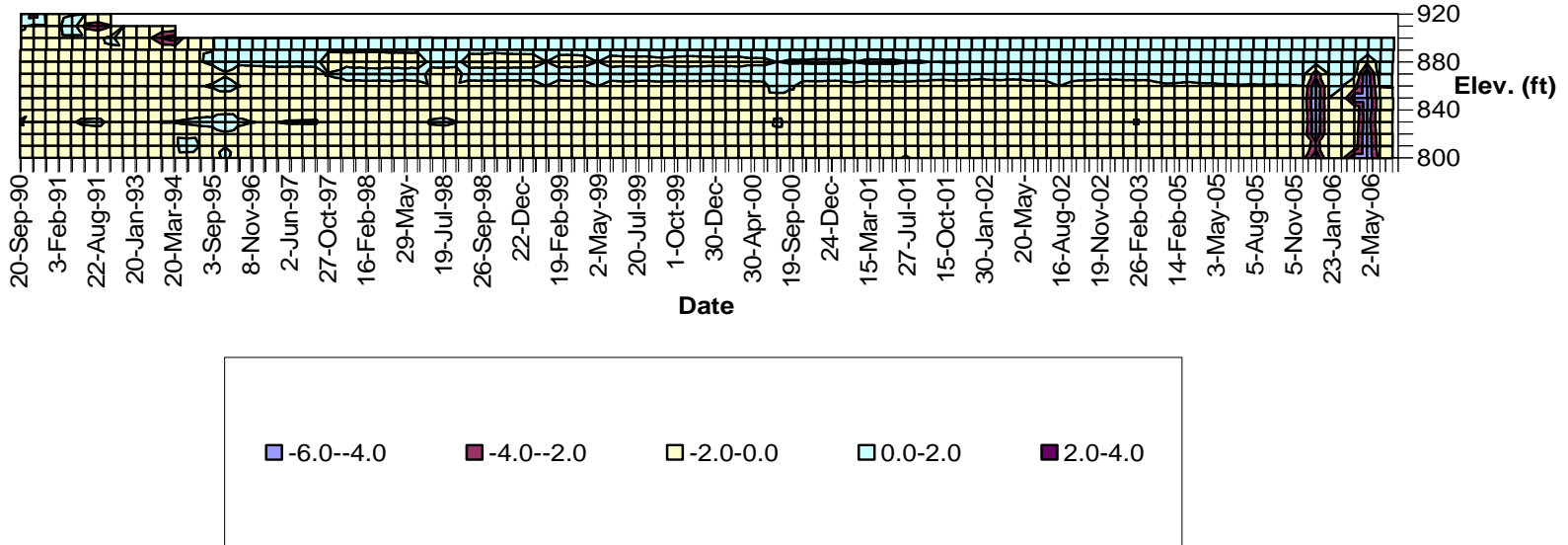
Job No. 33757098

Figure 7-4  
**Probabilistic Seismic Hazard Deaggregation for MDE**

# TDAM-T1



# TDAM-T15



URS Job No. 33757098



Figure 7-6  
**Historical Temperature Profile at Thermistor TDAM – T15**

Stability Analysis of Tailings Main Dam  
 Future Raises to Closure  
 Red Dog Mine, Alaska

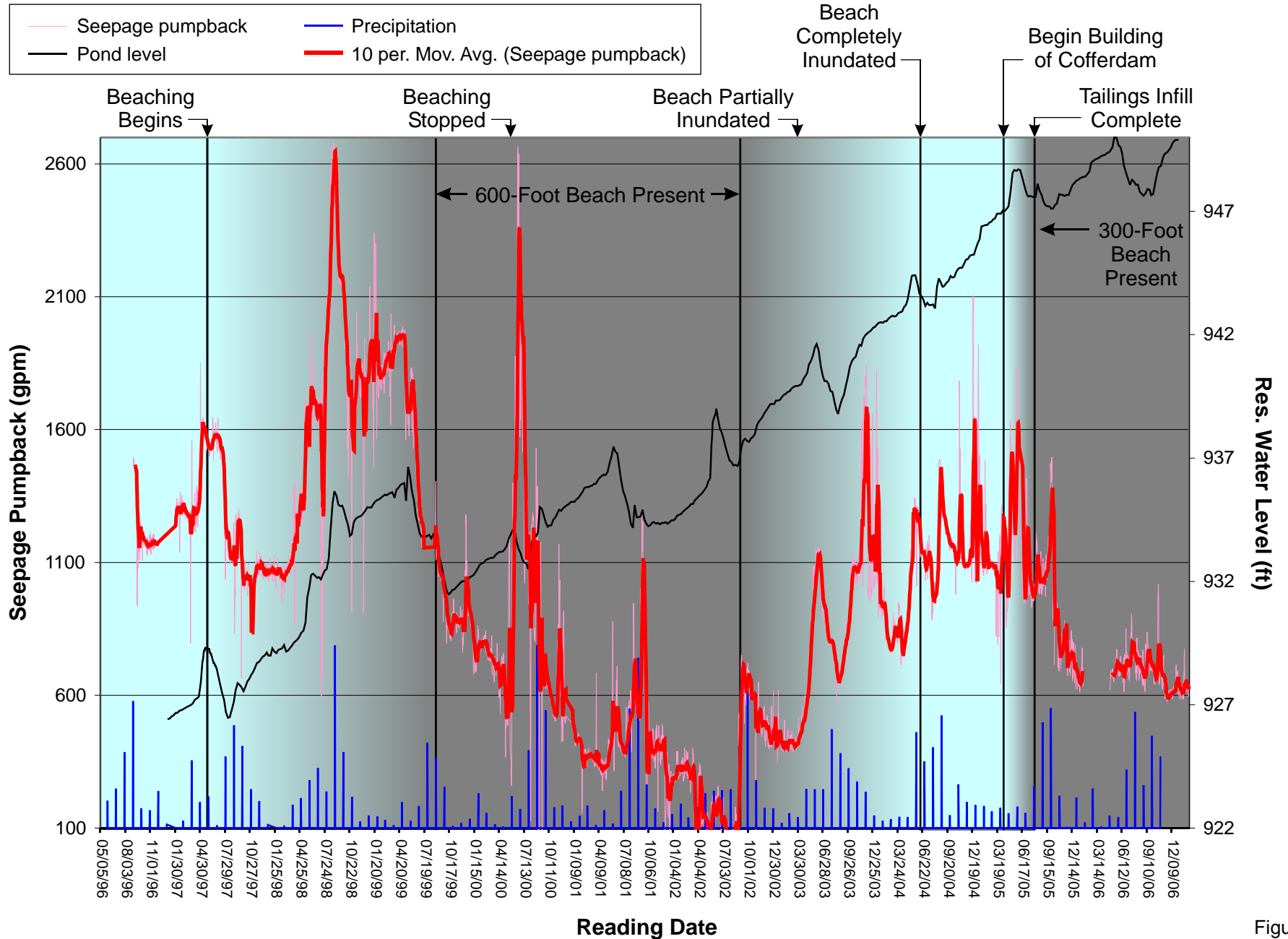


Figure 7-7  
**Historical Effectiveness of Tailings Beach on Seepage**

**Analysis Conditions:**  
 Downstream Slope 2.75H:1V  
 Failure Surface (Block/Circular): Block  
 Loading (Static/Seismic OBE/Seismic MDE): Seismic MDE  
 Long Term (LT)/ End of Construction (EOC) : LT

0.997

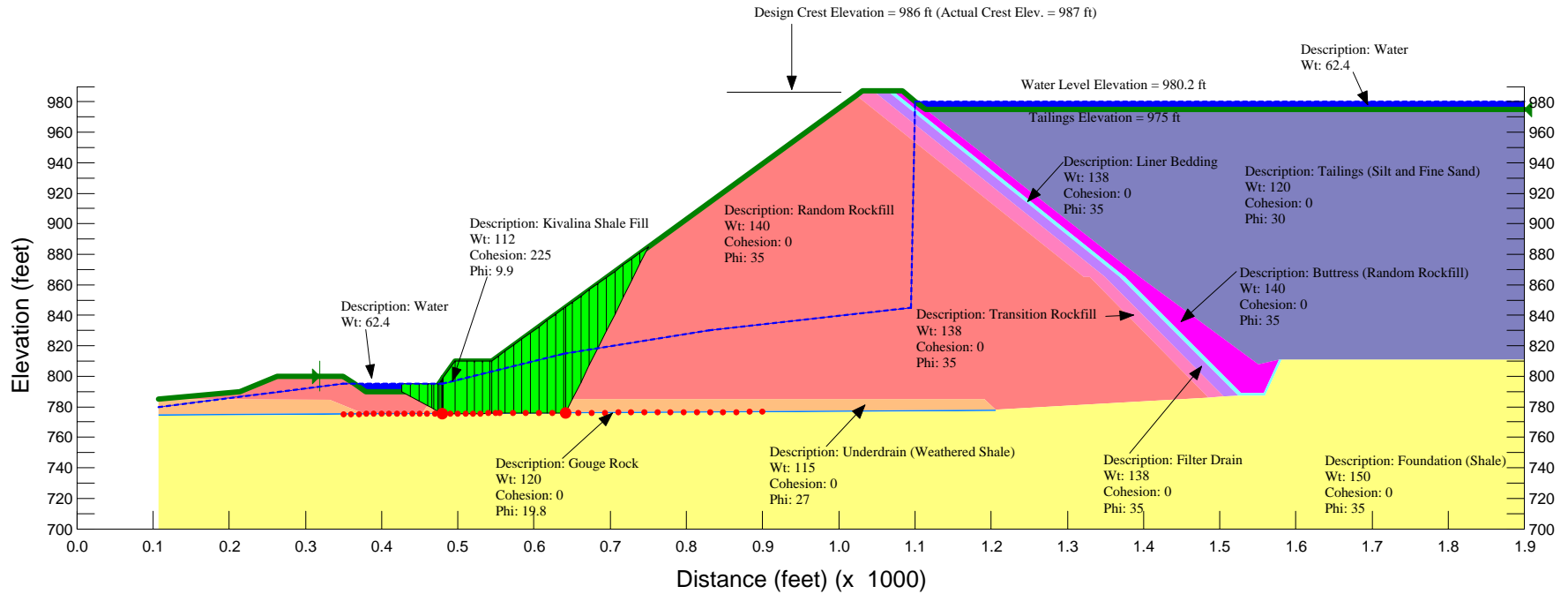


Figure 7-8

Critical Block Failure Surface - 2.75H:1V with Berm for Long Term Condition under MDE Loading

URS Project No.: 33757098

URS

G:\Red Dog Mine\Mine Closure & Reclamation\Tailings Main Dam\Main Dam Stability\Main Dam Closure Stability 2006\Slope 2.75 to 1\reduce shear strength\RedDog Block Seismic MCE=125 Ru=0 (Fig 7-8).gsz  
 Last Saved Date: 9/28/2006  
 Last Saved Time: 1:56:07 PM

Stability Analysis of Tailings Main Dam  
 Future Raises to Closure  
 Red Dog Mine, Alaska

**Analysis Conditions:**  
 Downstream Slope 2.75H:1V  
 Failure Surface (Block/Circular): **Block**  
 Loading (Static/Seismic OBE/Seismic MDE): Seismic MDE  
 Long Term (LT)/ End of Construction (EOC) : LT

0.955

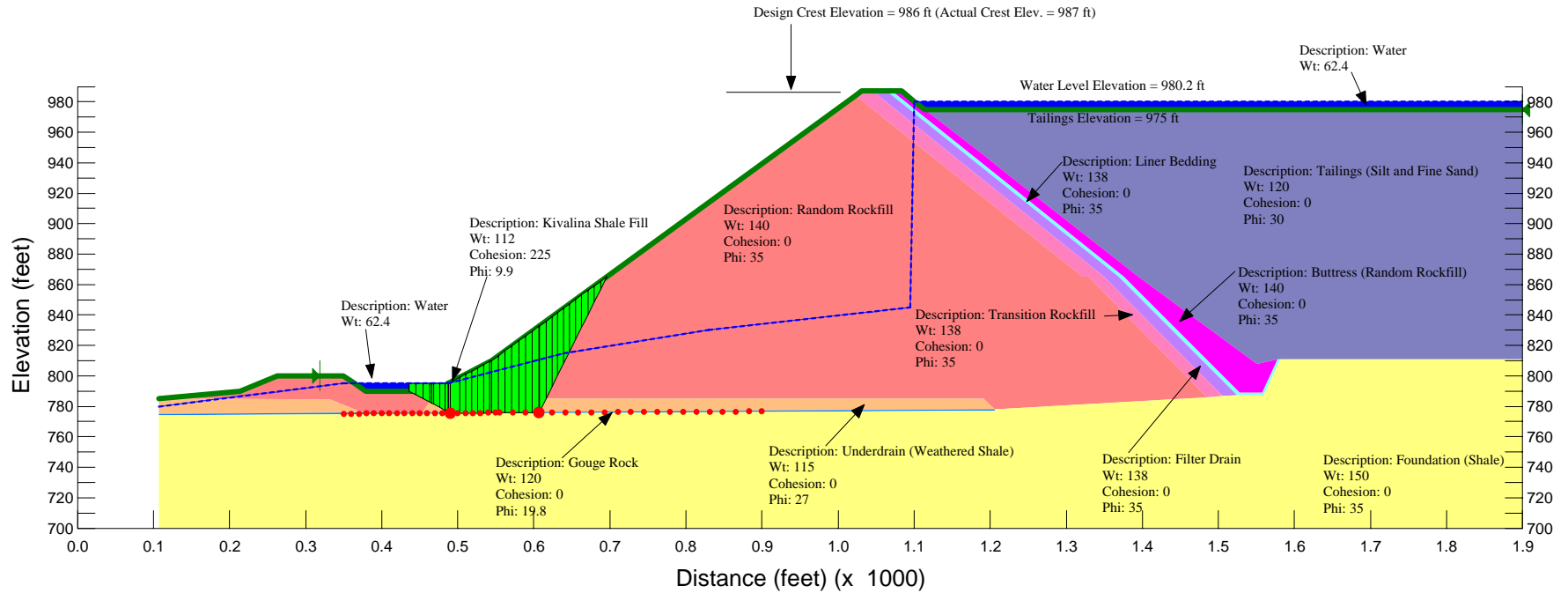


Figure 7-9

Critical Block Failure Surface - 2.75H:1V without Berm for Long Term Condition under MDE Loading

URS Project No.: 33757098

URS

G:\Red Dog Mine\Mine Closure & Reclamation\Tailings Main Dam\Main Dam Stability\Main Dam Closure Stability 2006\Slope 2.75 to 1\ reduce shear strength\RedDog Block Seismic MCE=.125 Ru=0 With Out Berm(Fig 7-9).gsx  
 Last Saved Date: 9/28/2006  
 Last Saved Time: 1:26:30 PM

Stability Analysis of Tailings Main Dam  
 Future Raises to Closure  
 Red Dog Mine, Alaska

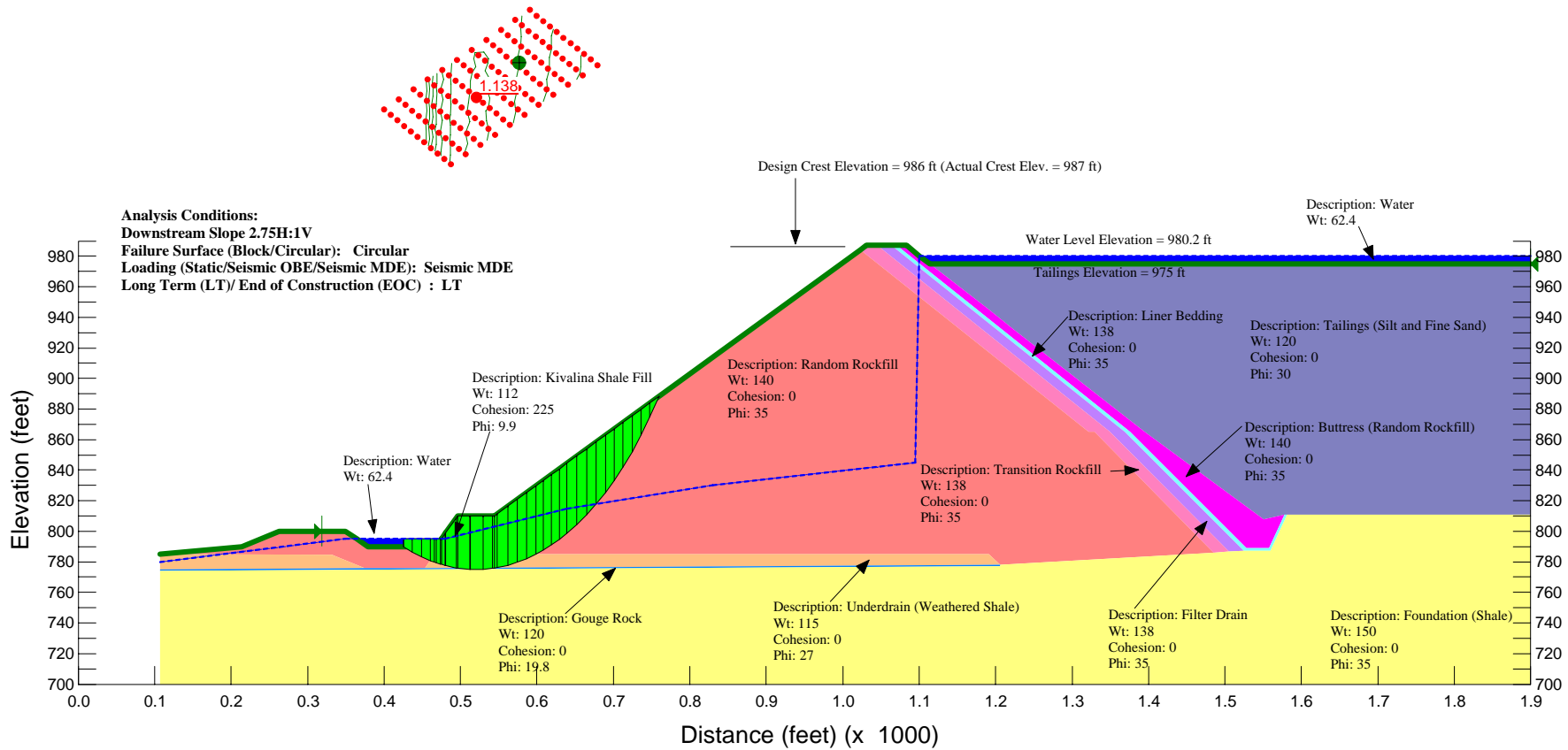


Figure 7-10

URS Project No.: 33757098

Critical Circular Failure Surface - 2.75H:1V with Berm for Long Term Condition under MDE Loading

URS

G:\Red Dog Mine\Mine Closure & Reclamation\Tailings Main Dam>Main Dam Stability/Main Dam Closure Stability 2006\Slope 2.75 to 1, reduce shear strength\RedDog Circular Seismic MCE=125 Ru=0\Fig 7-10).gsx  
 Last Saved Date: 9/28/2006  
 Last Saved Time: 1:51:13 PM

Stability Analysis of Tailings Main Dam  
 Future Raises to Closure  
 Red Dog Mine, Alaska

**Analysis Conditions:**  
 Downstream Slope 2.75H:1V  
 Failure Surface (Block/Circular): Circular  
 Loading (Static/Seismic OBE/Seismic MDE): Seismic MDE  
 Long Term (LT)/ End of Construction (EOC) : LT

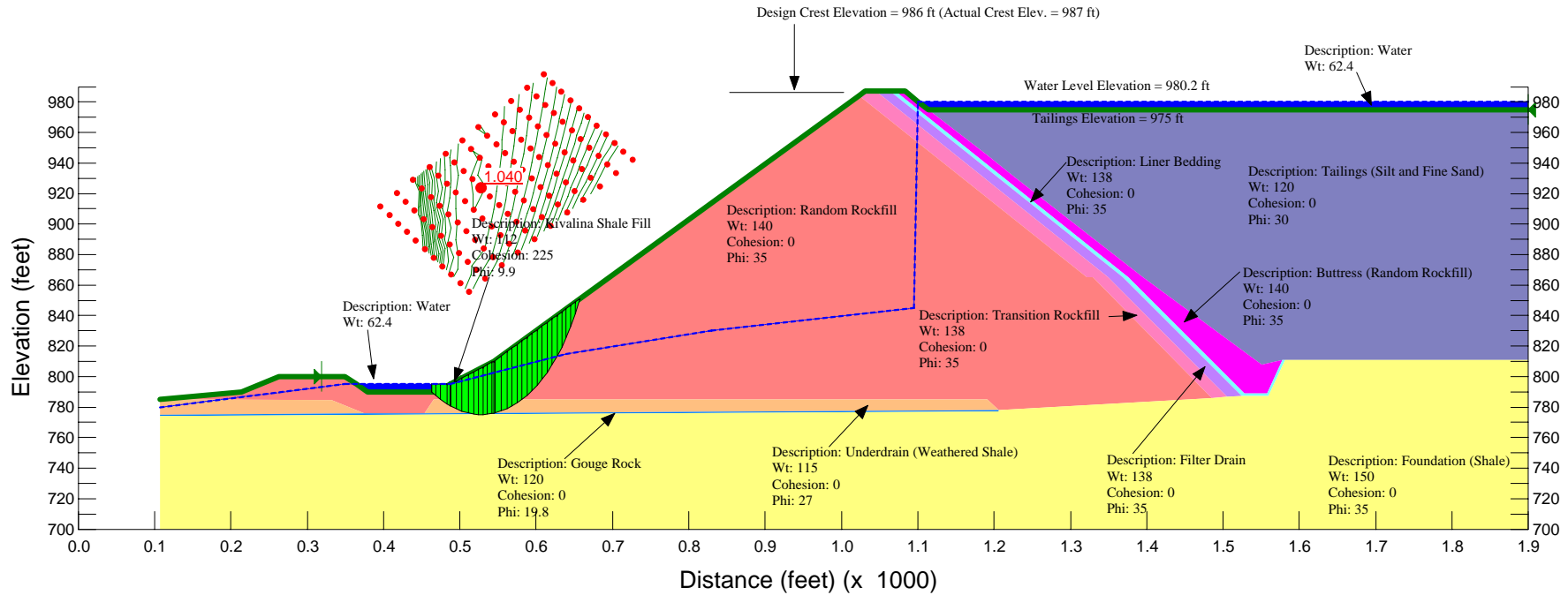


Figure 7-11

URS Project No.: 33757098

Critical Circular Failure Surface - 2.75H:1V without Berm for Long Term Condition under MDE Loading

URS

G:\Red Dog Mine\Mine Closure & Reclamation\Tailings Main Dam\Main Dam Stability\Main Dam Closure Stability 2006\Slope 2.75 to 1\reduce shear strength\RedDog Circular Seismic MCE=1.25 Ru=0 With Out Berm(Fig 7-11).gsz  
 Last Saved Date: 9/28/2006  
 Last Saved Time: 1:54:23 PM

Stability Analysis of Tailings Main Dam  
 Future Raises to Closure  
 Red Dog Mine, Alaska

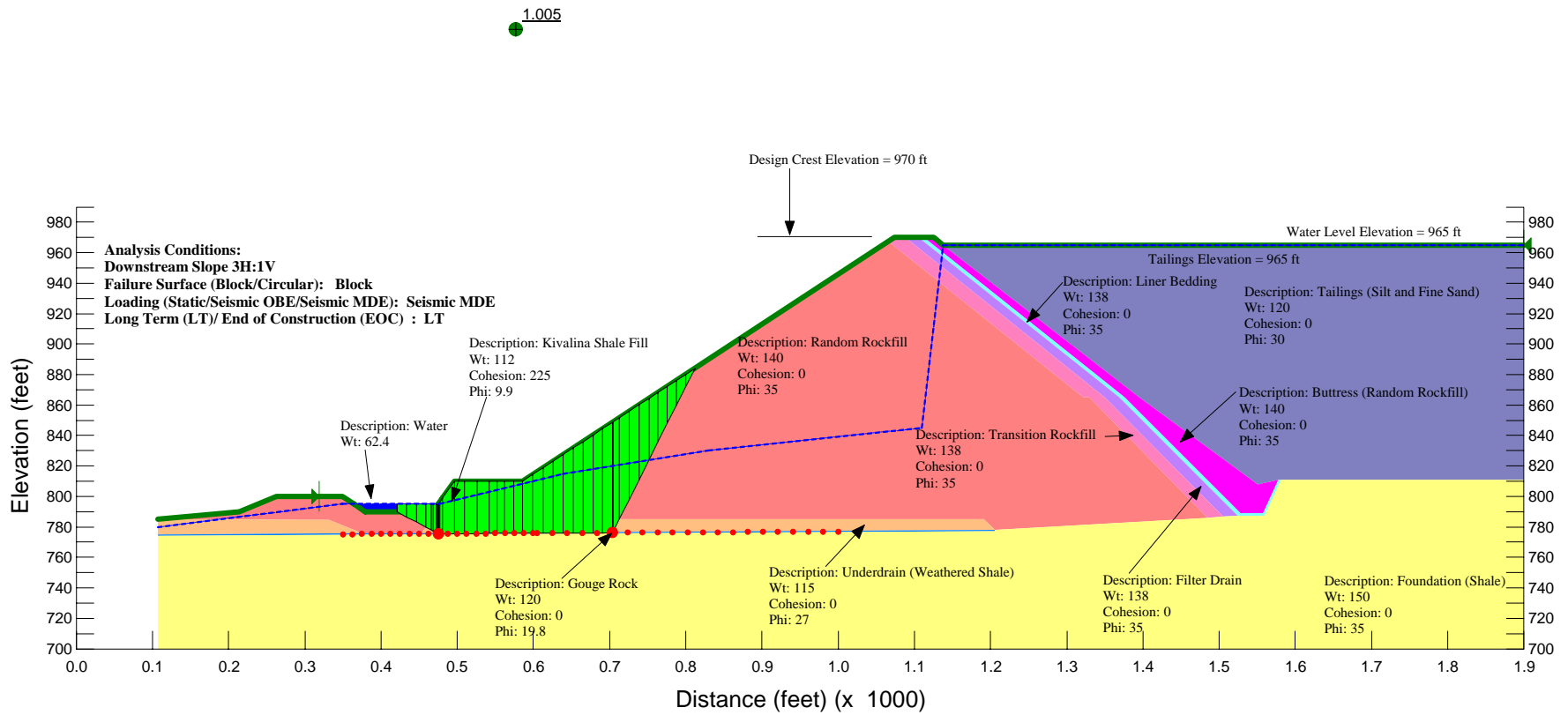


Figure 7-12

Critical Block Failure Surface - 3H:1V Slope for Stage VIII under MDE Loading

URS Project No.: 33757098

**URS**

G:\Red Dog Mine\Mine Closure & Reclamation\Tailings Main Dam\Main Dam Stability\Main Dam Closure Stability 2006\Stage VIII Slope 3 to 1\reduce shear strength\RedDog Block Seismic MCE=125 Ru=0(Fig 7-12).gsz  
 Last Saved Date: 9/28/2006  
 Last Saved Time: 2:57:54 PM

Stability Analysis of Tailings Main Dam  
 Future Raises to Stage VIII  
 Red Dog Mine, Alaska

**Analysis Conditions:**  
 Downstream Slope 2.75H:1V  
 Failure Surface (Block/Circular): Block  
 Loading (Static/Seismic OBE/Seismic MDE): Static  
 Long Term (LT)/ End of Construction (EOC) : EOC

1.451

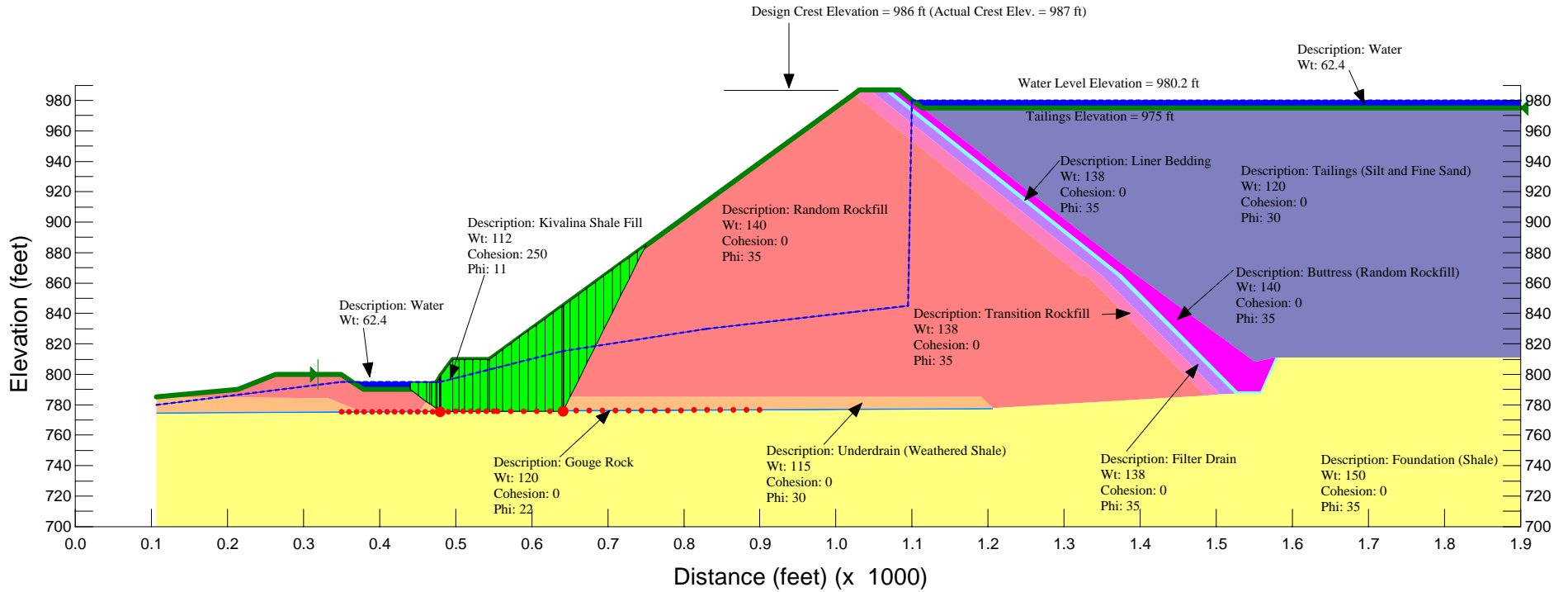


**Figure 7-13**  
**Critical Block Failure Surface with  $R_u = 0.1$  - Static, End-of-Construction Case; 2.75 H: 1 V Slope**

Job No. 33757098

**URS**

G:\Red Dog Mine\Mine Closure & Reclamation\Tailings Main Dam\Main Dam Stability\Main Dam Closure Stability 2006\Slope 2.75 to 1\phi=22\RedDog Block Static Ru=.1 (Fig 7-13).gsz  
 Last Saved Date: 2/22/2006  
 Last Saved Time: 3:22:29 PM

Stability Analysis of Tailings Main Dam  
 Future Raises to Closure  
 Red Dog Mine, Alaska

**Analysis Conditions:**  
 Downstream Slope 2.75H:1V  
 Failure Surface (Block/Circular): Block  
 Loading (Static/Seismic OBE/Seismic MDE): Static  
 Long Term (LT)/ End of Construction (EOC) : EOC

1.287

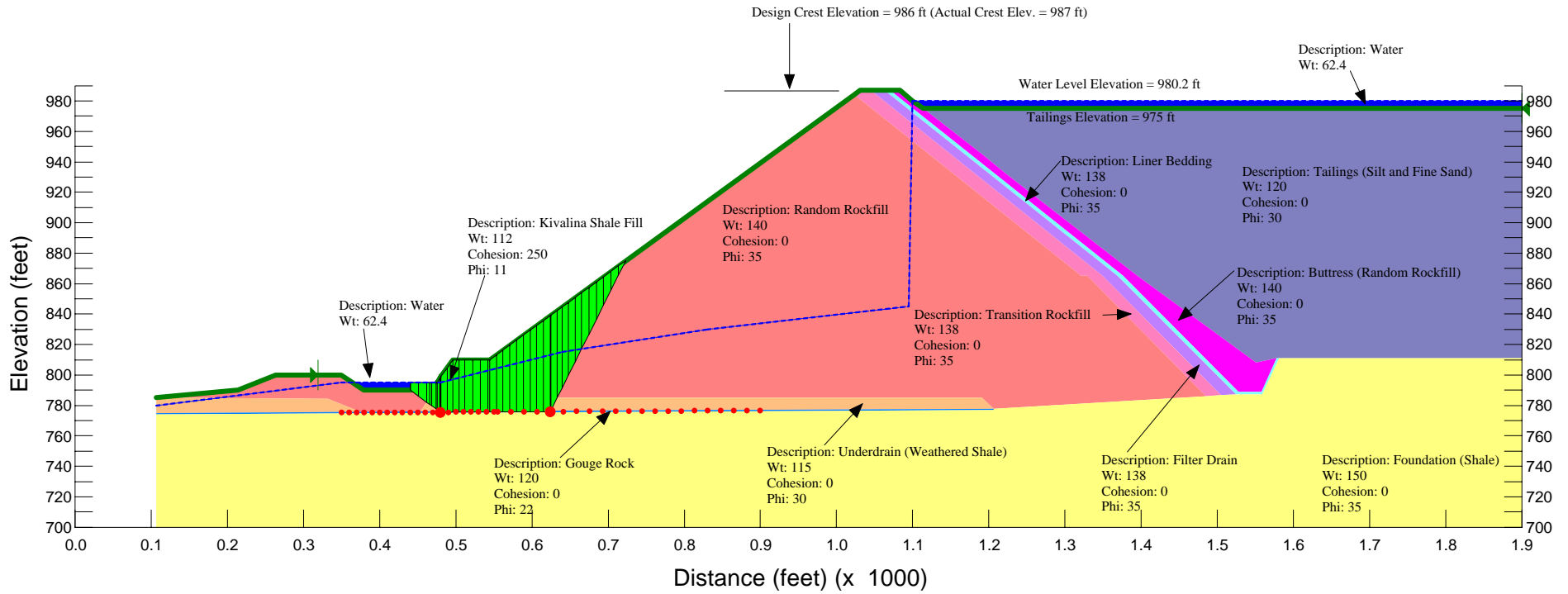


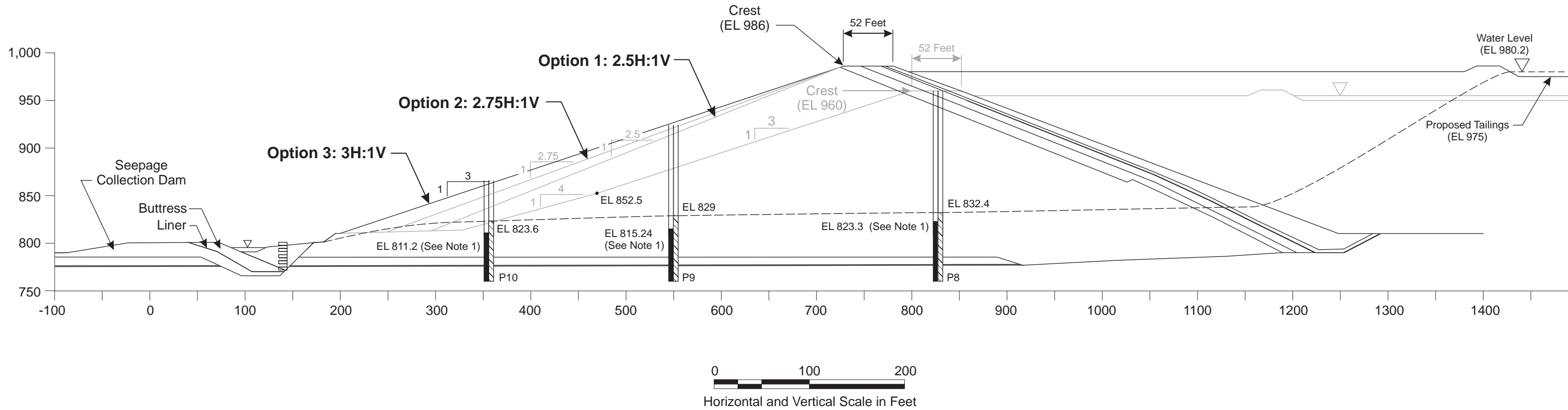
**Figure 7-14**  
 Critical Block Failure Surface with  $R_u = 0.2$  - Static, End-of-Construction Case; 2.75 H: 1 V Slope

Job No. 33757098

**URS**

G:\Red Dog Mine\Mine Closure & Reclamation\Tailings Main Dam\Main Dam Stability\Main Dam Closure Stability 2006\Slope 2.75 to 1\phi=22\RedDog Block Static Ru=2 (Fig 7-14).gsz  
 Last Saved Date: 3/21/2006  
 Last Saved Time: 2:53:03 PM

Stability Analysis of Tailings Main Dam  
 Future Raises to Closure  
 Red Dog Mine, Alaska



**LEGEND**

-  Maximum recorded water level (Stage VII-B)
-  Water levels from seepage analysis (closure, 900 beach, no liner)

**NOTE**

1. Maximum recorded phreatic levels shown correspond to operational conditions and dam configuration present till 2005 and do not reflect the potential phreatic surfaces for closure configuration and operations.

Figure 7-15  
**Downstream Phreatic Surface for Closure  
 900 Feet Beach, No Liner**

1.364

Analysis Conditions:  
Downstream Slope 3H:1V  
Failure Surface (Block/Circular): Block  
Loading (Static/Seismic OBE/Seismic MDE): Static  
Long Term (LT)/ End of Construction (EOC) : LT

Design Crest Elevation = 986 ft (Actual Crest Elev. = 987 ft)

Water Level Elevation = 980.2 ft

Tailings Elevation = 975 ft

Description: Water  
Wt: 62.4

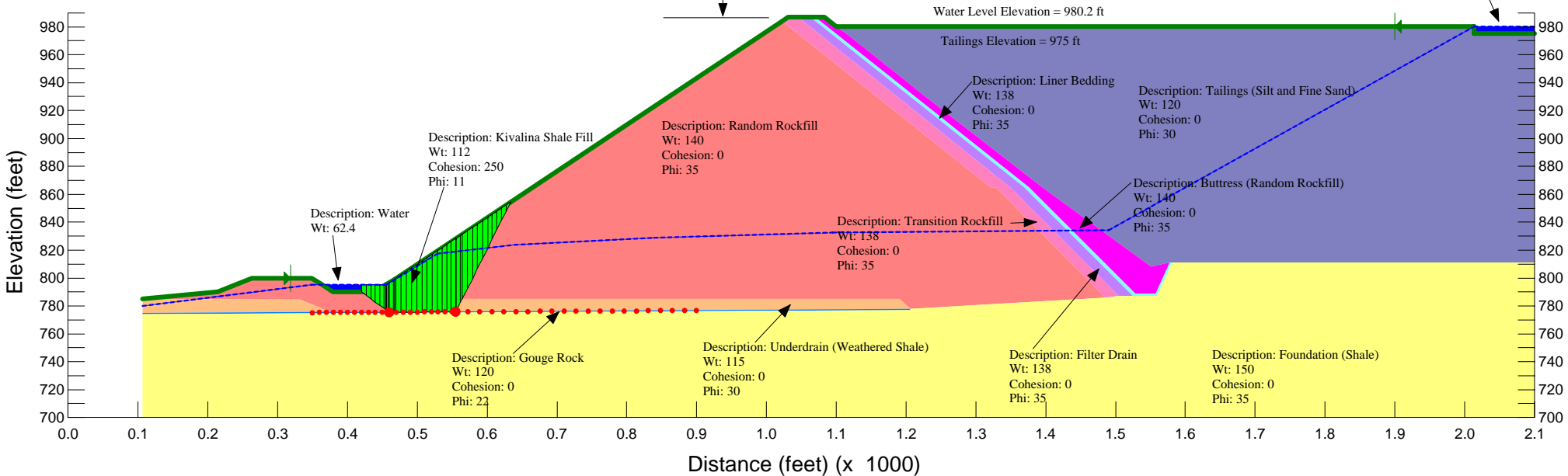


Figure 7-16

URS Project No.: 33757098

Critical Block Failure Surface with  $R_u = 0$  - Static, Long Term Design Condition Case, 900 beach, No Liner; 3H: 1 V Slope

URS

G:\Red Dog Mine\Mine Closure & Reclamation\Tailings Main Dam\Main Dam Stability\Main Dam Closure Stability 2006\Slope 3 to 1\woliner\RedDog Block Static Ru=0-Rev1.gsz  
Last Saved Date: 4/11/2007  
Last Saved Time: 9:15:47 AM

Stability Analysis of Tailings Main Dam  
Future Raises to Closure  
Red Dog Mine, Alaska